

For Reference

NOT TO BE TAKEN FROM THIS ROOM

Ex LIBRIS
UNIVERSITATIS
ALBERTAEANAE



THE UNIVERSITY OF ALBERTA

THE PHOTOCHEMISTRY OF DIMETHYLSILANE

by



ALBERT GORDON ALEXANDER

A THESIS

SUBMITTED TO THE FACULTY OF GRADUATE STUDIES AND RESEARCH
IN PARTIAL FULFILMENT OF THE REQUIREMENTS FOR THE DEGREE
OF DOCTOR OF PHILOSOPHY

DEPARTMENT OF CHEMISTRY

UNIVERSITY OF ALBERTA

EDMONTON, ALBERTA

CANADA

FALL, 1972



Digitized by the Internet Archive
in 2022 with funding from
University of Alberta Libraries

<https://archive.org/details/Alexander1972>

THE UNIVERSITY OF ALBERTA
FACULTY OF GRADUATE STUDIES AND RESEARCH

The undersigned certify that they have read, and
recommend to the Faculty of Graduate Studies and Research, for
acceptance a thesis entitled

THE PHOTOCHEMISTRY OF DIMETHYLSILANE

submitted by

ALBERT GORDON ALEXANDER

in partial fulfilment of the requirements for the degree of
Doctor of Philosophy.

ABSTRACT

The gas phase xenon resonance lamp photolysis of dimethylsilane and the cadmium lamp photolysis of hydrogen sulphide in the presence of dimethylsilane have been investigated in detail. The resulting product distribution was accounted for in both studies and mechanisms were proposed. The vacuum ultraviolet absorption spectra CH_3SiH_3 , CH_3SiD_3 , $(\text{CH}_3)_2\text{SiH}_2$, $(\text{CH}_3)_2\text{SiD}_2$, $(\text{CH}_3)_3\text{SiH}$, $(\text{CH}_3)_3\text{SiD}$, $(\text{CH}_3)_3\text{SiF}$ and $(\text{CH}_3)_4\text{Si}$ were recorded and used to help explain the results from the photolysis of dimethylsilane.

The photolytic decomposition of dimethylsilane yielded ten products and a polymer deposit on the cell window. The mechanism was deduced from the effect of pressure studies, time studies, radical scavengers such as nitric oxide and ethylene, and deuterium labeling. The photolysis was shown to proceed by thirteen primary steps, many of which can be subdivided because they involved the loss of two fragments. Although the 1470\AA resonance line of the xenon lamp lies predominantly in the silicon-hydrogen absorbing region, silicon-hydrogen cleavage is not the dominant mode of decomposition. The nature of the mechanism is a clear indication that absorption of photon energy in one moiety of a molecule can lead to decomposition along a variety of pathways. The results unambiguously indicate the intermediacy of two types of silylene diradicals, the silicon analogue of carbenes. They both readily insert into the Si-H bond of the substrate to give vibrationally excited methylated disilanes. The presence and importance of primary and secondary

photolysis isotope effects between $(\text{CH}_3)_2\text{SiH}_2$ and $(\text{CH}_3)_2\text{SiD}_2$ was illustrated in the kinetic evaluation of the data.

The photolysis of H_2S in the presence of dimethylsilane-d₂ led to the formation of large amounts of D₂. The exchange reaction $\text{H}^* + (\text{CH}_3)_2\text{SiD}_2 \rightarrow \text{D} + (\text{CH}_3)_2\text{SiHD}$ was proven not to be important. The recombination reaction of a dimethylsilyl radical and a thiol radical to form a silylmercaptan was the sole fate of the thiol radical. The silylmercaptan was photolyzed to give a hydrogen atom and a silylthiol radical which abstracted from substrate. The reformed silylmercaptan in turn, photolyzed to give a deuterium atom and the silylthiol radical again, which acted as a photochemical chain carrier. The photochemical chain was time dependent, having a length of about five in a fifteen minute photolysis and a length of about one and one-half in a one minute photolysis.

ACKNOWLEDGEMENTS

The author wishes to express his sincere gratitude to Dr. O. P. Strausz for his assistance, support and encouragement throughout the course of this study.

Special thanks and gratitude go to Dr. R. W. Fair whose help was invaluable in the interpretation of the work.

The experimental assistance and constructive criticisms of Drs. T. L. Pollock, K. Obi and A. W. Jackson and Messrs. W. Duholke and A. van Roodselaar are gratefully appreciated.

The author wishes to thank Dr. E. M. Lown for careful reading and assistance with the manuscript and Mrs. R. Tarnowski for her conscientious efforts in typing.

The assistance of the technical staff is appreciated.

The author would like to thank Dr. G. P. Semeluk for allowing him to use the vacuum ultraviolet spectrograph at the University of New Brunswick. The assistance of Dr. Semeluk in helping the author attain his academic goals is gratefully appreciated.

The author wishes to express his profound gratitude to his wife, Masako, whose cooperation and devotion did much to make this work possible. Her assistance in the preparation of the manuscript is gratefully welcomed and appreciated.

A bursary and three scholarships from the National Research Council of Canada, tuition fees from the Department of Veterans Affairs and teaching assistantships from the University of Alberta are gratefully acknowledged.

TABLE OF CONTENTS

	<u>Page</u>
ABSTRACT.....	i
ACKNOWLEDGEMENTS.....	iii
LIST OF TABLES.....	viii
LIST OF FIGURES.....	xi
CHAPTER I INTRODUCTION.....	1
A. Silicon Chemistry.....	1
1. Physical and Chemical Properties of Silicon Compounds.....	1
2. Thermodynamics.....	5
3. Silyl Radicals.....	6
4. Silylenes.....	9
5. Free Radical Attack on Silanes.....	11
6. Pyrolysis Studies.....	13
7. Radiolysis Studies.....	15
8. Mercury Photosensitization Studies.....	16
9. Photolysis Studies.....	21
B. Vacuum Ultraviolet Photochemistry.....	27
1. Carbon Dioxide.....	28
2. Alkanes.....	30
3. Theoretical Considerations.....	37
C. Present Investigation.....	39

TABLE OF CONTENTS (cont'd)

	<u>Page</u>
CHAPTER II EXPERIMENTAL.....	40
1. Vacuum System.....	40
2. Vacuum Ultraviolet Techniques.....	41
3. Photolysis System.....	48
4. Materials.....	51
5. Analytical System.....	51
6. Other Equipment.....	55
CHAPTER III THE XENON RESONANCE LAMP PHOTOLYSIS OF DIMETHYLSILANE.....	58
A. Results - Photolysis.....	58
1. Products.....	58
2. Effect of Substrate Pressure.....	59
3. Effect of Exposure Time.....	59
4. Effect of Nitric Oxide as a Scavenger...	63
5. Deuterium Labeling Studies.....	75
6. Effect of Ethylene as a Scavenger.....	75
B. Results - Spectra.....	78
Vacuum Ultraviolet Spectra.....	78
C. Kinetics and Mechanistic Deviations.....	78
D. Discussion.....	97
CHAPTER IV THE PHOTOLYSIS OF HYDROGEN SULPHIDE IN THE PRESENCE OF DIMETHYLSILANE.....	113

TABLE OF CONTENTS (cont'd)

	<u>Page</u>
A. Results	
1. Photolysis of D_2S in the Presence of Dimethylsilane-d ₂	114
2. Effect of Varying $H_2S/DMS-d_2$ Ratios at Constant Time.....	118
3. Effect of Exposure Time at Constant $H_2S/DMS-d_2$ Ratios.....	120
4. Test for Dark Reaction.....	120
5. Effect of Added Carbon Dioxide.....	120
6. Photolysis of CH_2O in the Presence of Dimethylsilane-d ₂	124
7. Photolysis of H_2S in the Presence of Trimethylsilane-d ₁	124
8. Photolysis of COS in the Presence of Dimethylsilane-d ₂	128
9. Ultraviolet Absorption Study.....	130
10. Flash Photolysis with Kinetic Absorption Spectroscopy.....	131
11. Flash Photolysis with Mass Spectrometry.	131
B. Discussion.....	132
CHAPTER V SUMMARY AND CONCLUSIONS.....	140
BIBLIOGRAPHY.....	143

TABLE OF CONTENTS (cont'd)

	<u>Page</u>
APPENDIX A. $(CH_3)_2SiH_2/(CH_3)_2SiD_2$ Kinetics.....	155
B. $C_2H_4/(CH_3)_2SiD_2$ Kinetics.....	161
C. $H_2S/(CH_3)_2SiD_2$ Kinetics.....	164

LIST OF TABLES

<u>Number</u>		<u>Page</u>
I-I	Selected Bond Energies of Silicon Compounds (kcal/mole)	7
I-II	Primary Processes in the Vacuum Ultraviolet Photolysis of Monomethylsilane Using a Xenon and a Krypton Lamp..	23
II-I	Wavelengths of Atomic Emission Lines Used in Vacuum Ultraviolet Photochemistry.....	43
II-II	Wavelengths of Emission Lines of Halogen Lamps.....	44
II-III	Approximate Wavelength Limits for Transmission of Various Optical Materials in the Vacuum Ultraviolet...	46
II-IV	Materials Used.....	52
II-V	Thermal Conductivity G.L.C. Operating Conditions.....	54
II-VI	Flame Ionization G.L.C. Operating Conditions.....	56
III-I	Relative Yield of Products as a Function of Pressure from the Xenon Lamp Photolysis of Dimethylsilane.....	60
III-II	Intensity of the Xenon Lamp as a Function of Time ($\times 10^{15}$, quanta/sec).....	64
III-III	Quantum Yield of Products as a Function of Time from the Xenon Lamp Photolysis of Dimethylsilane.....	66
III-IV	Quantum Yield of Products at Zero Time from the Xenon Lamp Photolysis of Dimethylsilane.....	70
III-V	Relative Yield of Products as a Function of Time from the Xenon Lamp Photolysis of Dimethylsilane.....	71
III-VI	Micromoles of Products as a Function of Added Nitric Oxide from the Xenon Lamp Photolysis of Dimethylsilane	73

LIST OF TABLES (cont'd)

<u>Number</u>		<u>Page</u>
III-VII	Isotopic Composition of Hydrogen and Methane from the Xenon Lamp Photolysis of Mixtures of Dimethylsilane and Dimethylsilane-d ₂	76
III-VIII	Isotopic Composition of Hydrogen and Methane from the Xenon Lamp Photolysis of Mixtures of Dimethylsilane-d ₂ and Ethylene.....	77
III-IX	Primary Mechanism for the Xenon Lamp Photolysis of Dimethylsilane-d ₂	96
IV-I	Isotopic Composition of Hydrogen from the Cadmium Lamp Photolysis of Deuterium Sulphide in the Presence of Dimethylsilane-d ₂	116
IV-II	Isotopic Composition of Hydrogen from the Cadmium Lamp Photolysis of Hydrogen Sulphide in the Presence of Dimethylsilane-d ₂ . Constant Time.....	119
IV-III	Isotopic Composition of Hydrogen from the Cadmium Lamp Photolysis of Hydrogen Sulphide in the Presence of Dimethylsilane-d ₂ . Constant H ₂ S/DMS-d ₂ Ratio....	121
IV-IV	Isotopic Composition of Hydrogen from the Cadmium Lamp Photolysis of Hydrogen Sulphide in the Presence of Dimethylsilane-d ₂ . Effect of Added Carbon Dioxide.....	123
IV-V	Isotopic Composition of Hydrogen from the Cadmium Lamp Photolysis of Formaldehyde in the Presence of Dimethylsilane-d ₂	125

LIST OF TABLES (cont'd)

<u>Number</u>		<u>Page</u>
IV-VI	Isotopic Composition of Hydrogen from the Cadmium Lamp Photolysis of Hydrogen Sulphide in the Presence of Trimethylsilane-d ₁	127
IV-VII	Isotopic Composition of Hydrogen from the Cadmium Lamp Photolysis of Carbonyl Sulphide in the Presence of Dimethylsilane-d ₂	129

LIST OF FIGURES

<u>Number</u>		<u>Page</u>
III-1	Relative Yields of H_2 , Tri-MDS, Tri-MS and C_2H_4 as a Function of Pressure from the Xenon Lamp Photolysis of Dimethylsilane.....	61
III-2	Relative Yields of DMDS, MES, Tet-MDS, CH_4 , C_2H_6 and MMS as a Function of Pressure from the Xenon Lamp Photolysis of Dimethylsilane.....	62
III-3	Intensity of the Xenon Lamp as a Function of Post Photolysis Time.....	65
III-4	Quantum Yields of CH_4 , H_2 , Tri-MS, Tri-MDS, C_2H_6 and DMDS as a Function of Time from the Xenon Lamp Photolysis of Dimethylsilane.....	68
III-5	Quantum Yields of MES, Tet-MDS, C_2H_4 and MMS as a Function of Time from the Xenon Lamp Photolysis of Dimethylsilane.....	69
III-6	Micromoles of Tet-MDS, Tri-MS and C_2H_6 as a Function of Added Nitric Oxide from the Xenon Lamp Photolysis of Dimethylsilane.....	74
III-7	Vacuum Ultraviolet Absorption Spectra of Mono- methylsilane and Monomethylsilane-d ₃	79
III-8	Vacuum Ultraviolet Absorption Spectra of Dimethyl- silane and Dimethylsilane-d ₂	80
III-9	Vacuum Ultraviolet Absorption Spectra of Trimethylsilane and Trimethylsilane-d ₁	81

LIST OF FIGURES (cont'd)

<u>Number</u>		<u>Page</u>
III-10	Vacuum Ultraviolet Absorption Spectra of Trimethylmonofluorosilane and Tetramethylsilane.....	82
III-11	X_{D_2}/F_{He} and X_{HD}/F_{He} as a Function of X_L from the Xenon Lamp Photolysis of Mixtures of Dimethylsilane and Dimethylsilane-d ₂	87
III-12	A Plot in Accordance with Equation [36] to Obtain the Isotope Effect for Abstraction in the Xenon Lamp Photolysis of Mixtures of Dimethylsilane and Dimethylsilane-d ₂	88
IV-1	X_{D_2} as a Function of Time from Cadmium Lamp Photolysis of Hydrogen Sulphide in the Presence of Dimethylsilane-d ₂ . Constant H ₂ S/DMS-d ₂ Ratio.....	122
IV-2	A Plot in Accordance with Equation [41] for the Cadmium Lamp Photolysis of Hydrogen Sulphide in the Presence of Dimethylsilane-d ₂ . Constant Time.....	134
IV-3	A Plot in Accordance with Equation [41] for the Cadmium Lamp Photolysis of Hydrogen Sulphide in the Presence of Dimethylsilane-d ₂ . Constant Time. Low H ₂ S/DMS-d ₂ Ratios.....	135

CHAPTER I

INTRODUCTION

A. Silicon Chemistry

The photochemistry of silicon compounds and in particular of silicon hydrides, is a relatively new and rapidly increasing field of interest. Information on this subject is scarce (1) and prior to the early 1960's, the main emphasis in silicon chemistry has been on the synthesis and characterization of new compounds (2). The photochemical work that has been done on silanes in this period, with few exceptions, was largely preparative with no effort to understand the kinetic-mechanistic aspects. The greatly increased practical importance of silicon chemistry, as well as its intrinsic interest, has led to much activity within the last ten years. Before reviewing the recent developments, let us turn our attention to the silicon atom, its properties and simple compounds.

1. Physical and Chemical Properties of Silicon Compounds

Silicon is the second member of the group IV B elements. The chemistry of the first element, carbon is very much different from the other members of the group and there is probably no other group of elements that shows such a striking difference in the physical and chemical properties as we proceed from the first to the second row. The salient features of the chemical properties of silicon in comparison with carbon can be summarized in the following

points.

(a) The main mode of bonding for both carbon and silicon is sp^3 hybrid bonding, such as hydrides, alkylated hydrides, halides, hydroxyl compounds, ethers, etc. Long chain bonding of silicon and oxygen gives rise to the industrially important compounds - siloxanes. Silicon can increase its coordination to six in some cases, by the use of d-orbitals, which will be discussed later.

(b) The tendency for catenation decreases drastically in going from carbon to silicon. Stable carbon-carbon linkages in the order of hundreds are well known while similar linkages involving silicon are unknown. Compounds having more than six silicon-silicon bonds have not been prepared in quantitative yields.

(c) Multiple bond formation, which plays a large and important role in carbon chemistry, is unknown in silanes. There have been many attempts to synthesize stable ($p \rightarrow p$) π double bonds but the products have invariably been proven to be dimers or polymers (3). The presence of silicon double bonds as transient intermediates has been proposed in pyrolysis systems (4). The reason for the lack of double or triple bond formation to silicon is not known with certainty. Some of the theories put forward are discussed below.

(i) It has been suggested (5) that silicon double bonds are not formed because σ bonds are stronger than π bonds. This rationalization seems to work in the case of Si-O vs Si=O bonds. The Si-O bond strength is about 106 kcal/mole while the C-O bond strength

is 86 kcal/mole. Although stable Si=O compounds do not exist, a bond strength of 190 kcal/mole has been found for gaseous SiO at high temperature, as against a value for carbon monoxide of 256 kcal/mole. Hence it would seem that $2E(Si-O)$ is greater than $E(Si=O)$ while $2E(C-O)$ is not as great as $E(C=O)$. This argument loses credibility when applied to Si=C and Si=Si bonds because the Si-C and Si-Si bonds are not particularly strong. Also, it must be remembered that $2E(C-C)$ is greater than $E(C=C)$ and olefins are well known. (A complete discussion of bond strengths will be given later).

- (ii) It has also been suggested that $(p \rightarrow p)\pi$ overlap is poor for higher row elements (6). That is, the (np) orbitals are diffuse for values of $n = 3$ or higher. However, quantum mechanical calculations involving Slater orbitals do not support this (7,8).
- (iii) Pitzer (9) has suggested that inner shell repulsions could become important at the short internuclear distances required for multiple bonding. This does not, however, explain why Si=O bonds are so unstable because P=O and S=O bonds are well known and the same effects should be operative.

The interrelation of all these factors could be so finely balanced that a slight shift in any one of them could explain the difference in carbon and silicon bonding.

(d) Another important difference between carbon and silicon is the ability of silicon to utilize its vacant d-orbitals. Although carbon has vacant d-orbitals, they lie in the order of 220 kcal/mole (10) above the 2p orbitals and would be of little importance in bonding or transition states (11). However, the 5-fold degenerate d-orbitals of silicon are only 130 kcal/mole (10) above the highest occupied orbital, which makes them potentially important in bond formation. It is more facile to promote a 3p-electron to a 3d-orbital than it is to promote a 3s inner shell electron to a 3p-orbital. Hence d-orbitals are important in the formation of additional bonds by mixing with s and p orbitals. The five coordinate sp^3d hybrids and the six coordinate sp^3d^2 hybrids are examples of this. Probably one of the most controversial aspects of the importance of the 3d-orbitals of silicon is that of $(p \rightarrow d)\pi$ bonding (12-14).

(e) Electronegativity is another property where carbon and silicon differ. Although the concept of electronegativity is somewhat vague and there are at least three different scales in popular use, the difference between carbon and silicon is still distinct. The electronegativities of some common elements using the Allred-Rochow scale follow: hydrogen = 2.20, carbon = 2.50, silicon = 1.74, nitrogen = 3.07, oxygen = 3.50, fluorine = 4.10, chlorine = 2.83, bromine = 2.74, iodine = 2.21, and sulphur = 2.44 (15). As far as the hydrides are concerned, we find that silicon would carry a partial positive charge. This means that silicon hydrides are more susceptible to nucleophilic attack by water or oxygen. Hence we find that the

simple alkyl silanes and silicon hydrides are less stable than their carbon analogues.

In light of the foregoing discussion it is not surprising that the chemical reactivity and stability of many silicon compounds differ markedly from their carbon analog. For example, silanols are very unstable and readily condense to siloxanes and water.



Silanediols are unknown. All the silanes, but in particular those that have more than one silicon atom, are very susceptible to hydrolysis during storage in glass containers.



The silicon hydrides, but not the alkyl silanes, burn spontaneously when exposed to oxygen.

2. Thermodynamics

Thermochemical data and bond dissociation energies for silanes are sparse. Uncontrollable explosions and the formation of polymeric SiO_2 makes the use of calorimetry difficult. Mass spectrometric results are often complicated by ion-pair formation and the difficulty in interpolation of the ionization curves. In addition, radical ionization potentials for silanes are not known.

Average bond enthalpies for some carbon and silicon derivatives have been obtained by explosion calorimetry, heats of hydrolysis and elaborate thermochemical reasoning (12). It can be seen that silicon forms weaker bonds to itself, carbon, and hydrogen

than does carbon. However, it forms stronger bonds with group V, VI, and VII elements. Table I-I gives some selected bond energies obtained by several different authors. The differences in bond strengths between carbon and silicon can be rationalized in terms of electronegativity. Bond energies, however, do not necessarily reflect reactivity. Although Si-Cl bonds are stronger than Si-C bonds, they are more reactive to the presence of water on glass surfaces. This is because the Si-Cl bond is more polar and hence susceptible to nucleophilic attack.

3. Silyl Radicals

The physical and chemical differences between carbon and silicon radicals are extensive. Great effort has gone into determining the structure of trivalent silyl radicals. The SiH_3 radical has been produced (25) in a krypton matrix at 4.2°K by γ -irradiation of SiH_4 . An ESR study of the radical showed that the orbital of the unpaired electron had 22% s-character and that the bond angle was 110.6°. This can be contrasted to the physical properties of methyl radicals which have an essentially planar structure and no s-character in the orbital of the unpaired electron. Similar studies on SiH_3 (26), CH_3SiH_2 (27) and $(\text{CH}_3)_3\text{Si}$ (27) radicals in a xenon matrix indicated bond angles of 113° - 114°. The non-planarity of silyl radicals has been predicted theoretically (28). It has also been shown that optically active α -naphthylphenylmethylsilyl radicals generated in solution (29) abstracted from CCl_4 to give a product with 85% retention of configuration.

TABLE I-I

Selected Bond Energies of Silicon Compounds (kcal/mole)

Compound	D(Bond)	Reference
$\text{H}_3\text{Si}-\text{H}$	94	21
$\text{Si}-\text{H}$	74	22
$\text{H}_5\text{Si}_2-\text{H}$	90	23
$\text{H}_3\text{Si}-\text{SiH}_3$	81	21
$\text{CH}_3\text{SiH}_2-\text{H}$	94	24
$(\text{CH}_3)_3\text{Si}-\text{H}$	81	17
	80.3	19
	79	18
$\text{H}(\text{CH}_3)_2\text{Si}-\text{CH}_3$	76.5	19
$(\text{CH}_3)_3\text{Si}-\text{CH}_3$	76	17
	76	18
	67.6	20
$(\text{CH}_3)_3\text{Si}-\text{Cl}$	88	17
	123	18
$(\text{CH}_3)_3\text{Si}-\text{Br}$	78.5	17
$(\text{CH}_3)_3\text{Si}-\text{I}$	69	17
$(\text{CH}_3)_3\text{Si}-\text{Si}(\text{CH}_3)_3$	67	16
	67	18

In contrast to carbon, there are few good sources of silyl radicals. Pyrolysis of the simple silanes is not suitable for kinetic studies because of competing silylene formation. Also, many of these compounds require very high temperatures for decomposition, sometimes in excess of 773°K. The pyrolysis of hexamethyl-disilane (16) at 796 - 828°K is one example where a thorough study of the trimethylsilyl radical was possible.

The use of silicon substituted ketones and azo compounds for the production of silyl radicals by photolysis has certain limitations. The extremely high bond strength of Si-O and Si-N means that these compounds are too stable to be good radical sources (30). This increased bond strength is probably due to interaction of the p-orbitals of oxygen and nitrogen with the vacant d-orbitals of silicon. At the energies required for photolysis there can be many competing modes of decomposition. The photolysis of silicon-mercury compounds, such as $((\text{CH}_3)_3\text{Si})_2\text{Hg}$, have proved to be useful sources of silyl radicals (31).

Kinetic studies of the reactions of silyl radicals are somewhat easier than those involving carbon radicals even though there are few good sources. Pyrolysis does not proceed by a radical chain mechanism as in hydrocarbons, although there can be complications from polymerization. Another important point is that disproportionation does not occur because silicon does not form double bonds. Hence complicating addition reactions do not occur. Extensive reviews of silyl radical reactions are available (32-34).

4. Silylenes

Divalent carbon radicals (carbenes) play an important role in carbon chemistry (35,36). In Group IV B there is a steady increase in the stability of the divalent species relative to that of trivalent species. That is, reaction [3] becomes less important with respect to reaction [4] and/or [5] where M is a Group IV B element.



Silylene reactions are extremely important in silicon chemistry and reviews (35,37) have appeared recently.

It is known that the ground state of methylene is a linear triplet, $^3\Sigma_g^-$, and the first excited state is a bent singlet, 1A_1 (38). The various bond lengths, energies, and other physical properties of methylene and its derivatives have been well established. The same cannot be said of silylene and its derivatives however, Dubois, Herzberg and Verma (39) found two electronic states in SiH_2 . In the lower electronic state, 1A_1 , the $HSiH$ angle is $92^\circ 5'$ and the Si-H distance is 1.516\AA . In the upper electronic state, 1B_1 , these parameters are 123° and 1.487\AA respectively. They were unable, however, to find a lower triplet ground state analogous to methylene. Also, they could not determine if the 1A_1 or the 1B_1 were the ground state. Theoretical calculations by Jordan (40) indicated a singlet ground state for SiH_2 . Recently, Milligan and Jacox (41) have shown, by photolysis of silane in an argon matrix

at 4° and 14°K and analysis by infrared and ultraviolet spectroscopy, that the 1A_1 state is the ground state.

Silylenes have been formed by a variety of means (37); pyrolysis, flash photolysis, photolysis, neutron irradiation, and glow discharge. However, in all these methods, there is a fine balance between silylene formation and single bond homolysis to form silyl radicals. This balance seems to be a function of the starting material. For example, hexamethyldisilane yields two trimethylsilyl radicals when pyrolyzed (16). However, substitution of a methoxy group for one of the methyl groups on each of the silicon atoms will give rise to dimethylsilylene upon pyrolysis (42). The most likely mechanism in the latter case involves an α -elimination. The driving force for this process is probably the strong affinity of oxygen for silicon. The pyrolysis of 7-silanorbornadienes and metal silyls, such as $AlMe_2(SiMe_3)$ have given good yields of silylenes (37).

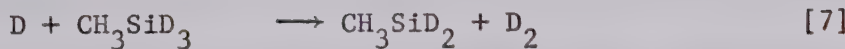
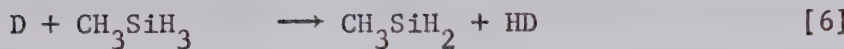
The study of silylene reactions has been difficult because of their great reactivity. Silylenes polymerize, insert into single bonds, and add to carbon-carbon multiple bonds. In the absence of other reagents, silylenes readily polymerize. This reaction is analogous to olefin formation with carbenes but since silicon does not form double bonds, polymer formation occurs. In the presence of a precursor or a trapping agent, there is ready insertion into single bonds. They readily insert into silicon-hydrogen bonds and into any bond between silicon and a more electronegative atom, such as halogens, oxygen or nitrogen. However, they do not insert

into silicon-carbon, carbon-hydrogen or carbon-carbon bonds even at high temperature. Because of this, it has been suggested that silylenes are less reactive than carbenes (43). Silylenes will also add to unsaturated organic compounds. However, no stable silacyclopropane has ever been isolated. Although they are thought to be an intermediate, it appears that they dimerize to a 1,4-disilacyclo compound or rearrange to give a vinyl silane (43,44).

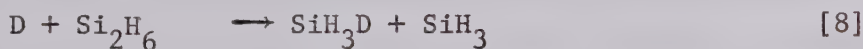
5. Free Radical Attack on Silicon Compounds

The reactions of alkyl radicals (45-48) and halogen substituted alkyl radicals (49-55) with silanes have been the object of extensive studies over the last few years. The transfer reactions of alkyl radicals with non-halogenated silanes indicated that the logarithms of the Arrhenius A factors are, in most cases, between 11.0 and 12.0. This agrees very well with the A factors for alkyl radical attack on hydrocarbons. The activation energies in the case of silanes, 5 - 8 kcal/mole, are lower than for the hydrocarbons, 11 - 18 kcal/mole (47). This decrease has been attributed to the weaker Si-H bond. Substitution of one or more halogen atoms on the silane or the use of halogen substituted attacking radicals markedly alters the activation energy but has little effect on the A factor. This result has been attributed to polar effects associated with the interaction of the reactants.

The reaction of hydrogen atoms with silanes has not received much attention. The vacuum ultraviolet photolysis of monomethyl-silane (91) has led to the determination of the isotope ratio



$k_6/k_7 = 3.2$. The iodine lamp photolysis of mixtures of ethylene- d_4 and the appropriate non-deuterated silane enabled the determination of a series of abstraction rate constants (56). It has been shown (57) that D-atoms will undergo a displacement reaction with disilane with an efficiency approximately equal to the abstraction reaction



The rate constant for the reaction of D-atoms with $(CH_3)_3SiH$ has been shown (58) to be $1.11 \times 10^{11} \text{ cc mole}^{-1} \text{ sec}^{-1}$ in a flow system.

The 1849A photolysis of C_2D_4 in the presence of SiH_4 suggested the transient formation of SiH_4D and allowed the determination of the rate constant for abstraction (59).

An extensive study of the reactions of methylene with silanes has been carried out by Simons and his co-workers (60-62). Unlike silylene, singlet methylene will insert into both carbon-hydrogen and silicon-hydrogen bonds. The ratio for Si-H to C-H bond insertion is: monomethylsilane = 8.9, dimethylsilane = 6.9 and trimethylsilane = 7.2. These values were found to be independent of wavelength and silicon-carbon insertion did not occur. It is believed that methylene insertion into silanes is as fast or faster than addition to olefins. RRKM theoretical calculations on the decomposition of the chemical activated species indicates that the A-factor is 10^{15} to 10^{16} sec^{-1} .

6. Pyrolysis of Silicon Compounds

The first serious attempt to understand the mechanism of monosilane pyrolysis was not undertaken until 1966 by Purnell and Walsh (63) and later by Ring et al. (64). Not surprisingly, there is disagreement on the mechanism. Purnell favours molecular elimination of hydrogen to form silylene which subsequently inserts into substrate. Ring, however, favours atomic hydrogen loss to form a monosilyl radical which undergoes a displacement reaction with substrate. The latter mechanism is critically dependent on the presence of HD in equimolar mixtures of SiH_4 and SiD_4 . However, they do not report the absolute yields of HD. Pollock et al. (57) have shown that monosilyl radicals do not recombine at atmospheric pressure. These results indicate that a SiH_3 radical in collision with a SiD_3 radical would give rise to H_2 , HD, or D_2 plus the appropriate diradical. Also, thermodynamic calculations by Purnell (65) and Davidson (66), indicate that SiH_3 is totally unstable with respect to SiH_2 at typical silane pyrolysis temperatures. Hence it would seem that silylene formation is the chief mode of decomposition in the pyrolysis of monosilane.

The pyrolysis of trimethylsilane between 943°K and 1031°K by Davidson (19,67) established that the primary step was the formation of silyl radicals and not silylenes. Most notable among the products were di-, tri-, and tetramethyl-1,3-disilacyclobutanes. It was necessary to postulate the formation of the double bonded intermediates, $(\text{CH}_2=\text{Si}(\text{CH}_3)_2)$ and $(\text{CH}_2=\text{SiHCH}_3)$, by disproportionation

reactions of the initial radicals and subsequent dimerization.

Clifford et al. (20) obtained similar results on the pyrolysis of tetramethylsilane. The presence of silicon double bonded intermediates in the thermal decomposition of 1,1-dimethyl-1-silacyclobutane was proven by Flowers and L. E. Gusel'nikov (4). The addition of methanol to the system yielded trimethylsilanol while the addition of ammonia yielded trimethylsilylamine. These compounds in turn dimerized to hexamethyldisiloxane and hexamethyldisilazane.

A very thorough study of the pyrolysis of disilane has been carried out by Bowrey and Purnell (68) who showed that the only primary step was silyl formation. The initial formation of silylene was verified independently by Ring (69,70). Both authors showed, by the addition of alkylsilanes to their systems, that insertion of silylene into carbon-silicon and carbon-hydrogen bonds does not occur even at elevated temperatures.

Ring (71) has carried out the thermal decomposition of methyldisilane and 1,2-dimethyldisilane. The initial steps were silylene formation. The trisilanes formed in each case resulted from insertion of the appropriate silylene into a silicon-hydrogen bond. The thermal decomposition of pentamethyldisilane (72) proceeds by silylene formation rather than silyl radical formation. The pyrolysis of methoxymethyldisilanes involves the migration of the methoxy group and subsequent silylene formation (42,44). The pyrolysis of hexamethyldisilane (16,73,74), however, has been shown to proceed by a radical mechanism.

It is evident that the factor influencing the importance of

silyl versus silylene formation in the primary step of the pyrolysis of a disilane is the ability of the substrate to form a transient three-member ring, that is, an α -elimination mechanism. Hydrogen and oxygen readily form such bridges while carbon does not. If the disilane is not symmetrical as in methyldisilane then there are two silylenes possible and the formation of the more complex monosilane seems to be slightly favoured.

Gusel'nikov and co-workers (75,76) have shown that the pyrolysis of large methylcyclosiloxanes leads to the formation of transient silicon-oxygen double bonded species which, in turn, readily polymerize.

7. Radiolysis of Silicon Compounds

The radiolysis of silanes has mostly been concerned with industrial applications (77) and the emphasis has been on increasing the yield of the desired products. The reactions are not particularly clean and a large variety of products are formed in addition to the desired material. The mechanisms of such radiolysis studies have been interpreted in terms of free radicals and/or ionic species.

The γ -ray radiolysis of monosilane (78) at room temperature produces only hydrogen and disilane with G yields of 17.0 and 5.3 respectively as the measureable products. A light brown polymeric deposit forms on the cell surfaces. Monosilane is consumed with a G value of approximately 22. The primary steps involve both free radical and ionic processes.

More recently, Mains and Dedinas (79,80) have carried

out a radiolysis study on tetramethylsilane in both the vapor and liquid phase. It was felt that the mechanism can be explained exclusively by neutral radical formation and molecular elimination. The formation of ionic species and subsequent ion-molecule reactions were not considered to be important. It was shown that 81% of the hydrogen arises from thermal hydrogen atoms, 12% from molecular elimination and 7% from hot hydrogen atoms. Thermal methyl radicals account for 35% of the methane while 40% arises from molecular elimination and 25% from hot methyl radical abstraction. Ethane and the silane products arise almost exclusively from radical recombination. Olefinic internal free radical scavengers, acetylene, ethylene and propylene, are formed in significant G yields in the presence of oxygen or nitric oxide. A 1,2-diradical arising from molecular elimination of methane is thought to be of minor importance. The silylenes formed by molecular elimination do not give rise to measurable products. This finding is in keeping with the inefficiency of silylene insertion into carbon-silicon and carbon-hydrogen bonds. The principal alkylsilane products arise from the intercombination of CH_3 , $(\text{CH}_3)_3\text{Si}$, and $(\text{CH}_3)_3\text{SiCH}_2$ radicals. Minor carbosilane products could arise from radical addition reactions to the olefins and the 1,2-diradical mentioned above. All G yields were lower in the liquid phase than in the vapor phase due to geminate recombination.

8. Mercury Photosensitization of Silicon Compounds

The mercury photosensitization of monosilane was first reported by Emeléus and Stewart (81) who detected hydrogen formation

and a brown film of polymeric silicon hydride. Mercury photosensitization should be a good method of studying silane decomposition since a known quantity of energy can be transferred in one step. Also, it has been shown that the cross sections for decomposition of the silicon hydrides are very much larger than their carbon counterparts (82). Niki and Mains (83) studied the sensitized decomposition of monosilane and found that quantum yield of hydrogen production was 1.8 but it was admitted that this value was subject to considerable uncertainty. Disilane, trisilane and other higher condensation products were detected.

A detailed investigation of the mercury photosensitized decomposition of the simple silanes has been undertaken by Strausz and co-workers. The mercury photosensitization of monomethylsilane, monomethylsilane-d₃, dimethylsilane, trimethylsilane, tetramethylsilane and dimethyldifluorosilane (84) were all found to involve exclusive initial loss of an H or D atom from the Si-H or Si-D bond, if available; otherwise, C-H scission occurs. The main products found in all of the systems were hydrogen and the appropriate disilane, formed by silyl radical recombination, in equal amounts. Although the quantum yields of hydrogen and the appropriate disilane were approximately equal, they were less than unity. This deficiency can be attributed to side reactions since smaller yields of higher silanes and polymer were noticed. Addition of small amounts of nitric oxide to these systems resulted in the complete suppression of disilane formation and the simultaneous appearance of the corresponding disiloxane via a chain mechanism.

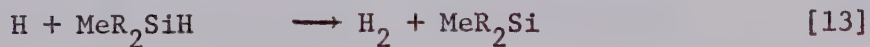
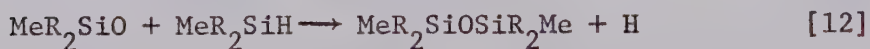
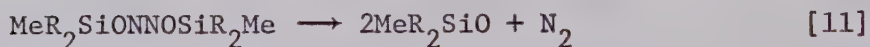
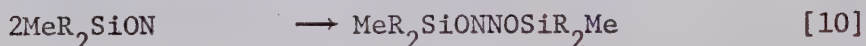
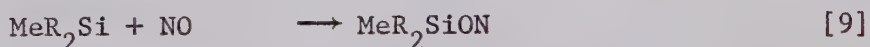
The mercury photosensitization of monosilane (84) proved to be more complex. The reaction was extremely surface dependent with values of $\phi(H_2)$ ranging from 10 in a clean cell, to 3 in a conditioned cell. Other products were disilane, trisilane, tetrasilane, and a solid polymer. It was necessary to postulate five primary steps and a very efficient wall reaction to account for the results.

The sole primary step in the sensitized decomposition of disilane (57) is Si-H cleavage. The hydrogen atoms react with disilane via two competing reactions having comparable rate constants, abstraction and a displacement reaction to give monosilane and a monosilyl radical. Disilyl radicals recombine to give tetrasilane in a pressure dependent reaction up to 400 torr of disilane. Recombination of a monosilyl and a disilyl radical to give trisilane is pressure dependent up to 1000 torr. Monosilyl radicals do not recombine at atmospheric pressure but disproportionate to give SiH_4 and SiH_2 . Rate theoretical calculations indicate that recombination could occur only at pressures above ca. 10 atmospheres. There was substantial polymer formation.

The sensitized decomposition of phenylsilane (85) occurs via three primary steps. Silicon-hydrogen cleavage accounts for approximately 80% of the primary quantum yield. The remaining two steps, silicon-carbon cleavage to form a silyl radical and a phenyl radical and a rearrangement process to form silylene and benzene, each constitute approximately 10% of the overall primary process. Small quantities of benzene and phenyldisilane and trace amounts of

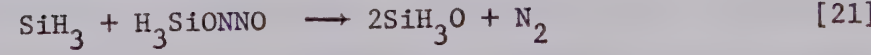
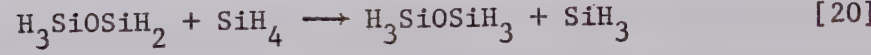
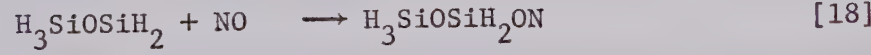
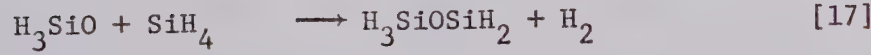
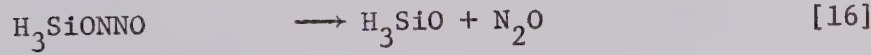
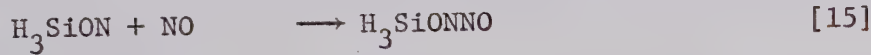
diphenyl, diphenylsilane and diphenyldisilane were detected. It was necessary to postulate that approximately 70% of the hydrogen atoms add to the phenyl ring of the substrate. The most probable fate of the silyl substituted cyclohexadienyl radical thus formed is combination or disproportionation with another radical or addition to a substrate molecule to form a higher molecular weight compound. The silylcyclohexadiene formed by disproportionation could not be detected. These results contrast markedly with those found for toluene where no decomposition was observed on photosensitization at room temperature and the quantum yield of hydrogen was only 0.1 at 673°K (86).

The use of nitric oxide as a scavenger of monoradicals in alkyl radical chemistry is well established (87). Its role in the scavenging of the monoradicals formed in the mercury photosensitization of the methyl silanes (84) was dramatically illustrated by the complete suppression of the disilanes. Large amounts of the corresponding disiloxane, hydrogen, nitrogen, and nitrous oxide were formed. A tentative chain mechanism was proposed by Strausz et al. (84) which is given below:



where $R = CH_3$ or H. The addition of nitric oxide to the silyl radical occurs at the O-atom whereas in alkyl radical systems bonding takes place at the N-atom (87). This addition is readily explained by the much higher affinity of silicon atoms for oxygen over nitrogen. It is interesting that a radical scavenger like nitric oxide has initiated a chain reaction in a non-chain system. Since the integrity of the primary radical is preserved in the siloxane product, we have a means of radical identification.

The inverse addition of nitric oxide to the silyl radical has been verified by Kamaratos and Lampe (88) by a mass spectrometric study of the mercury photosensitized reactions of silane and methyl-silane with nitric oxide. They revised the mechanism somewhat in order to account for the formation of nitrous oxide. The mechanism is given below:



The formation of large molecular weight siloxanes can be readily

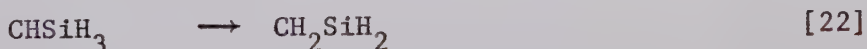
accounted for by the chain nature of the reaction mechanism. This investigation showed that the mechanism is very dependent on the amount of nitric oxide present. In the presence of excess nitric oxide, the double addition of NO will take place as indicated in reaction [15]. However, as the nitric oxide is depleted, then reaction [10] will become important. A very involved mechanism of eighteen steps for the scavenging of disilyl radicals formed in the mercury photosensitization of disilane has been proposed, which combines the main features of the two studies mentioned above (89).

9. Photolysis of Silicon Compounds

The direct photolysis of the simple silicon hydrides was first reported by Strausz and co-workers (90,91). Monosilane and the methylated monosilanes absorb only in the vacuum ultraviolet (92,93) while disilane photolysis can be initiated by a medium pressure mercury lamp because the absorption is significant between 2000°A and 2100°A (94).

Preliminary accounts of the vacuum ultraviolet photolysis of monomethylsilane using a xenon lamp and a krypton lamp have been reported (90,91). In both cases, the products were hydrogen, 1,2-dimethyldisilane, methyldisilane, methane, ethane, dimethylsilane, monosilane, and a solid polymer. The primary steps of the reactions, their quantum yields, and the mechanism of the overall processes were established from the nature of products, their dependence on conversion, pressure, the addition of scavengers such as nitric oxide and ethylene, and from the use of deuterium labeling. The effect of

wavelength was also examined. The proposed mechanism and the primary quantum yields for the various steps using the xenon and krypton lamps are given in Table I-II. In the xenon photolysis, the total primary quantum yield was 1.03 which means that it is not necessary to postulate further polyfragmentation steps. In the krypton photolysis, however, the total primary quantum yield was 1.23. In the absence of chain processes, the primary quantum yield must equal 1.0 to within experimental error. It was felt that step three, the 1,2 loss of hydrogen, has too high a value for a primary yield and it was postulated that all the CH_2SiH_2 decomposes to CHSiH and 64% of this species decomposes to CSi . Methylsilylene forms in two possible primary steps with the molecular process predominating. This species inserts quantitatively into the SiH bond of substrate to give 1,2-dimethyldisilane. Silylene also forms by two primary steps but radical cleavage predominates. Silylene quantitatively inserts to give methyldisilane. The 1,2 diradical formed in step three does not undergo further reaction to give measurable products but rather, contributes to polymer formation. The silylmethylene diradical formed in step four does not insert but undergoes unimolecular isomerization to give a 1,2 diradical:



This process is favoured thermochemically by the fact that the carbon-hydrogen bond is stronger than the silicon-hydrogen bond. Polyfragmentation, as indicated in step seven, does not occur in the xenon photolysis. Single bond homolysis, as indicated in step eight is

TABLE I-II

Primary Processes in the Vacuum Ultraviolet Photolysis of
Monomethylsilane Using a Xenon and a Krypton Lamp

		<u>ϕ (Xe)</u>	<u>ϕ (Kr)</u>
$\text{CH}_3\text{SiH}_3 + h\nu \xrightarrow{1}$	$\text{CH}_3\text{SiH} + \text{H}_2$	0.32	0.16
$\xrightarrow{2}$	$\text{CH}_3\text{SiH} + 2\text{H}$	0.05	0.09
$\xrightarrow{3}$	$\text{CH}_2\text{SiH}_2 + \text{H}_2$	0.23	<0.37 (0.14)
$\xrightarrow{4}$	$\text{CHSiH}_3 + \text{H}_2$	0.07	0.11
$\xrightarrow{5}$	$\text{CH}_4 + \text{SiH}_2$	0.09	0.08
$\xrightarrow{6}$	$\text{CH}_3 + \text{H} + \text{SiH}_2$	0.26	0.25
$\xrightarrow{7}$	$\text{CH}_3 + \text{H}_2 + \text{H} + \text{Si}$	0.00	0.17
$\xrightarrow{8}$	$\text{CH}_3 + \text{SiH}_3$	<u>0.01</u>	<u>0.00</u>
	total	1.03	<1.23 (1.00)

not important. Steps one to four can be considered as special cases of one type of cleavage while steps five to eight can be considered as special cases of another type of cleavage. It is obvious that increasing photonic energy increases the relative importance of polyfragmentation.

Unpublished work from this laboratory on the iodine lamp photolysis of monomethylsilane (95) is in keeping with the above results, but with differences reflecting the decrease in photon energy. Polyfragmentation decreased and single bond homolysis increased at the expense of molecular elimination.

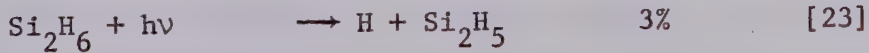
The final member of this series, tetramethylsilane, is currently being studied with the xenon lamp (96). Preliminary results can be summarized as follows. Methane and ethane account for nearly two-thirds of the products. Hydrogen is less than seven per cent while the remaining is made up of fourteen other products with trimethylsilane being about one-half of this. The nature of the products could best be explained by the almost exclusive formation of diradicals in the primary step and their subsequent polymerization since silylene insertion into Si-C or C-H bonds is much less favoured than insertion into Si-H bonds.

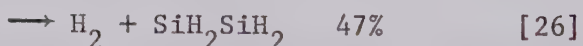
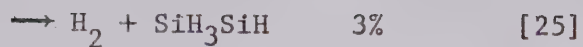
An attempt at the solid phase photolysis of dimethylsilane (96) with a xenon lamp led to unmeasurably small product yields due to monolayer absorption and geminate recombination.

A preliminary study of the photolysis of monosilane (97) by a xenon lamp has shown that silylene formation is the primary mode of decomposition. Photolysis of equimolar quantitites of SiH_4 and

SiD_4 lead to some HD formation but it is thought to arise from the decomposition of hot insertion products and not from H or D atom abstraction. The lack of $\text{Si}_2\text{H}_3\text{D}_3$ formation is the strongest argument against silyl radical formation. This fact by itself, however, is not valid evidence for the primary silylene mechanism because it has been shown (57) that silyl radicals do not recombine but instead disproportionate to give monosilane and silylene which would give rise to the products detected. The vibrationally hot disilanes can be pressure stabilized or undergo decomposition to give various isotopic hydrogen species and the appropriate silane fragment which can undergo further reaction with the substrate or polymerize. The pyrolysis of monosilane, as discussed previously, proceeds by the formation of silylene in the primary step and hence the mechanism for the photolysis as given above is probably correct. However, product analysis alone is not adequate to determine a mechanism in silane chemistry and the mechanism proposed by Ring et al. (97), for the photolysis of monosilane has to be considered tentative until a complete kinetic study is done.

The direct photolysis of disilane (94) has been carried out by a low pressure mercury arc and the results are more in keeping with the photolysis of monomethylsilane (90,91) than with monosilane (97). It was necessary to postulate five primary steps with molecular elimination predominating over single bond homolysis. The primary steps and their relative importance are given below:





The photolysis of perdueterodisilane yielded greater amounts of monosilane than hydrogen, while the reverse was true for disilane itself. Trisilane and tetrasilane were formed in secondary reactions. The primary mode of molecular hydrogen formation is via 1,2 cleavage rather than 1,1 cleavage which is in contrast to ethane and the hydrocarbons in general (98). The 1,2 diradical does not abstract from substrate or undergo other reactions to give detectable products, but rather, it acts as the polymer precursor. Unlike ethylidene (98), disilylene does not undergo unimolecular isomerization but inserts into the substrate as does silylene. The major secondary reactions of the radicals are the same as previously discussed in the mercury photosensitization of disilane.

In summary, it can be concluded that while triplet mercury sensitization in general is a good source of silyl radicals, the direct photolysis of silanes provides an excellent source of the divalent silicon radicals - silylenes, the silicon analogs of carbenes. The silylenes, such as silylene itself, silylsilylene and methyl-silylene undergo insertion reactions with the silicon-hydrogen bond but not with the carbon-hydrogen bond.

The direct photolysis of silicon hydrides is a complex process which is characterized by the occurrence of numerous parallel

primary modes of decomposition: molecular eliminations, free radical splits and polyfragmentations. On the whole, the photolytic behavior of silicon hydrides resembles that of the paraffins with some significant differences originating from the characteristic differences between the physico-chemical properties of the carbon and silicon atoms.

B. Vacuum Ultraviolet Photochemistry

The preceding sections have given us a fairly lucid picture of the physical chemistry of the simple silanes. It is obvious however, that the photochemistry of these compounds is sparse and somewhat tentative. Since all the simple monosilanes absorb below 2000\AA (92,93), their study could only be undertaken with the advent and development of vacuum ultraviolet techniques. The vacuum ultraviolet photolysis of the simple hydrocarbons has done much to further our understanding of the interaction of photonic energy with molecules and it was felt that similar studies on silanes would be fruitful. Since the results of these studies are to be compared and contrasted to the already existing body of information on the direct photolysis of paraffins in the vacuum ultraviolet, it would seem useful and necessary to discuss this information and its significance. A thorough discussion of the experimental methods of vacuum ultraviolet photochemistry will appear in another chapter.

There have been many recent reviews (98-106) of the chemistry

associated with the vacuum ultraviolet region and hence a comprehensive survey will not be undertaken here. This short review will be concerned only with the most recent work directly relevant to the object of this thesis study.

1. Carbon Dioxide

The photochemistry of carbon dioxide has been the object of much study due to its use as a chemical actinometer and its role in planetary atmospheres. Early work by Groth (107) and later by Mahan (108) established that the main products of the photolysis were oxygen and carbon monoxide. Evidence was found for ozone formation but it could not be measured quantitatively. The initial step in the mechanism was shown to be dissociation of the excited substrate molecule to form carbon monoxide and an oxygen atom. This step is in keeping with the spectroscopy of carbon dioxide in that the spectrum is essentially a continuum (109). Depending on the wavelength of light used for irradiation, it is possible to generate various species of carbon monoxide and atomic oxygen. In the vacuum ultraviolet region, however, only ground state carbon monoxide is formed. Below 1650 \AA the oxygen atom is formed in the ^1D state and below 1273 \AA , it is formed in the ^1S state as well (110). The fate of the ^1D or ^1S atoms is thought to be deactivation to the ground ^3P state and subsequent recombination to form molecular oxygen which in turn could act as a sink for ozone formation. The quantum yield of carbon monoxide formation was found to be near unity at both 1470 \AA and 1236 \AA . This mechanism would mean that the ratio O_2/CO should equal 0.5

whereas values ranging from 0 - ~0.5 were obtained experimentally.

The low values found were explained by ozone formation.

Katakis and Taube (111) suggested that the low O_2/CO ratio could be explained by the $O(^1D)$ atom reacting with substrate to form CO_3 . The carbon trioxide molecule could diffuse to the wall and form solid carbonate products and thus result in a reduced O_2 yield. The time dependence (112), pressure dependence (113), temperature dependence (114) and surface effects (113) of the O_2/CO ratio have been attributed to the CO_3 molecule. Spectroscopic evidence for CO_3 formation was provided by Jacox and Milligan (115) who photolyzed CO_2 at 77°K. Sach (116) photolyzed CO_2 in the presence of ^{14}CO and apparently found evidence for CO_3 oxidation of carbon monoxide. Also, some of these authors found values of $\phi(CO)$ ranging from 0.25 to 2.0.

Slanger and Black in 1971 (117) examined the carbon dioxide problem in detail and showed that the quantum yield of carbon monoxide formation is indeed unity. It was also shown that each photon absorbed produced an $O(^3P)$ atom and thus the $CO_3 + CO$ oxidation reaction cannot explain the anomalies of the carbon dioxide photolysis. In keeping with this result, Ausloos (106) has suggested that $O(^3P)$ could arise from the dissociation of CO_3 . That is, deactivation of $O(^1D)$ atoms is not a simple quenching process but, rather, involves a short-lived intermediate. Both authors (106,117) attribute the low yield of oxygen to $O(^3P)$ atom adsorption on the cell walls.

The most recent work on the CO_2 photolysis problem by Cvetanović (118) has shown that ozone is the species responsible for the discordant results in the literature. It was shown that the

photolysis of water acts as a catalyst for the decomposition of ozone and that pressure and surface effects are important. Material balance could be obtained from the yields of CO, O₂ and O₃.

2. Alkanes

The vacuum ultraviolet photochemistry of the simple alkanes has been widely studied and much relevant and valuable information concerning the decomposition of highly excited molecules has been gained. The absorption spectra of methane, ethane, propane, and n-butane were first measured by Okabe and Becker (119) under low resolution with a single beam instrument. Subsequent to this, more detailed results have been obtained on all the normal paraffin hydrocarbons from C₁ to C₈ as well as some branched chain paraffins by Sandorfy and co-workers (120-123). The absorption spectra are broad and continuous over the region studied with very little structure. The ethane spectrum is the most interesting in that it has a broad, slightly structured band around 1300^oÅ. The generally structureless features of the spectra would indicate that the excited states are essentially repulsive (although the existence of many close-lying electronic states, the large number of rotational isomers and the increasing number of totally symmetrical vibrations could contribute to the structureless features) with very short lifetimes, however, ethane would be expected to have a longer lifetime due to its greater structure. The onset of absorption increases with increasing complexity of the molecule. Methane photolysis cannot be effected by the xenon lamp ($\lambda = 1470\text{Å}$) but lies well within the region of the

krypton lamp, ($\lambda = 1236\text{\AA}$) while all other paraffins can be photolyzed by both lamp systems. Since the absorption is strong throughout the spectral region, the transitions are allowed and the excited states are probably singlets. Near the onsets, deuterated and non-deuterated species can have significantly different extinction coefficients. However, in the spectral region of the xenon and krypton lamp, the differences in extinction coefficients are not so important. The strong absorption of the molecules makes photochemical study facile, in that large enough product yields can be obtained in reasonably short periods of time.

Photolysis of the simple alkanes in the vacuum ultraviolet leads to decomposition with a quantum yield of essentially unity. Although fluorescence has been observed for n-pentane, its quantum yield is of the order of 6×10^{-5} (124) and is therefore negligible. Efficient photochemical decomposition of the substrate molecule in this region does not, however, simplify the mechanistic evaluation, since the energy available usually greatly exceeds that required. The initial steps in the photolysis are usually single bond cleavage to form two radicals, or molecular elimination from a neutral excited molecule to leave a diradical. Formation of three or more fragments in the primary step is unlikely because such an efficient randomization and simultaneous accumulation of energy in two or more bonds is not very probable. Mechanistic derivation may indicate such decomposition at first glance but it is more likely that there is secondary decomposition of the vibrationally excited fragment left behind after the primary decomposition. The excess photonic energy available

in vacuum ultraviolet photolysis studies means that there are usually several parallel primary steps, many of which can lead to secondary decompositions. All the species thus formed, excluding molecular products, can undergo further reactions leading to final measureable products. The unravelling of this complex process is difficult and it is sometimes impossible to unambiguously establish all the steps in the mechanism. In the vacuum ultraviolet study of the simple hydrocarbons, the task is made conceptually easier, in that all the fragments can be identified in the form of material balance. In similar studies on silanes however, there are additional complications, in that many of the silane fragments polymerize.

The main techniques used in elucidating the mechanistic details of these systems are: pressure studies; time studies; addition of scavengers such as nitric oxide, olefins, and hydrogen sulfide; selective deuterium labeling; addition of large excesses of inert foreign gases; and wavelength studies. It should be emphasized that most of the molecules studied have been in the gas phase. Liquid and solid phase studies are sparse indeed, mainly because of the additional complicating factors of geminate combination and disproportionation. Probably the single most powerful tool used in vacuum ultraviolet studies has been selective deuterium labeling. This method introduces a decomposition isotope effect into the system being studied. This phenomenon is quite important in the photolysis of monomethylsilane and dimethylsilane and will be discussed in greater detail in another chapter.

(a) Ethane

The mechanism of the photochemical decomposition of ethane has been established by the efforts of several workers (125-133). The xenon, krypton and argon photolyses have shown that the primary mechanism consists of the following four steps.

(i) Molecular loss of hydrogen by either a 1,1 or a 1,2 cleavage.

(ii) Single atomic hydrogen loss to yield an excited ethyl radical which loses another hydrogen atom to yield ethylene.

(iii) Carbon-carbon cleavage to form molecular methane and methylene.

(iv) Carbon-carbon cleavage to form two methyl radicals.

In the argon lamp photolysis there was a small (5%) additional process of ionization. Process (i) decreased with increasing energy, processes (ii) and (iv) increased and process (iii) went through a maximum. There are two types of processes operative in the system; direct bond cleavages (processes (ii) and (iv)) and rearrangement molecular cleavages (processes (i) and (iii)). Direct bond cleavages account for 13% of the mechanism at 8.4 ev (Xe), 38% at 10.0 ev (Kr) and 56% at 11.6 - 11.8 ev (Ar). Thus at higher energies, the excited molecule has a shorter lifetime and hence is less susceptible to a rearrangement process.

The ethylidene produced in process (i) does not insert into the substrate but rather, undergoes unimolecular isomerization to form a vibrationally hot ethylene molecule which can lose hydrogen to yield

acetylene as the final product. The ethylene produced by the 1,2 molecular loss of hydrogen does not, however, undergo further decomposition. Ethyl radical formation is not operative because of the excess energy left behind in the species after single bond homolysis and the driving force of double bond formation. The resulting ethylene from process (ii) does not decompose further. The methylene diradical inserts into substrate to yield an excited propane molecule which can decompose to yield methyl and ethyl radicals. The hydrogen atoms can abstract from substrate or add to ethylene to yield ethyl radicals which can recombine or disproportionate, and methyl and ethyl radicals can recombine to give propane.

The xenon sensitized decomposition of ethane has been carried out by Bünau and co-workers (134). The same products were formed as in the direct photolysis but in different amounts. Overall, xenon sensitization tends to enhance radical reactions at the expense of molecular reactions.

Tanaka and co-workers (135) applied the RRKM unimolecular decomposition theory to the energized ethylene formed in the 1470 \AA photolysis of ethane. The experimental rate constant was 1.01×10^9 sec $^{-1}$ while the calculated values from two assumed models were 0.33×10^9 sec $^{-1}$ and 1.21×10^9 sec $^{-1}$. It was not possible to choose between the rigid and semi-rigid models with the data available. However, the excellent agreement obtained testifies to how far our understanding of the vacuum ultraviolet photochemistry of ethane has progressed.

(b) Propane

The efforts of several workers (132,136-140) have established the five primary steps in the photolysis of propane.

(i) Two types of molecular hydrogen loss to form normal and iso-propylidenes.

(ii) Two types of atomic hydrogen loss to form normal and iso-propyl radicals, which lose an additional hydrogen atom.

(iii) Two types of methane loss to form either a 1,2 or a 1,3 diradical.

(iv) Carbon-carbon cleavage to form a methyl and an ethyl radical, which loses a hydrogen atom.

(v) Formation of methylene and an ethane molecule.

The normal and iso-propylidenes produced in step (i) do not react with substrate but rather, undergo unimolecular isomerization to form propylene which can decompose further. The reactions of the other radicals are in keeping with the previous discussion on ethane photolysis.

Ausloos and Lias (139) carried out the argon lamp photolysis (11.6 - 11.8 ev) of propane and showed that the ionization quantum yield is approximately 0.25. Hence, mechanistic elucidation at these energies must take into consideration ionic reactions as well. We need not worry about ionic reactions in the xenon and krypton lamp photolysis because the ionization potential of propane, 11.2 ev (139), is well above the 8.4 ev energy of the xenon lamp and the 10.0 ev energy of the krypton lamp.

The primary quantum yields for the xenon and krypton lamp

photolysis of propane were reported by Tanaka and co-workers (141) in 1971. The five primary steps and their quantum yields are given below at the two wavelengths studied.

		<u>Xe</u>	<u>Kr</u>	
C_3H_8^*	$\rightarrow \text{H}_2 + \text{C}_3\text{H}_6$	0.67	0.32	[28]
	$\rightarrow \text{H} + \text{C}_3\text{H}_7^*$	}		[29]
	$\rightarrow \text{CH}_2 + \text{C}_2\text{H}_6^*$	0.05	0.10	[30]
	$\rightarrow \text{CH}_3 + \text{C}_2\text{H}_5^*$	0.17	0.43	[31]
	$\rightarrow \text{CH}_4 + \text{C}_2\text{H}_4$	0.11	0.15	[32]

The C_3H_7^* and C_2H_5^* radicals undergo further hydrogen loss to give the following two apparent primary steps.



Subsequent reactions are in keeping with the results presented previously. It was not possible to determine the relative amounts of molecular and atomic hydrogen loss. However, one would suspect, on the basis of previous results on the photolysis of ethane, that atomic hydrogen loss would increase with respect to molecular hydrogen loss with increasing photonic energy. This would be due to the shorter lifetime of the excited state with increased photon energy, not allowing for a rearrangement mechanism. Although this rationalization seems quite sound in explaining hydrogen loss, it cannot explain the increased methylene and methane yields. The theoretical aspects of these hydrocarbon systems are not well enough understood to adequately explain all aspects of the mechanism.

Unimolecular decomposition theory, RRKM, has been applied to propane as it has to ethane (135). As before, rigid and semi-rigid models were considered for the activated complex. The experimental rate constant for decomposition was found to be $1.78 \times 10^9 \text{ sec}^{-1}$ while the calculated value from one model was $1.00 \times 10^9 \text{ sec}^{-1}$ and from the other, $2.90 \times 10^9 \text{ sec}^{-1}$.

3. Theoretical Considerations

Although attempts at understanding the photochemical decomposition of molecules in the vacuum ultraviolet have been undertaken, they have not been overly successful. In fact, the treatments would have to be considered as qualitative rationalizations. If we take ethane as an example, we could explain the molecular loss of hydrogen by saying that in the excited state the carbon-hydrogen bonds are in an anti-bonding configuration and the hydrogen-hydrogen bonds are in a bonding configuration.

One of the first attempts at understanding the experimental findings on the photolysis of the simple alkanes was done by Peters (142). In the case of ethane it was felt that 1,1 and 1,2 molecular elimination of hydrogen occurred from the same excited state as atomic loss of hydrogen, while methyl and methylene radical formation occurred from different states.

Since methane is the simplest hydrocarbon, it has received a significant amount of theoretical consideration. Karplus and Bersohn (143) showed that atomic loss of hydrogen should be favoured over molecular loss of hydrogen, while Lindholm (144) feels that molecular loss is more important. In actual fact

the two primary processes are about equal (106).

The interpretation of the absorption spectra (120-123) of the simple hydrocarbons in theoretical terms is somewhat rudimentary at best. It has been suggested by Raymonda and Simpson (145) that there are two types of (σ, σ^*) transitions in the hydrocarbons. In the longer wavelength region, there is a promotion of a (C-C) σ bonding electron to an upper state, and in the shorter wavelength region there is a promotion of a (C-H) σ bonding electron to an upper state. Hence we should get more carbon-carbon bond cleavage at longer wavelength photolysis than carbon-hydrogen cleavage. The opposite would be true at shorter wavelengths. The previous discussion, however, shows that this is not the case. That is, absorption in one moiety of a saturated hydride molecule can lead to rupture of other bonds in the molecule. This is a clear indication that we are dealing with strongly delocalized orbitals in the excited state.

Lombos et al. (120-123) measured the absorption spectra of the simple alkanes and carried out Pariser-Parr calculations on methane, ethane and propane. Obi et al. (141) used the wavefunctions thus derived to obtain the bond orders corresponding to the allowed transitions in ethane. The experimental results are in excellent agreement with the bond orders derived at the five transitions. However, the experimental and theoretical findings are not in agreement in the case of propane. Work on the higher alkanes was not done due to the absence of reliable wavefunctions. It is obvious that much theoretical work remains to be done before a thorough understanding of the photochemistry of paraffins is achieved.

C. Present Investigation

The only previous study published in the literature on the photochemistry of methylated silanes was carried out in this laboratory (90,91). As a continuation and extension of this program, a study of the xenon lamp photolysis of dimethylsilane was undertaken in the present research. The principal aim was to examine the effect of the presence of an additional methyl group in the molecule on the primary step and to investigate the chemistry of the various new intermediate radicals produced in the decomposition sequence.

In the course of this work, it became necessary to study the reactions of hydrogen atoms with silanes. Hence the photolysis of hydrogen sulphide in the presence of dimethylsilane was done, and the subsequent kinetic data were incorporated into the dimethylsilane system. The vacuum ultraviolet spectra of all the simple methylated silanes and their deuterated counterparts were recorded, in order to correlate with the photolysis work.

It was also anticipated that this detailed examination of the photobehaviour of dimethylsilane, coupled with auxiliary studies from this laboratory on other silane systems and others from the literature, would lead to a more thorough understanding and revision of the photodecomposition of monomethylsilane.

Since this work complements and extends the earlier data on the vacuum ultraviolet photolysis of monomethylsilane, it was hoped that some trends could be established with the hydrocarbon series.

CHAPTER II

EXPERIMENTAL

1. Vacuum System

Two conventional vacuum systems were employed for the study. The actual photolyses were carried out in a grease-free vacuum system pumped by a two-stage mercury diffusion pump, backed by a Welsh Duo Seal oil rotary pump. Delmar mercury float valves and Hoke metal diaphragm valves (numbers TY440, C413K, and C415K) were used. The system was capable of achieving pressures of 10^{-6} torr of foreign gas, although the vapour pressure of mercury in the system was of the order of 10^{-3} torr. Pressures were measured with a MacLeod gauge and a constant volume mercury manometer. Gas transfers and distillations were followed on a Pirani Vacuum Gauge (Consolidated Vacuum Corporation type GP-140) using Pirani tubes as the sensing head (number GP-001). Samples could be introduced to the attached gas chromatograph via a Toepler pump and gas burette assembly or directly from the system. A three stage trapping assembly could be used in conjunction with the gas chromatograph for preparative purification or product separation. A low pressure system was used to operate the float valves, manometer and Toepler pump.

The second vacuum system was mercury free and was used to prepare the vacuum ultraviolet photolysis lamps. It was pumped by a three stage oil diffusion pump (Octoil S oil) and backed by a Welsh

Duo Seal rotary pump. Greased stopcocks (Apiezon N grease) and Hoke (type 425106 Y-316-SS) were used. Pirani Vacuum Gauge and tubes and an oil manometer (silicon oil DC200) were used to measure pressures.

2. Vacuum Ultraviolet Techniques

There are many recent reviews (98,101,146,147) of vacuum ultraviolet techniques available. Hence only a short review will be given here.

(a) Lamps

There have been two types of light sources employed in the vacuum ultraviolet. The continuum lamp such as hydrogen (148) or a rare gas (149,150) discharge at a pressure of a few hundred torr have been used in conjunction with a vacuum monochromator to obtain monochromatic light sources. The poor efficiency of monochromators in the vacuum ultraviolet means that it is difficult to obtain high enough intensity for meaningful product yields. The most practical light sources should have enough intensity so as to create several micromoles of product in a relatively short period of time.

The second, and by far the best source of vacuum ultraviolet light has been the rare gas resonance lamps. There are many reasons for their wide popularity.

(i) High intensity is quite easily obtained, lamp outputs of 10^{15} - 10^{16} quanta/sec are quite common.

(ii) Most of the lamps have a high degree of monochromatic purity; in some cases, krypton lamps for example, the use of

appropriate window material will absorb an interfering resonance line.

(iii) Due to the monochromatic nature of the emission, it is possible to define exactly how much energy is absorbed by the molecule under study. The use of several different lamps emitting their own distinct lines makes a wavelength study possible which in turn can yield much valuable information on the dissociation of highly excited molecules.

(iv) It is possible to carry out photolysis studies without the interference of ionization; in turn it is possible to carry out a selected ionization that can yield information that is pertinent to radiolysis work.

(v) Ease of operation makes their use particularly attractive.

(vi) It is possible to add quenchers and scavengers such that a particular lamp will not photolyze them but can decompose the substrate.

The main lamps used in the vacuum ultraviolet and their emission lines are given in Table II-I. The emission lines of the halogen lamps are listed in Table II-II. The relative intensities vary somewhat with halogen pressure. The main emission line of the xenon lamp is 1470\AA with the line at 1295\AA being about 2% of that at 1470\AA . The 1165\AA line of the krypton lamp is 28% of the 1236\AA line. The 1067\AA and 1048\AA lines in the argon lamp are about equal in intensity.

Electrode discharge halogen lamps were first developed by Harteck and co-workers (151,152). Their ease of use has been greatly

TABLE II-I
Wavelengths of Atomic Emission Lines Used in
Vacuum Ultraviolet Photochemistry

Light Source	Emission lines ° Å
Iodine	2062, 1876-1783
Low Pressure Mercury	1849
Bromine	1634, 1583-1450
Xenon	1470, 1295
Krypton	1236, 1165
Hydrogen	1216
Argon	1067, 1048
Neon	744, 736
Helium	584

TABLE II-II
Wavelengths of Emission Lines of Halogen Lamps^a

Iodine Lamp ^b		Bromine Lamp ^c	
Wavelength Å	Relative Intensity	Wavelength Å	Relative Intensity
2062	100	1634	100
1876	16	1583	36
1845	13	1577*, 1575	65
1830*	21	1541*	71
1799	14	1532	25
1783*	33	1489*	29
1702	4	1450*	5
1642*	2		
1618*	1		

^a K. Obi, Ph.D. Thesis, Tokyo Institute of Technology (1966).

^b Iodine pressure 40 microns.

^c Bromine pressure 50 microns

* Resonance line.

facilitated by modification to microwave discharge (153,154). Loucks and Cvetanović (118) have recently reported a spherical bromine lamp of fairly high intensity. Iodine lamps can be used with a quartz window and bromine lamps with a sapphire window. The relative output of both lamps can be adjusted by the use of an appropriate refrigerant around the cold finger because the relative intensities of the lamps are pressure dependent.

The rare gas resonance lamps can be operated at room temperature if a getter (Ba-Al-Ni alloy) is used. In the absence of a getter, a refrigerant such as liquid oxygen would suffice. However, the potential danger associated with the use of liquid oxygen makes the use of getters somewhat obvious. The best resonance lamps are achieved by having a 5 - 10 times excess of carrier gas such as neon or helium over the emitting gas (xenon, krypton or argon); the total pressure should be in the 1 - 2 torr range. The hydrogen Lyman α lamp can be made the same way using argon as the carrier gas (155, 156).

(b) Window Materials

Window materials through which the photon must be propagated are an important consideration and a restricting requirement in vacuum ultraviolet photochemical studies. The materials most commonly used in vacuum ultraviolet photochemistry are listed in Table II-III along with the approximate onset for 10% transmission. These low wavelength transmittance cutoffs shift to the red with increasing temperature (157).

Quartz is the most suitable window material for photochemical

TABLE II-III

Approximate Wavelength Limits for Transmission of Various
Optical Materials in the Vacuum Ultraviolet^a

Material	Thickness (mm)	Wavelength (Å) for 10% transmission
LiF	1	1050
LiF (x-rayed)	1	1200
CaF ₂ (synthetic)	3	1220
Sapphire (synthetic)	0.5	1425
Suprasil	1	1550
Quartz, clear fused	10	1720
Quartz, crystal	10	1860

^a H. Friedman, in J. A. Ratcliffe, ed., Physics of the Upper Atmosphere, Academic Press, New York, 1960, p. 160. J. G. Calvert and J. N. Pitts, Jr., Photochemistry, John Wiley & Sons, Inc., New York, 1966, p. 748.

experiments at wavelengths longer than the 1700-1800 \AA region. Suprasil, a synthetic quartz, is transparent down to 1550 \AA . These materials are convenient to use because they can be attached directly to quartz reaction vessels. Synthetic sapphire can be used for experiments at wavelengths as short as 1450 \AA and it is possible to make a graded seal to pyrex (158). This seal is capable of withstanding a temperature range of 77 - 700 $^{\circ}\text{K}$ and like a quartz to quartz seal, it is quite resistant to thermal shock. Sapphire has the added advantage of being able to selectively transmit the 1470 \AA line of the xenon resonance lamp and cutting off the 1295 \AA resonance line.

Synthetic calcium fluoride is transparent down to 1220 \AA and has the merit of being able to absorb the 1165 \AA resonance line of the krypton lamp and transmitting the more intense 1236 \AA line. Lithium fluoride has the shortest wavelength cutoff (1050 \AA) of the readily available optical materials. It can transmit the 1067 \AA resonance line of the argon lamp and the hydrogen Lyman α (1216 \AA) line as well as the longer wavelengths of the xenon and krypton lamps. The most convenient way of sealing CaF_2 and LiF to the lamp is by means of black wax. This method, however, restricts the temperature range of the lamp to ambient temperature. It is possible to affix LiF to pyrex by means of a $\text{LiF} - \text{AgCl} - \text{Ag} - \text{AgCl} - \text{Pyrex}$ seal (98) which is capable of withstanding temperature up to 673 $^{\circ}\text{K}$. During such low wavelength irradiation, an F-center is formed in the LiF window, which decreases the transparency and hence the lifetime of the lamps are in the order of 10 - 20 hours.

Below the lithium fluoride cutoff, there is a tremendous increase in experimental difficulty. The two methods used in this region are differential pumping in windowless systems, and thin films. For example, Back and Walker (159) derived an intensity of 3×10^{14} quanta/sec at 584\AA by using the differential pumping technique. Rebbert and Ausloos (160) obtained an intensity of 10^{13} quanta/sec by employing a thin aluminium film ($2000 - 4000\text{\AA}$ thick) attached to a fine mesh backing. This window was leak-free and capable of withstanding a pressure differential of 25 torr. Thin silicon oxide films are transparent to wavelengths shorter than 1000\AA but are very fragile. A very thorough discussion of window materials is available (161).

3. Photolysis System

Two different cells were used in the various stages of the work and all runs were carried out under static conditions.

(a) A cylindrical Pyrex reaction cell 22 mm in diameter and 190 mm in length with a volume of 99 cc including cold finger and valve attachment was used in the xenon resonance lamp photolysis of dimethylsilane. It had a single lithium fluoride window, 28 mm in diameter and 2 mm thick, and was affixed to the cell by means of black wax (Apiezon W). The window was polished after each run with Cerium Oxide (Optical Equipment Company) to remove the polymer formed on the surface. The window of the lamp was placed in contact with the entrance window of the cell and surrounded with a column of flowing nitrogen gas in order to remove oxygen which would strongly

absorb the emitted radiation.

(b) A cylindrical quartz reaction cell, 36 mm in diameter and 150 mm in length with a volume of 166 cc including cold finger and valve attachment was used in the photolysis of hydrogen sulphide in the presence of dimethylsilane. It was equipped with 2 mm thick quartz windows. The cell could be easily baked with a hand torch.

The xenon lamp was a cylindrical Pyrex vessel, 22 mm in diameter and 175 mm in length. A 2 mm thick by 28 mm in diameter lithium fluoride window was attached to one end by means of black wax (Apiezon W). A barium (Ba-Al-Ni alloy) getter (Kemet Division, Union Carbide) was imbedded through the bottom of the cold finger. The lamp was connected to the mercury free Pyrex vacuum system by means of a graded seal and evacuated for several days during which time it was frequently baked with a hand torch. The lamp was filled to a pressure of about ten torr with neon and the system discharged by a 2450-Mc/sec Hg 198 Microwave Exciter (Baird-Atomic Inc.) operated at 15% power through a V-shaped antenna which was kept from one to two mm from the lamp surface. This was done to remove residual absorbed oxygen and water on the lamp surface that would lead to spectral impurities. When significant amounts of impurities are present, the neon would not discharge for more than a few minutes. The initial bright scarlet colour quickly became pink and the discharge ceased. When the lamp was thoroughly purged, the neon discharge remained bright scarlet for several hours. The barium getter was heated by means of a rheostat (1-2 volts) to degas the metal. When the lamp was thoroughly purged, the barium getter was melted (4-5 volts) and

a barium mirror formed on the lower part of the cold finger. This barium mirror would absorb water discharged off the lamp walls during use. The lamp was then filled with 0.2 - 0.3 torr of xenon and 1.5 - 2.0 torr of neon as carrier gas. The lamp was sealed off with a hand torch and removed from the system. The lamp was operated at ambient temperature with 15 - 20% power from the microwave generator. The main emission line of the xenon lamp was 1470 \AA . During the course of the work, several xenon lamps were used as they have a tendency to deteriorate after about ten hours of use. All the vacuum ultraviolet lamps require the use of a tessla coil to initiate the discharge. Carbon dioxide was used as an actinometer taking $\phi(\text{CO}) = 1.0$. The pressure of CO_2 was 100 mm, the photolysis time was 5 min. and the ratio O_2/CO equaled 0.348. A more thorough discussion of vacuum ultraviolet techniques will be given later.

The cadmium lamp was a commercial model manufactured by George Gates and Company. It was operated at 1.5 volts and the main emission line was 2288 \AA . A Pyrex sleeve was used to cut out the 2288 \AA line and only allow the next strongest 3261 \AA line. A ten to fifteen minutes warm-up period was required for steady operation of the lamp.

A medium pressure mercury arc, Hanovia Type 30620 was also used. The lines around 2800 \AA , 2650 \AA and 1950-2050 \AA were used for various experiments; a 20 - 30 minutes warm-up period was employed. In both the cadmium and the mercury lamps, provision was made for the use of cutoff filters, interference filters and neutral density filters.

4. Materials

The materials used, their source, and their purification are given in Table II-IV.

5. Analytical System

The main analytical method used in the study was gas chromatography. Both separation and identification of compounds were routinely carried out. Two types of gas chromatography were employed; (a) thermal conductivity and (b) flame ionization.

(a) The thermal conductivity gas chromatograph was a component type that was coupled directly to the high vacuum system. The detector was a Gow-Mac TR-11-B operated at 140°C. The power supply was a Gow-Mac 9999C and the results were read out on a Sargent model RS recorder. The power supply control unit was operated at 140 ma when argon was the carrier gas and at 250 ma when helium was the carrier gas. The gases were passed through a column of molecular sieves 13x and the single stream flow rate was controlled by an Edwards needle valve. This detector was used only to measure non-condensable (-196°C) gases. Relative response factors were determined. These gases were measured in the gas burette and a portion thereof was transferred to the evacuated sample loop of the G.C. from which it was introduced to the column. The columns used, the conditions of use, and the compounds analyzed are given in Table II-V.

(b) The flame ionization chromatograph used for the dimethyl-silane photolysis work was a Hewlett-Packard model 5750. Results were

TABLE II-IV

Materials Used

Material	Supplier	Purification
CH_3SiH_3	Merck, Sharpe, and Dohme	Degassed at -196°C Distilled at -130°C
CH_3SiD_3	Merck, Sharpe, and Dohme	Degassed at -196°C Distilled at -130°C
$(\text{CH}_3)_2\text{SiH}_2$	Peninsular ChemResearch	Degassed at -196°C Distilled at -130°C
$(\text{CH}_3)_2\text{SiD}_2$	Merck, Sharpe, and Dohme	Degassed at -196°C Distilled at -130°C
$(\text{CH}_3)_3\text{SiH}$	Chemical Procurement	Degassed at -196°C Distilled at -112°C
$(\text{CH}_3)_3\text{SiD}$	Merck, Sharpe, and Dohme	Degassed at -196°C Distilled at -112°C
$(\text{CH}_3)_3\text{SiF}$	Peninsular ChemResearch	Degassed at -196°C Distilled at -112°C
$(\text{CH}_3)_4\text{Si}$	Aldrich Chemical Co.	Degassed at -196°C Distilled at -98°C
$(\text{CH}_3)_3\text{SiSi}(\text{CH}_3)_3$	Pierce Chemical Co.	Degassed at -196°C
CH_4	Phillips Petroleum Co.	Degassed at -196°C
C_2H_6	Phillips Petroleum Co.	Degassed at -196°C
C_3H_8	Phillips Petroleum Co.	Degassed at -196°C
$n\text{-C}_4\text{H}_{10}$	Phillips Petroleum Co.	Degassed at -196°C
C_2H_4	Phillips Petroleum Co.	Degassed at -196°C
C_2D_4	Merck, Sharpe, and Dohme	Degassed at -196°C
C_2H_2	Matheson	Degassed at -196°C
H_2S	Matheson	Degassed at -196°C
D_2S	Merck, Sharpe, and Dohme	Degassed at -196°C
COS	Matheson	Passed through sodium hydroxide and lead acetate solutions and then through a drierite column. Degassed at -196°C

TABLE II-IV (cont'd)

Materials Used

Material	Supplier	Purification
$(H_2CO)_x$	Shawinigan	Degassed at ambient temperature. Heated with hand torch to form H_2CO vapor.
CO_2	Airco	Assayed Reagent
O_2	Airco	Assayed Reagent
CO	Airco	Assayed Reagent
H_2	Airco	Assayed Reagent
N_2	Airco	Assayed Reagent
NO	Matheson	Passed through soda lime trap at $-78^{\circ}C$ and P_2O_5 column at ambient temperature. Degassed at $-196^{\circ}C$ Distilled at $-186^{\circ}C$
Xe	Airco	Assayed Reagent
Kr	Airco	Assayed Reagent
Ne	Airco	Assayed Reagent
He	Canadian Liquid Air (for G.C.)	Passed through column of molecular sieves at ambient temperature
Ar	Union Carbide (for G.C.)	Passed through column of molecular sieves at ambient temperature
LiF	Harshaw	None

TABLE II-V
Thermal Conductivity G.L.C. Operating Conditions

Column	Flow Rate	Temperature	Construction	Compounds Analyzed
Silica Gel High Activity	30 cc/min He	room temperature	4 ft x 6 mm o.d. glass	CO_2
Molecular Sieve 13X, 45-60 mesh	30 cc/min He	room temperature	6 ft x 6 mm o.d. glass	O_2 , CO
Molecular Sieve 13X, 45-60 mesh	30 cc/min Ar	room temperature	6 ft x 6 mm o.d. glass	H_2 , CH_4 , N_2 , NO

displayed on a Sargent Model RS recorder. The carrier gas, helium, was passed through a column of molecular sieves 13x. The entire condensable (-196°C) reaction mixture, substrate plus products, was frozen into a Pyrex ampoule equipped with a Burrell Silicone rubber seal. The internal pressure was raised to atmospheric with helium introduced from a gas syringe and a sample was withdrawn with a syringe for injection onto the appropriate column. Relative response factors and linearity of the substrate were determined. The columns used, the conditions of use, and the compounds analyzed are given in Table II-VI.

6. Other Equipment

- (a) Mass spectra were determined on Associated Electronics Industries Model numbers MS2, MS9 and MS12.
- (b) Hydrogen isotope ratios were determined on an Associated Electronic Industries Model MS10. The response of the instrument to H₂, HD, and D₂ was checked periodically.
- (c) Nuclear Magnetic Resonance Spectra were obtained on a Varian 100 Mc machine. This instrument was used to check the isotopic purity of the deuterated silanes.
- (d) Ultraviolet spectra were determined on a Cary Model 14 spectrometer.
- (e) The flash photolysis-kinetic absorption spectroscopy apparatus has been described previously (162).
- (f) The flash photolysis-mass spectroscopy apparatus has been described previously (163).

TABLE II-VI

Flame Ionization G.I.C. Operating Conditions

Column	Flow Rate	Temperature	Construction	Compounds Analyzed
Silica Gel Medium Activity	50 cc/min He	50°C	12 ft x 1/4 in stainless steel	C_2H_6 , C_2H_4 , monomethylsilane dimethylsilane (DMS)
Silicon oil DC200, 10% on Chromsorb W.A.W. 60 - 80 mesh	50 cc/min He	70°C	16 ft x 1/4 in stainless steel	dimethylsilane (DMS) trimethylsilane (Tri-MS) methyllethylsilane (MES) 1,1-dimethylsilane (DMS) 1,1,2-trimethylsilane (Tri-MDS) 1,1,2,2-tetramethylsilane (Tet-MDS)
Tricresyl Phosphate, 10% on Chromsorb W 30 - 60 mesh	50 cc/min He	50°C	22 ft x 1/4 in stainless steel	Used for same compounds as silicon oil column above, but gave a better separation of Tri-MDS and Tet-MDS and a poorer separation of DMS and Tri-MS.

(g) Since there were no double beam recording vacuum ultraviolet spectrometers available at the University of Alberta, it was necessary to do this work elsewhere. The work was carried out in the Department of Chemistry at the University of New Brunswick, Fredericton, New Brunswick. The instrument used was a commercial Jarrell-Ash, one meter 15° Robin vacuum ultraviolet double beam spectrophotometer, with a spectral range of $1150^{\circ}\text{A} - 3600^{\circ}\text{A}$. A detailed description of this apparatus can be found in the literature (164). However, due to deteriorated MgF_2 optics the actual operative spectral range was $1350^{\circ}\text{A} - 2000^{\circ}\text{A}$. The light source was the continuum of a deuterium discharge lamp. Four centimeter cells with 2 mm thick LiF windows were used; the pressure range employed was 0.1 - 0.5 torr.

CHAPTER III

THE XENON RESONANCE LAMP PHOTOLYSIS
OF DIMETHYLSILANEA. Results - Photolysis

The direct photolysis of dimethylsilane by the xenon resonance lamp was studied as a function of substrate pressure, exposure time, and concentration of free radical scavengers nitric oxide and ethylene. The photolysis of dimethylsilane-d₂ and mixtures of dimethylsilane and dimethylsilane-d₂, were carried out in order to determine the nature of the primary processes. All runs were done at room temperature and under static conditions.

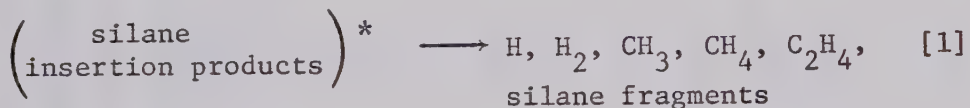
1. Products

The photolysis yielded ten products. In decreasing order of importance they were: hydrogen, 1,1,2-trimethyldisilane (Tri-MDS); methane; ethane; 1,1,2,2-tetramethyldisilane (Tet-MDS); trimethylsilane (Tri-MS); 1,1-dimethyldisilane (DMDS); monomethylsilane (MMS); methyleethylsilane (MES); and ethylene. Two other products detected in trace amounts, hereafter referred to as A and B, which could not be identified have been neglected in the kinetic treatment. A solid polymeric material formed during the photolysis was deposited on the cell walls and caused a decrease in the transparency of the LiF window.

2. Effect of Substrate Pressure

The effect of substrate pressure on product yields was studied in 16 min photolyses. The relative yields are given in Table III-I and are shown graphically in Figures III-1 and III-2 (with the exception of A and B).

The observed pressure dependence of C_2H_6 , C_2H_4 , CH_4 , H_2 , MES, Tri-MS, DMDS, Tri-MDS and Tet-MDS can be rationalized in terms of pressure stabilization of hot silane insertion products,



The silane fragments would presumably contribute to the formation of polymer.

MMS is unaffected by substrate pressure. It will be shown later that it is formed in a molecular process. To avoid complications due to pressure-dependent fragmentations, all subsequent experiments were conducted at a pressure of 100 torr or higher.

3. Effect of Exposure Time

A time study was carried out to determine the quantum yields because of increasing attenuation of the incident light intensity by the polymer deposition. Carbon dioxide actinometry was done before and after each run and $\phi(CO)$ was taken as 1.0 (Chapter I, section B-1). Light intensities were corrected to a constant initial photon input and a plot was made of post run intensity corrected vs time.

TABLE III-I

Relative Yield of Products as a Function of Pressure from the
Xenon Lamp Photolysis of Dimethylsilane

Relative Yield (Per cent)	Pressure (mm)						400.0		
	10.1	20.5	32.5	53.6	79.4	100.0			
H ₂	37.3	38.0	35.6	28.6	27.0	23.3	25.0	17.1	22.8
Tri-MDS	16.9	19.3	20.6	25.0	25.5	28.1	29.1	35.3	31.1
CH ₄	13.7	10.4	11.3	9.38	9.01	7.74	7.54	8.65	7.92
C ₂ H ₆	7.78	6.75	5.98	6.11	6.08	5.60	4.74	4.14	1.87
Tet-MDS	7.07	8.10	8.52	10.6	10.1	11.9	11.5	13.0	10.7
Tri-MS	7.46	7.40	8.10	9.57	10.6	11.6	10.5	11.2	14.3
DMDS	4.98	4.91	5.07	5.54	5.64	5.55	5.82	5.08	5.23
MMS	2.40	2.65	2.35	2.51	2.71	2.98	2.06	2.43	2.17
MES	0.83	0.87	1.13	1.41	1.72	1.79	1.94	1.79	2.46
C ₂ H ₄	0.64	0.59	0.39	0.37	0.29	0.24	0.21	0.12	0.031
A	0.68	0.76	0.82	0.82	1.03	0.91	1.16	1.09	1.08
B	0.25	0.17	0.14	0.14	0.30	0.31	0.39	0.20	0.32

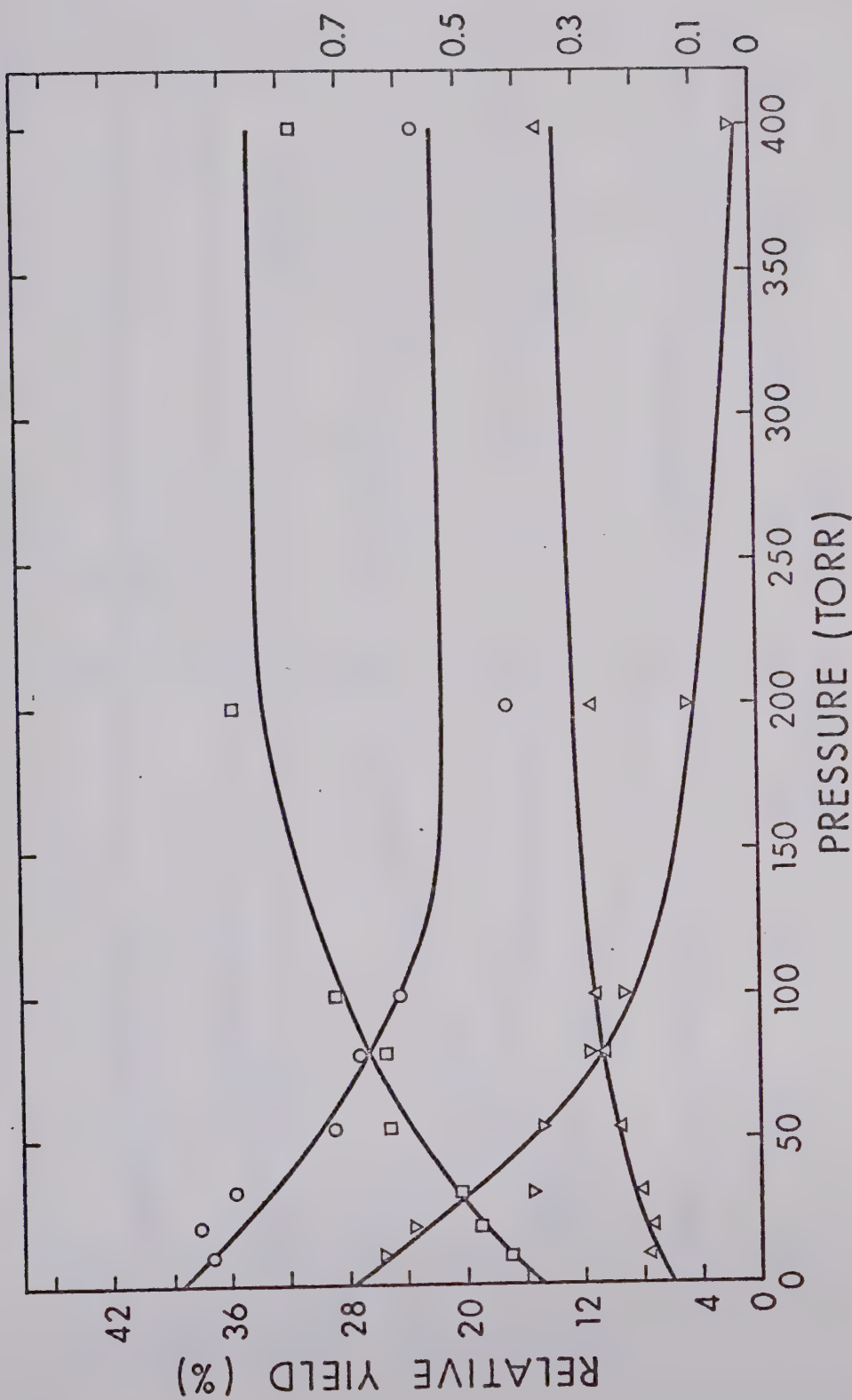


FIGURE III-1. Relative Yields of H_2 , Tri-MDS, Tri-MS and C_2H_4 as a Function of Pressure from the Xenon Lamp Photolysis of Dimethylsilsilane. $\circ \text{H}_2$ (L.H.S.), \square Tri-MDS (L.H.S.), Δ Tri-MS (L.H.S.), $\nabla \text{C}_2\text{H}_4$ (R.H.S.).

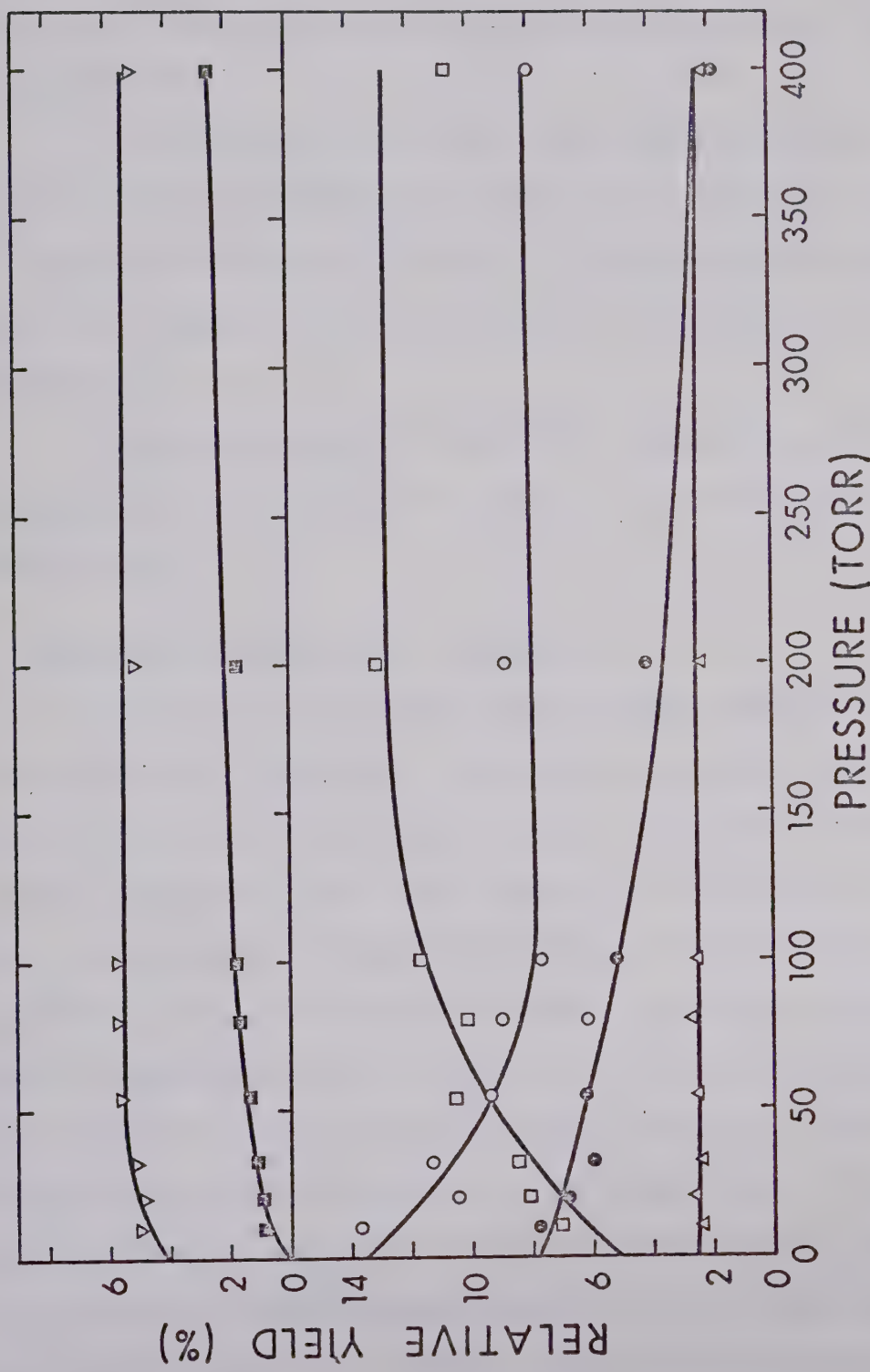


FIGURE III-2. Relative Yields of DMDS, MES, Tet-MDS, CH₄, C₂H₆ and MMS as a Function of Pressure from the Xenon Lamp Photolysis of Dimethylsilylane. ∇ DMDS, \blacksquare MES, \square Tet-MDS, \circ CH₄, \bullet C₂H₆, \triangle MMS.

This graph was integrated to yield the total photon input at any given time. The intensity measurements are given in Table III-II and Figure III-3.

The results of the quantum yield study are listed in Table III-III and are shown graphically in Figures III-4 and III-5 (with the exception of compounds A and B). A graphical extrapolation of the data to zero exposure time gave the quantum yield values listed in Table III-IV.

The results given in Table III-V show that the products are invariant with respect to exposure time and consequently they are of primary origin.

4. Effect of Nitric Oxide as a Scavenger

It has been shown in the mercury photosensitization of silanes (84) and in the direct photolysis of monomethylsilane (90,91) that nitric oxide is an efficient scavenger of monovalent silyl radicals. Silylenes on the other hand, are not affected by nitric oxide, hence relatively small concentrations of nitric oxide should suppress all radical recombination products. In order to differentiate products originating from monoradical and diradical precursors, experiments were carried out in the presence of a few torr of nitric oxide. The results are shown in Table III-VI and Figure III-6. As can be seen, 51% of the Tet-MDS, 83% of the Tri-MS, and 100% of the C_2H_6 are scavengeable. The unscavengeable Tet-MDS, Tri-MS, Tri-MDS, DMDS, MES must arise from insertion of various diradicals into the substrate. MMS was not scavengeable but it will be shown that this product

TABLE III-II
Intensity of the Xenon Lamp as a Function
of Time ($\times 10^{15}$, quanta/sec)

Time min	Pre Run Intensity Uncorrected	Post Run Intensity Uncorrected	Pre Run Intensity Corrected	Post Run Intensity Corrected	Total Intensity
1	5.47	2.99	6.00	3.28	273
1	8.10	4.24	6.00	3.14	273
1	7.96	5.24	6.00	3.95	273
2	5.32	3.86	6.00	4.35	486
2	6.23	3.86	6.00	3.72	486
3	6.98	3.24	6.00	2.78	669
5	5.47	4.05	6.00	4.44	954
5	5.43	2.49	6.00	2.76	954
5	4.49	1.63	6.00	2.17	954
5	7.85	2.25	6.00	1.72	954
5	7.48	2.54	6.00	2.04	954
10	5.43	2.68	6.00	2.97	1380
10	5.43	0.87	6.00	0.97	1380
10	4.49	0.94	6.00	1.26	1380
16	9.35	1.12	6.00	0.72	1662
16	5.78	4.18	6.00	4.34	1662
20	5.43	0.56	6.00	0.62	1836
20	5.12	0.81	6.00	0.95	1836

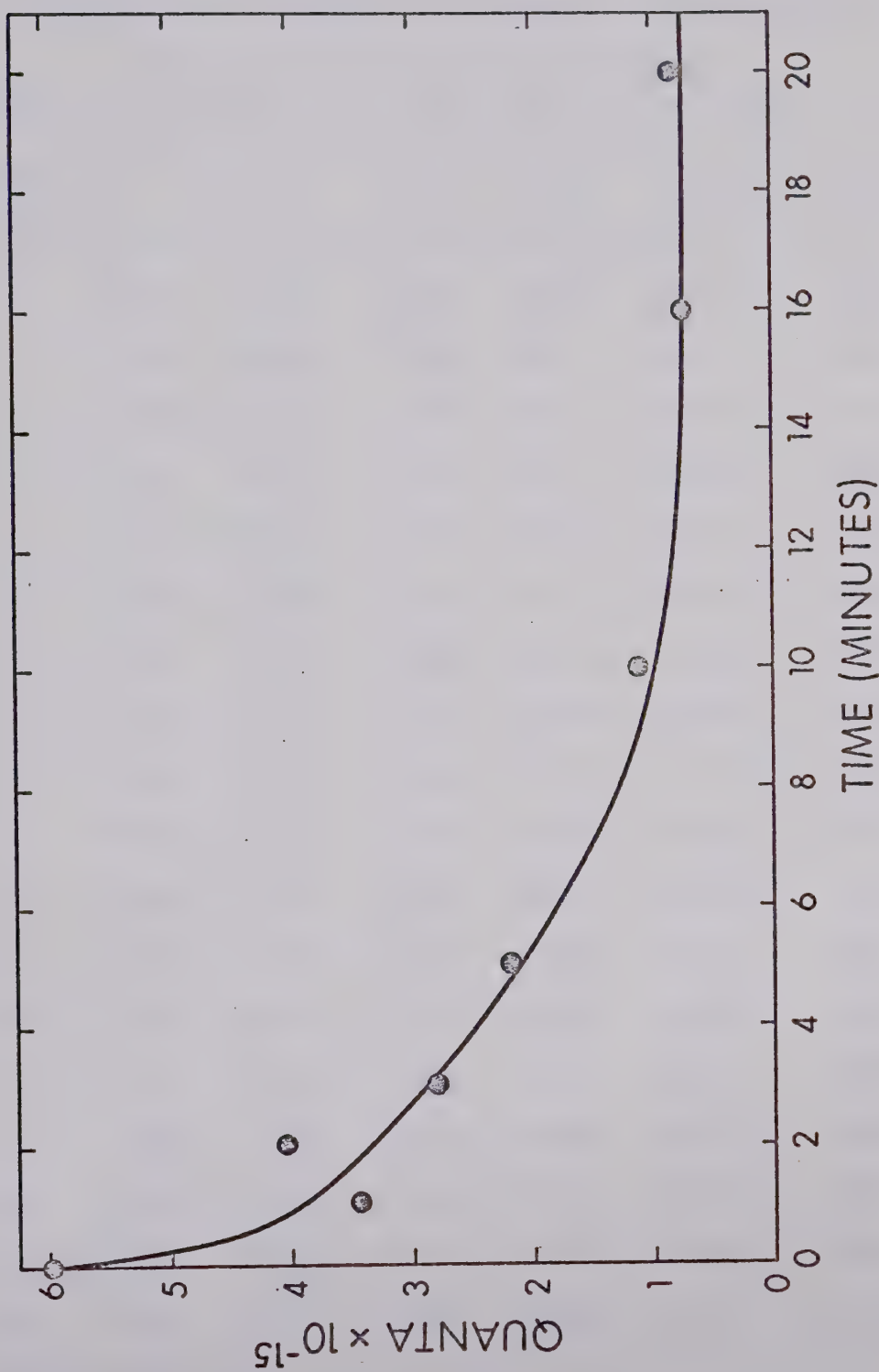


FIGURE III-3. Intensity of the Xenon Lamp as a Function of Post Photolysis Time.

TABLE III-III

Quantum Yield of Products as a Function of Time from the
Xenon Lamp Photolysis of Dimethylsilane

Time min	Quantum Yield					
	H ₂	Tri-MDS	CH ₄	C ₂ H ₆	Tet-MDS	Tri-MS
1	0.89	0.32	0.20	0.15	0.13	0.11
1	0.85	0.29	0.20	0.14	0.11	0.10
1	0.80	0.33	0.18	0.11	0.14	0.10
2	0.85	0.23	0.20	0.11	0.098	0.067
2	0.85	0.32	0.24	0.14	0.15	0.11
3	0.68	0.28	0.17	0.11	0.12	0.091
5	0.72	0.21	0.21	0.11	0.087	0.065
5	0.55	0.19	0.16	0.084	0.078	0.065
5	0.70	0.23	0.21	0.14	0.10	0.082
5	0.50	0.16	0.15	0.085	0.081	0.071
5	0.55	0.20	0.13	0.070	0.074	0.068
10	0.56	0.16	0.18	0.072	0.064	0.054
10	0.48	0.16	0.14	0.075	0.063	0.050
10	0.77	0.21	0.26	0.11	0.063	0.084
16	0.42	0.13	0.14	0.072	0.055	0.054
16	0.60	0.18	0.18	0.081	0.071	0.065
20	0.44	0.14	0.14	0.063	0.060	0.048
20	0.49	0.13	0.17	0.061	0.059	0.048

TABLE III-III (cont'd)

Quantum Yield of Products as a Function of Time from the
Xenon Lamp Photolysis of Dimethylsilane

Time min	Quantum Yield					
	DMDS	MMS	MES	C_2H_4	A	B
1	0.067	0.039	0.017	0.018	0.009(3)	-
1	0.064	0.010	0.016	0.012	0.011	0.002(2)
1	0.066	0.017	0.017	0.013	0.009(7)	0.001(2)
2	0.056	0.015	0.013	0.017	0.009(1)	-
2	0.071	0.035	0.017	0.012	0.011	0.001(8)
3	0.060	0.029	0.015	0.010	0.008(4)	0.002(4)
5	0.044	0.005(9)	0.011	0.009(0)	0.006(6)	0.002(2)
5	0.042	0.012	0.012	0.007(4)	0.006(5)	0.001(9)
5	0.050	0.038	0.014	0.011	0.008(0)	0.002(8)
5	0.042	0.025	0.012	0.006(5)	0.006(6)	0.001(5)
5	0.039	0.020	0.010	0.004(4)	0.007(7)	0.001(5)
10	0.034	0.006(4)	0.010	0.005(3)	0.006(3)	0.001(6)
10	0.030	0.012	0.007(2)	0.005(7)	0.003(7)	0.000(7)
10	0.048	0.039	0.013	0.006(9)	0.008(0)	0.002(4)
16	0.026	0.038	0.008(3)	0.003(1)	0.004(3)	0.001(4)
16	0.036	0.035	0.012	0.003(7)	0.007(2)	0.002(4)
20	0.026	0.000(4)	0.008(0)	0.003(9)	0.005(0)	0.001(5)
20	0.025	0.023	0.007(9)	0.003(5)	0.005(2)	0.001(2)

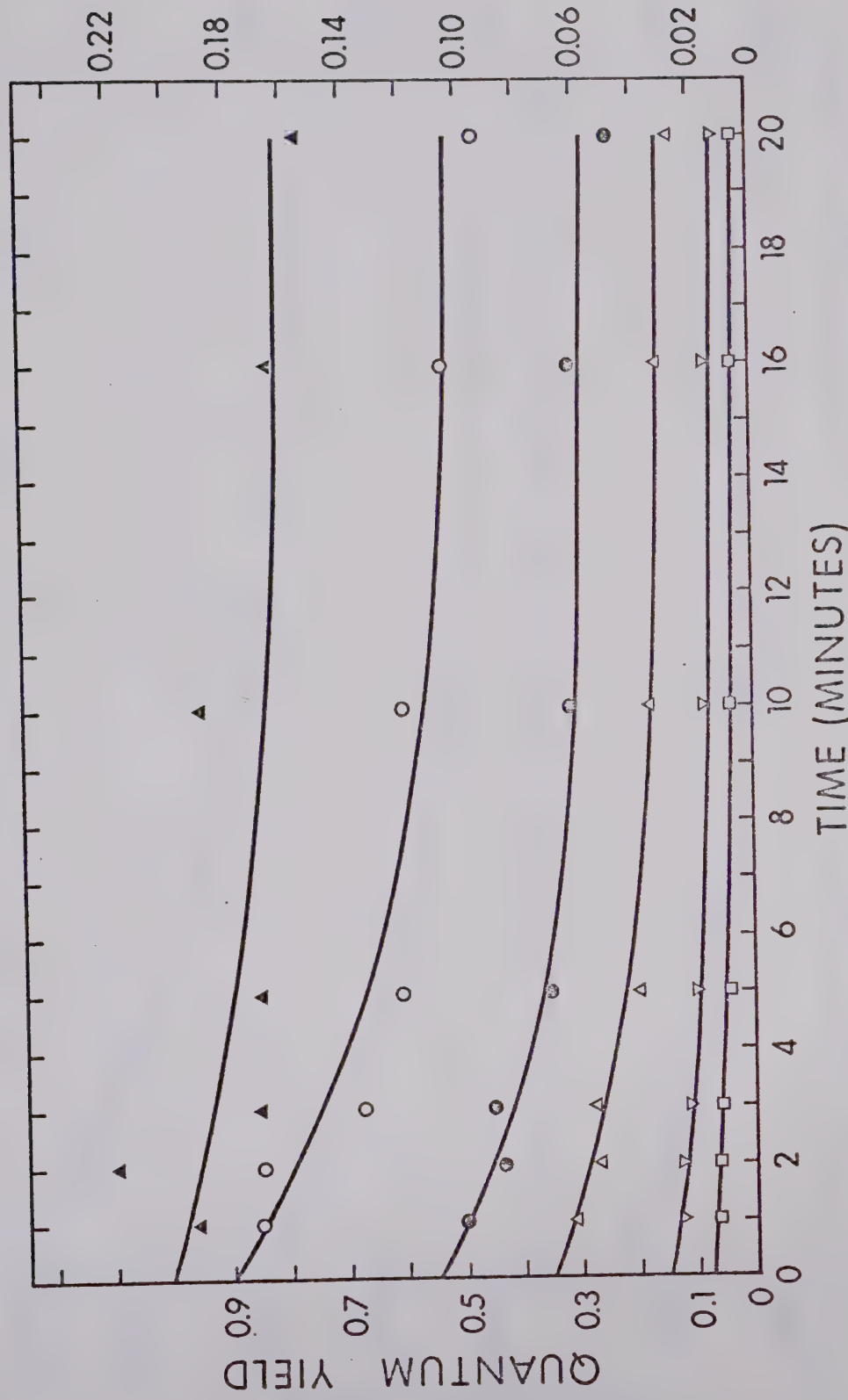


FIGURE III-4. Quantum Yields of CH_4 , H_2 , Tri-MS, C_2H_6 and DMDS as a Function of Time from the Xenon Lamp Photolysis of Dimethylsilsilane. ▲ CH_4 (R.H.S.), ○ H_2 (L.H.S.), ● Tri-MS (R.H.S.), △ Tri-MS (L.H.S.), ▽ C_2H_6 (L.H.S.), □ DMDS (L.H.S.).

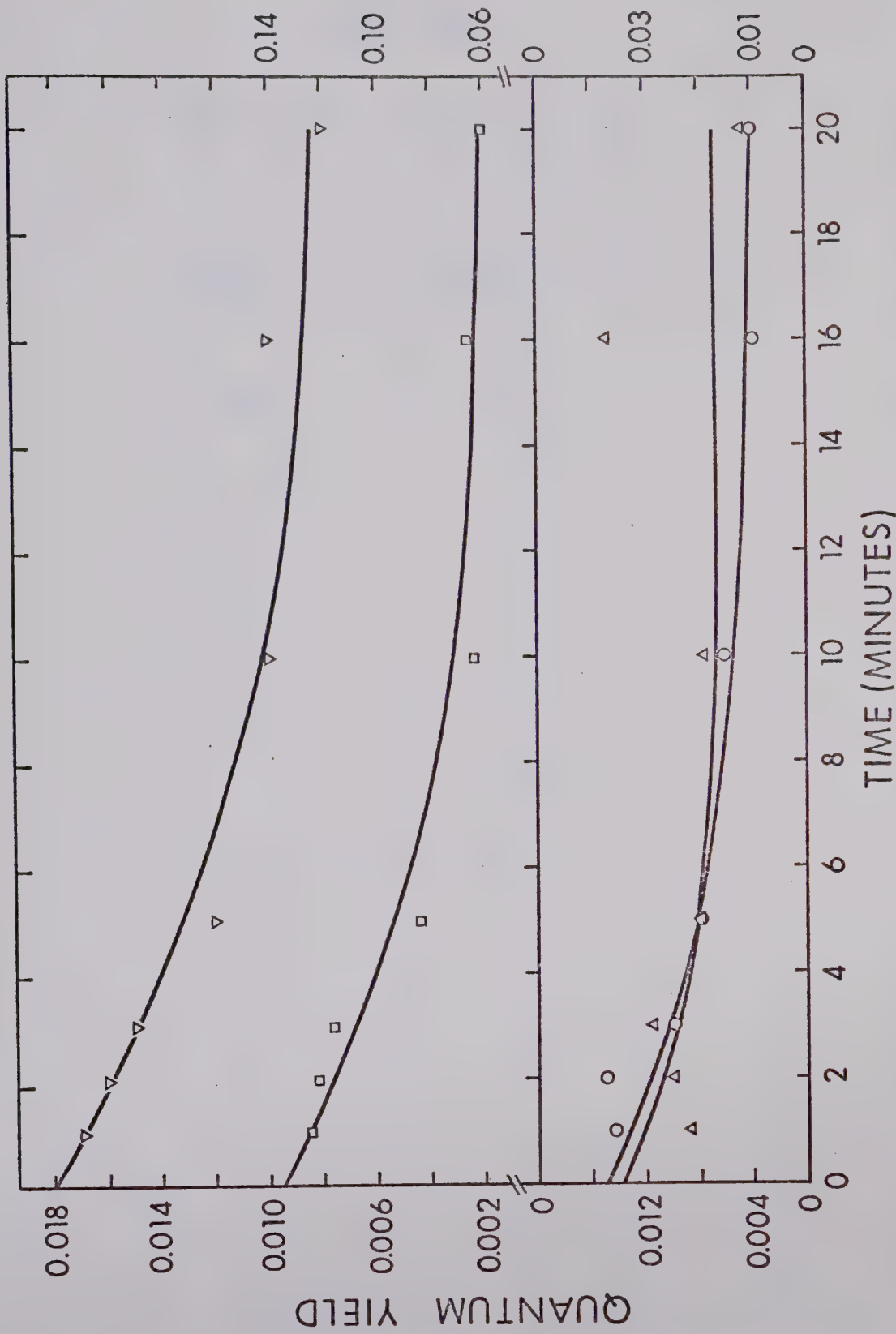


FIGURE III-5. Quantum Yields of MES, Tet-MDS, C_2H_4 and MMS as a Function of Time from the Xenon Lamp Photolysis of Dimethylsilsilane. \triangledown MES (L.H.S.), \square Tet-MDS (R.H.S.), \circ C_2H_4 (L.H.S.), Δ MMS (R.H.S.).

TABLE III-IV

Quantum Yield of Products at Zero
 Time from the Xenon Lamp Photolysis
 of Dimethylsilane

Product	Quantum Yield, ϕ°
H_2	0.90
Tri-MDS	0.35
CH_4	0.20
C_2H_6	0.15
Tet-MDS	0.13(5)
Tri-MS	0.11
DMDS	0.075
MMS	0.035
MES	0.018
C_2H_4	0.015

TABLE III-V

Relative Yield of Products as a Function of Time from the
Xenon Lamp Photolysis of Dimethylsilane

Time min	Relative Yield, %					
	H ₂	Tri-MDS	CH ₄	C ₂ H ₆	Tet-MDS	Tri-MS
1	45.7	16.7	10.1	7.63	6.63	5.53
1	47.3	15.9	11.3	7.49	6.11	5.59
1	44.9	18.7	9.89	6.11	7.73	5.66
2	51.1	13.5	12.1	6.73	5.89	4.01
2	43.8	16.5	12.2	6.95	7.54	5.45
3	43.1	17.6	10.9	7.23	7.43	5.84
5	48.8	13.9	14.2	7.62	5.87	4.39
5	45.3	16.0	13.2	6.94	6.46	5.40
5	44.0	14.6	13.1	9.02	6.30	5.12
5	43.9	14.3	12.7	7.45	7.11	6.22
5	47.0	16.8	11.1	5.95	6.32	5.82
10	48.9	13.9	15.2	6.28	5.56	4.66
10	46.8	15.6	13.3	7.43	6.23	4.93
10	47.8	13.0	16.0	6.82	3.88	5.22
16	44.3	13.6	14.7	7.53	5.76	5.61
16	47.2	14.1	14.2	6.34	5.56	5.07
20	46.6	15.1	15.2	6.72	6.43	5.17
20	48.2	12.7	16.4	5.93	5.80	4.64

TABLE III-V (cont'd)

Relative Yield of Products as a Function of Time from the
Xenon Lamp Photolysis of Dimethylsilane

Time min	Relative Yield, %					
	DMDS	MMS	MES	C_2H_4	A	B
1	3.43	2.00	0.88	0.92	0.48	-
1	3.56	0.58	0.86	0.64	0.62	0.13
1	3.71	0.96	0.94	0.72	0.55	0.068
2	3.38	0.91	0.75	1.01	0.55	-
2	3.67	1.79	0.89	0.63	0.55	0.092
3	3.85	1.84	0.96	0.65	0.54	0.15
5	2.96	0.40	0.77	0.61	0.44	0.15
5	3.51	0.99	0.95	0.61	0.54	0.15
5	3.16	2.37	0.89	0.69	0.50	0.18
5	3.68	2.20	1.07	0.57	0.58	0.13
5	3.30	1.70	0.87	0.37	0.66	0.13
10	2.96	0.56	0.90	0.46	0.55	0.14
10	2.92	1.16	0.70	0.56	0.36	0.073
10	2.99	2.45	0.79	0.43	0.50	0.15
16	2.69	4.00	0.87	0.32	0.44	0.15
16	2.81	2.76	0.94	0.29	0.56	0.19
20	2.83	0.043	0.85	0.42	0.54	0.16
20	2.40	2.24	0.77	0.34	0.51	0.11

TABLE III-VI

Micromoles of Products as a Function of Added
 Nitric Oxide from the Xenon Lamp Photolysis
 of Dimethylsilane

Products	Nitric Oxide, %				
	0	0.97	4.19	6.94	15.5
H ₂	0.96	1.37	1.73	a	a
Tri-MDS	0.31	a	a	0.27	0.36
CH ₄	0.27	0.59	0.62	a	a
C ₂ H ₆	0.16	0.058	0.009	0.002	0.004
Tet-MDS	0.13	0.057	0.070	0.047	0.087
Tri-MS	0.11	0.016	0.022	a	a
DMDS	0.069	0.079	0.10	0.086	0.12
MMS	0.032	0.052	0.13	0.019	0.073
MES	0.019	0.013	0.024	0.018	0.032
C ₂ H ₄	0.012	0.022	0.092	0.026	0.051
A	0.011	a	a	a	a
B	0.003	0.011	0.005	0.00	0.00
Tri-MDSO	0.00	0.10	0.14	0.13	0.26
Tet-MDSO	0.00	a	a	0.23	0.76
N ₂	0.00	0.45	0.90	a	a

a: not determined

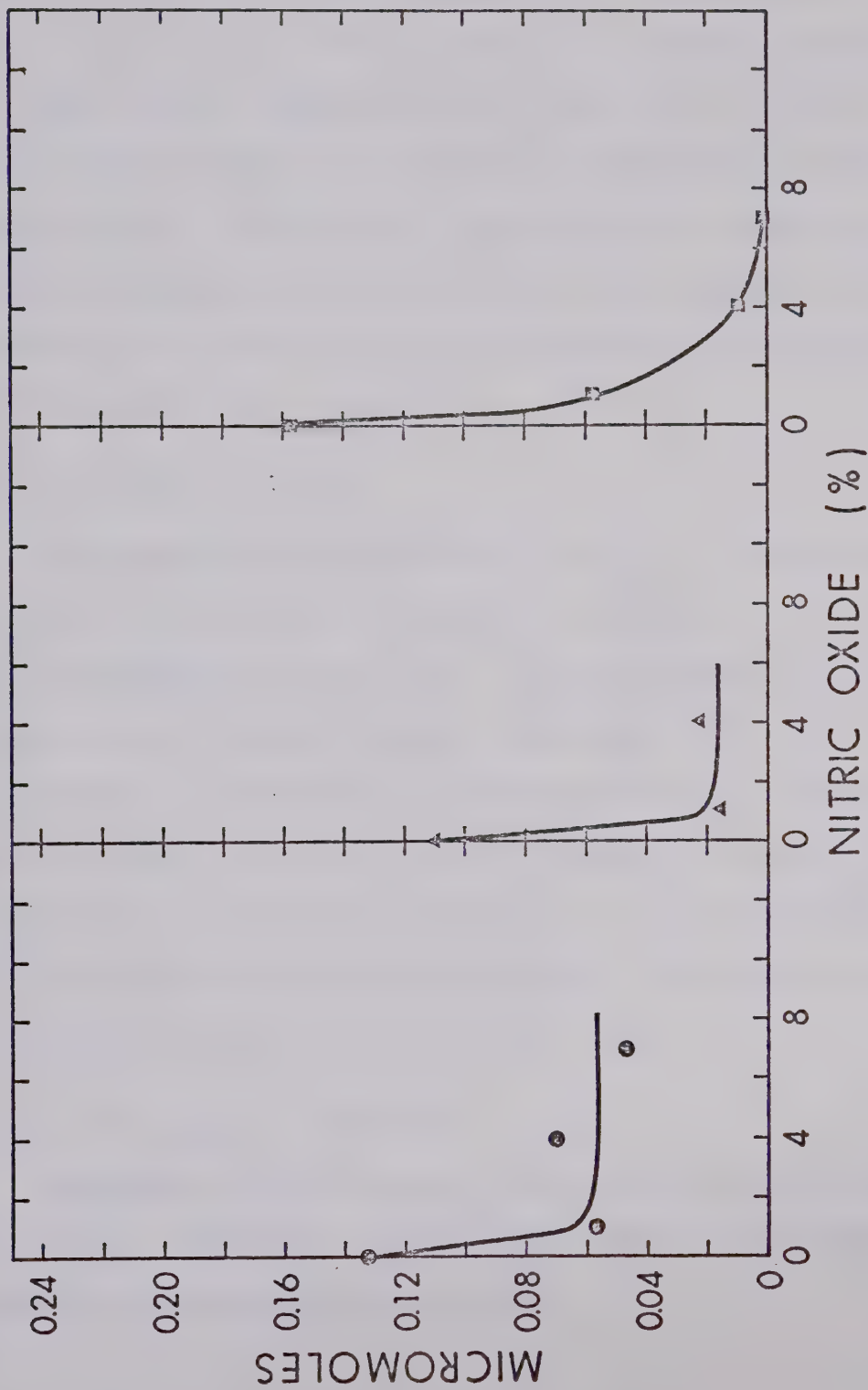


FIGURE III-6. Micromoles of Tet-MDS, Tri-MS and C_2H_6 as a Function of Added Nitric Oxide from the Xenon Lamp Photolysis of Dimethylsilane. ● Tet-MDS, ▲ Tri-MS, ■ C_2H_6 .

arises from a molecular mode of decomposition of the substrate. The increase in H_2 , CH_4 , C_2H_4 , and N_2 yields with increasing concentration of nitric oxide is indicative of the chain nature of the NO reaction. The same trend in the yield of the new products 1,1,2-trimethyldisiloxane (Tri-MDSO) and 1,1,2,2-tetramethyldisiloxane (Tet-MDSO) also supports the operativeness of short chains as well as demonstrates the presence of the radicals $CH_3\dot{S}iH_2$ and $(CH_3)_2\dot{S}iH$ (Chapter I, section A-8).

5. Deuterium Labeling Studies

The photolysis of dimethylsilane can lead to various types of atomic and molecular losses of hydrogen and methane. In order to examine this phenomenon in more detail, and to determine the relative and absolute values of these processes, experiments were carried out with isotopically labelled substrate (dimethylsilane-d₂). Various mixtures of undeuterated dimethylsilane and deuterated dimethylsilane were photolyzed and the isotopic composition of the noncondensable products (hydrogen and methane) were determined. The results, using the xenon lamp, are shown in Table III-VII.

6. Effect of Ethylene as a Scavenger

Mixtures of dimethylsilane-d₂ and ethylene were photolyzed and the isotopic composition of hydrogen and methane was recorded. The results are presented in Table III-VIII.

TABLE III-VII

Isotopic Composition of Hydrogen and Methane from the Xenon Lamp
 Photolysis of Mixtures of Dimethylsilane and Dimethylsilane-d₂

Mole Fraction Substrate	(CH ₃) ₂ SiH ₂	(CH ₃) ₂ SiD ₂	Mole Fraction Hydrogen			Mole Fraction Methane	
			H ₂	HD	D ₂	CH ₄	CH ₃ D
0.000	1.000		0.096	0.421	0.483	0.269	0.731
0.000	1.000		0.120	0.406	0.475	0.267	0.733
0.000	1.000		0.108	0.395	0.494	0.260	0.740
0.000	1.000		0.150	0.391	0.459	a	a
0.103	0.897		0.262	0.406	0.332	a	a
0.101	0.899		0.143	0.431	0.426	0.414	0.586
0.250	0.750		0.389	0.369	0.241	0.539	0.461
0.498	0.502		0.586	0.286	0.126	0.690	0.310
0.754	0.246		0.813	0.144	0.043	0.860	0.140
0.900	0.100		0.921	0.063	0.016	0.937	0.063

a: not determined

TABLE III-VIII

Isotopic Composition of Hydrogen and Methane from the Xenon Lamp

Photolysis of Mixtures of Dimethylsilane-d₂ and Ethylene

Mole Fraction Substrate	Mole Fraction Hydrogen			Mole Fraction Methane			
	(CH ₃) ₂ SiD ₂	C ₂ H ₄	H ₂	HD	D ₂	CH ₄	CH ₃ D
0.953	0.047		0.194	0.398	0.408	0.347	0.652
0.947	0.053		0.214	0.394	0.394	0.340	0.660

B. Results - Spectra

Spectroscopic data on the lower silicon hydrides and their methyl derivatives are sparse. Harada et al. (92) reported low resolution vacuum ultraviolet spectra for five of these molecules, namely SiH_4 , $(\text{CH}_3)_2\text{SiH}_2$, $(\text{CH}_3)_3\text{SiH}$, $(\text{CH}_3)_4\text{Si}$, and $(\text{CH}_3)_6\text{Si}_2$. The structureless continuum common to all these spectra resembles those observed in the hydrocarbon ultraviolet spectra except that they are shifted to the red with enhanced intensity. In all the silicon hydrides examined, there was no indicated of transitions from the bonding orbitals of the CH_3 group to the vacant 3d orbitals of the silicon.

In the present study the vacuum ultraviolet spectra of all the methylated monosilanes, the deuterium substituted analogs, and trimethylfluorosilane were recorded. The spectra are presented in Figures III-7, III-8, III-9, and III-10.

C. Kinetics and Mechanistic Derivations

The photolysis of dimethylsilane can lead to various types of atomic and molecular loss of hydrogen and methane. In order to sort out these possibilities, experiments were carried out with isotopically labelled substrate (dimethylsilane-d₂). For ease of writing, we will use the symbol L (light) for dimethylsilane and the symbol He (heavy) for dimethylsilane-d₂. The following kinetic scheme for the primary loss of hydrogen in the photolysis of dimethylsilane should be considered.



[3]

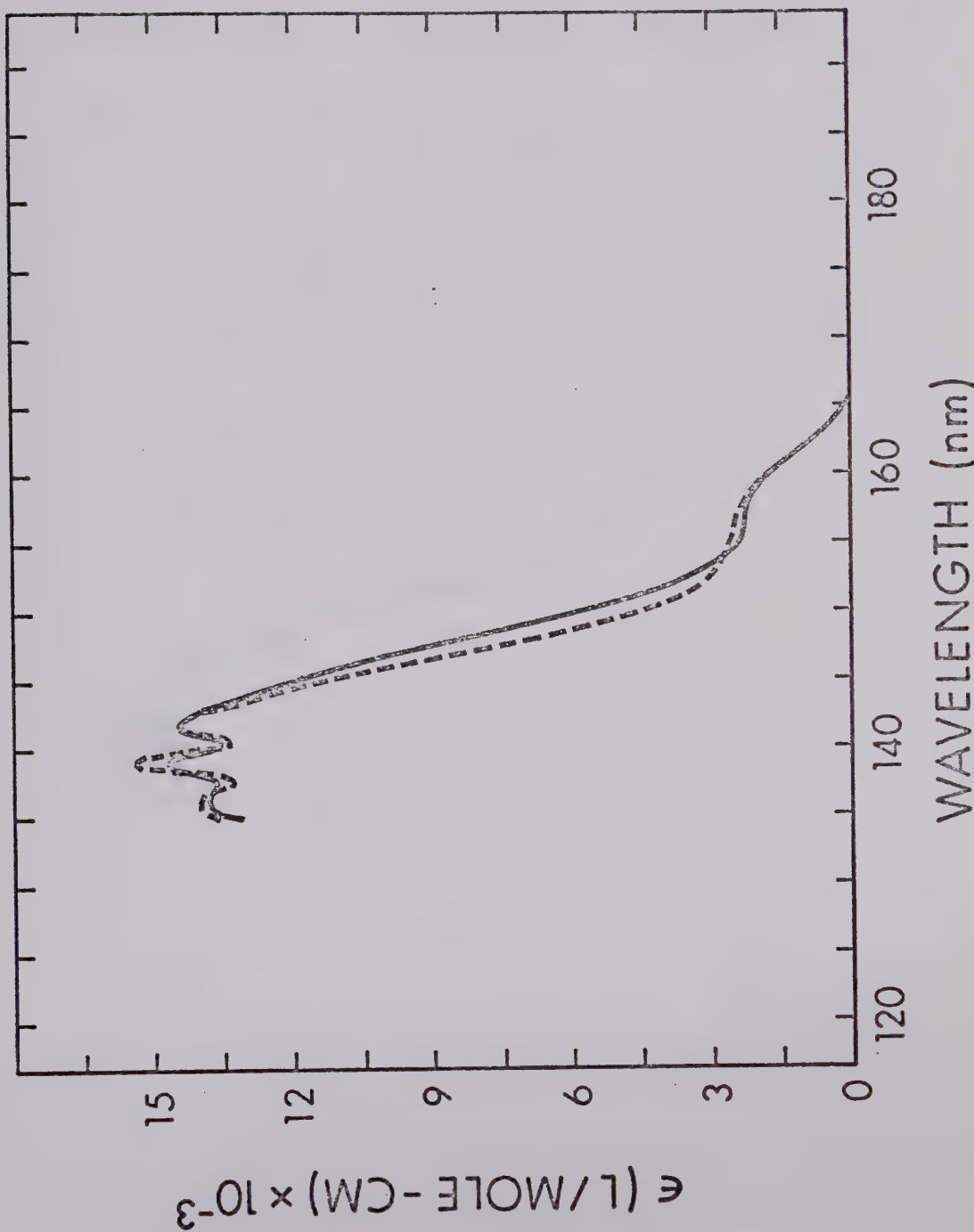


FIGURE III-7. Vacuum Ultraviolet Absorption Spectra of Monomethylsilane and Monomethylsilane-d₃. — MMS, - - - MMS-d₃.

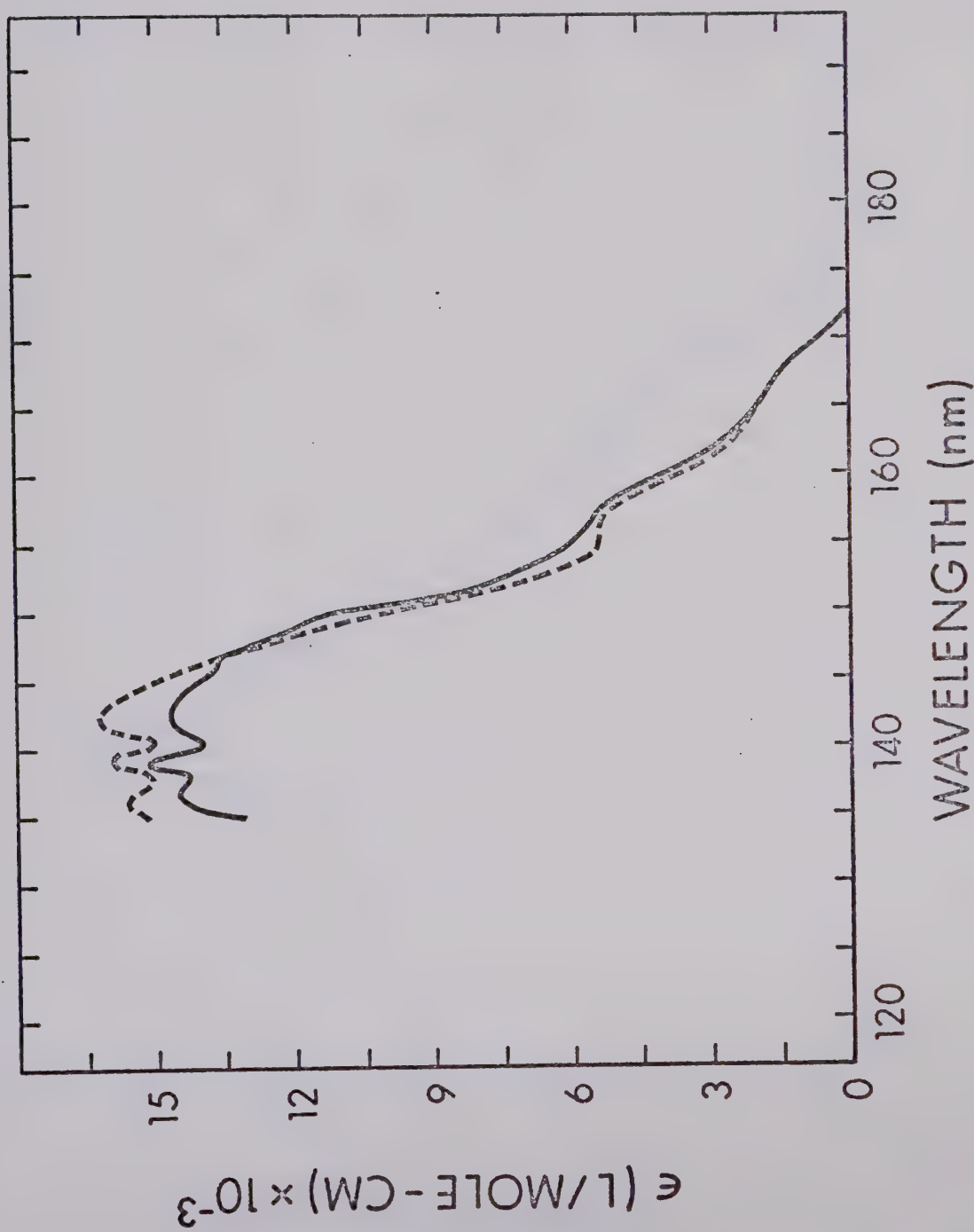


FIGURE III-8. Vacuum Ultraviolet Absorption Spectra of Dimethylsilsilane and Dimethylsilsilane-d₂. — DMS, --- DMS-d₂.

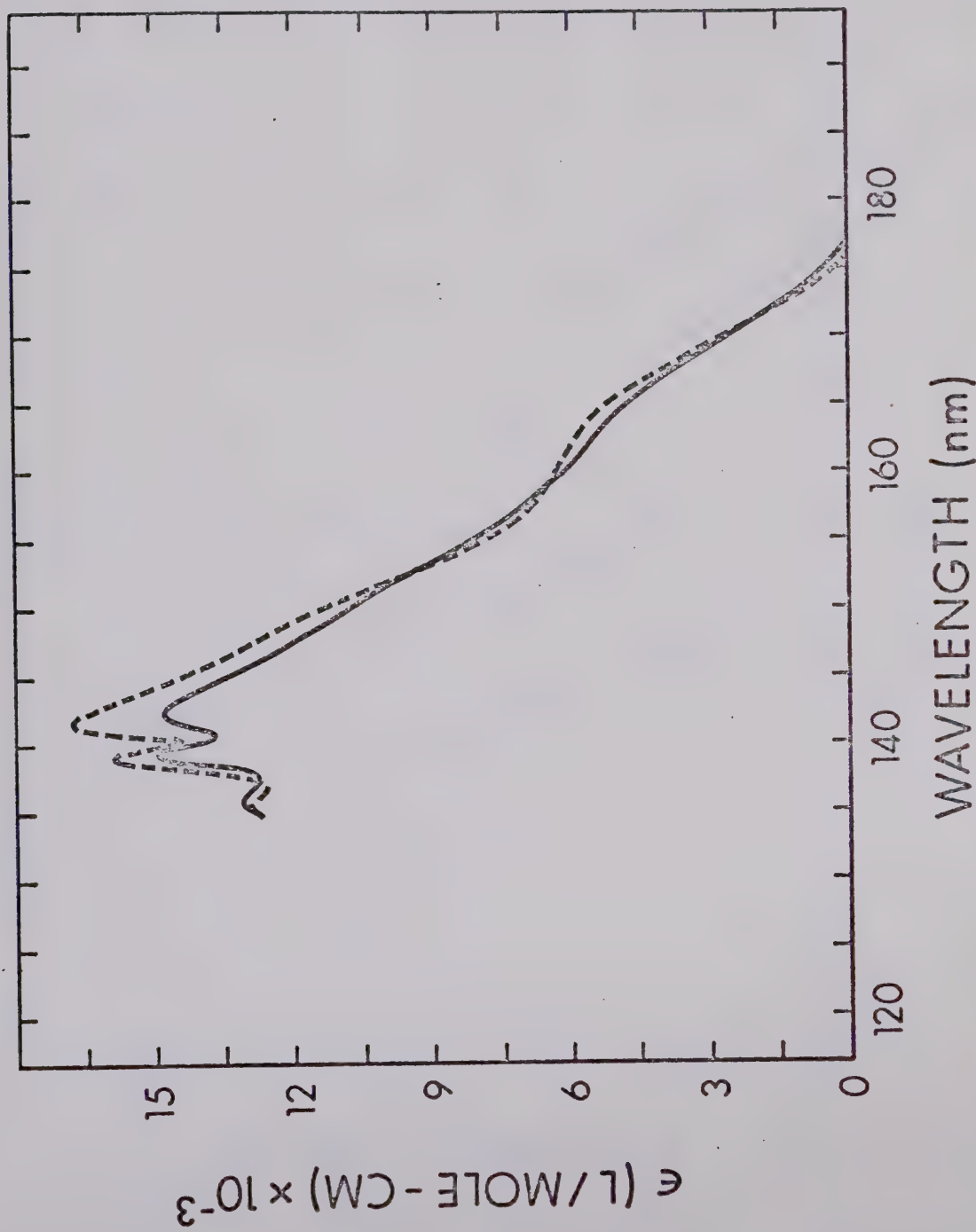


FIGURE III-9. Vacuum Ultraviolet Absorption Spectra of Trimethylsilsilane and Trimethylsilsilane-d₁. —— Tri-MS, --- Tri-MS-d₁.

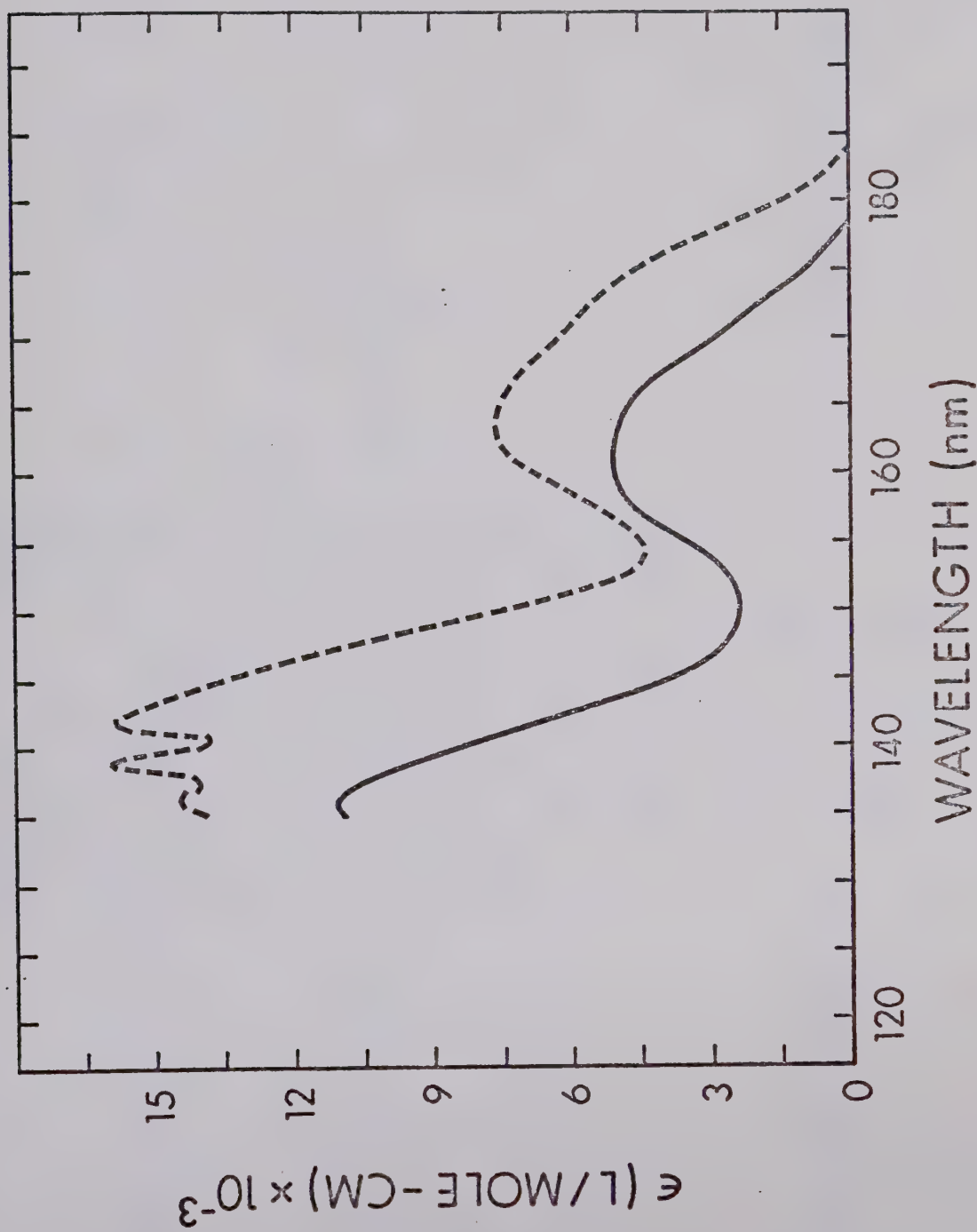


FIGURE III-10. Vacuum Ultraviolet Absorption Spectra of Trimethylmonofluorosilane and Tetramethylsilane. — Tet-MS, - - - Tri-MMFS.

He*	\rightarrow	H	[4]
	\rightarrow	D	[5]
	\rightarrow	D ₂	[6]
	\rightarrow	HD	[7]
	\rightarrow	H ₂	[8]
L + hν	\rightarrow	L*	[9]
L*	\rightarrow	H	[10]
	\rightarrow	H	[11]
	\rightarrow	H ₂	[12]
	\rightarrow	H ₂	[13]
	\rightarrow	H ₂	[14]

Equations [10] - [14] in the undeuterated (L) system correspond to equations [4] - [8] in the deuterated (He) system.

The hydrogen and deuterium atoms can carry various amounts of excess translational energy but are assumed to be thermalized in the kinetic treatment. The following abstraction and exchange reactions with both He and L are then possible; (for clarity, the resulting silane fragments will not be written).

H + L	\rightarrow	H ₂	[15]
H + He	\rightarrow	HD	[16]
D + L	\rightarrow	HD	[17]
D + He	\rightarrow	D ₂	[18]
H + He	\rightarrow	D	[19]
D + L	\rightarrow	H	[20]
H + L	\rightarrow	CH ₃	[21]
H + He	\rightarrow	CH ₃	[22]



Since there was no monosilane among the products, the exchange reactions [21] - [24] are not important. In order to determine the importance of the exchange reactions [19] and [20], H-atoms from the photolysis of hydrogen sulphide were allowed to react with dimethylsilane-d₂. It was thus shown that the exchange reactions [19] and [20] do not occur to any significant extent. The auxiliary study forms Chapter IV in this thesis.

Abstraction from the methyl groups of the substrate has not been included in the scheme because it has been shown that abstraction from the silicon end of the molecule is several orders of magnitude faster (47). Similarly, exchange with the methyl groups was omitted because any exchange mechanism must involve a five-bond complex as an intermediate; since the silicon atom can form such a complex more readily than the carbon atom, it was felt that if exchange does take place, it would be exclusively with the silicon end of the molecule. This aspect was further verified in auxiliary studies (Chapter IV).

Steady state treatment of the above set of equations gave

$$(He^*) = \frac{I_a F_{He}}{k_4 + k_5 + k_6 + k_7 + k_8} \quad [25]$$

$$(L^*) = \frac{I_a F_L}{k_{10} + k_{11} + k_{12} + k_{13} + k_{14}} \quad [26]$$

Where I_a is the incident light intensity, $k_4 - k_8$ and $k_{10} - k_{14}$ are the rate constants for reactions [4] - [8] and [10] - [14] respectively,

$$F_{He} = \varepsilon_{He}(He) / (\varepsilon_{He}(He) + \varepsilon_L(L))$$

$$F_L = \varepsilon_L(L) / (\varepsilon_{He}(He) + \varepsilon_L(L)),$$

and ε_{He} and ε_L are the extinction coefficients of He and L respectively.

Hence we obtain,

$$\frac{X_{D_2}}{F_{He}} = \frac{1}{\Sigma\phi} \left[\phi_6 + \frac{k_{18}X_{He}}{k_{17}X_L + k_{18}X_{He}} \phi_5 \right] \quad [27]$$

$$\begin{aligned} \frac{X_{HD}}{F_{He}} = & \frac{1}{\Sigma\phi} \left[\phi_7 + \frac{k_{16}X_{He}}{k_{15}X_L + k_{16}X_{He}} \phi_4 + \frac{k_{17}X_L}{k_{17}X_L + k_{18}X_{He}} \phi_5 \right. \\ & \left. + \frac{\varepsilon_L}{\varepsilon_{He}} \left(\frac{k_{16}X_L}{k_{15}X_L + k_{16}X_{He}} \right) (\phi_{10} + \phi_{11}) \right] \quad [28] \end{aligned}$$

$$\begin{aligned} \frac{X_{H_2}}{F_{He}} = & \frac{1}{\Sigma\phi} \left[\phi_8 + \frac{\varepsilon_L}{\varepsilon_{He}} \frac{X_L}{X_{He}} \left(\phi_{12} + \phi_{13} + \phi_{14} \right) \right. \\ & \left. + \frac{k_{15}X_L}{k_{15}X_L + k_{16}X_{He}} \left(\phi_4 + \frac{\varepsilon_L}{\varepsilon_{He}} \frac{X_L}{X_{He}} (\phi_{10} + \phi_{11}) \right) \right] \quad [29] \end{aligned}$$

Where X_{D_2} , X_{HD} , and X_{H_2} are the experimentally determined isotopic hydrogen yields, $\Sigma\phi$ is the total experimentally determined quantum yield, $\phi_4 - \phi_8$ and $\phi_{10} - \phi_{14}$ are the quantum yields corresponding to reaction [4] - [8] and [10] - [14] respectively and X_L and X_{He} are the mole fractions of L and He respectively. A complete kinetic derivation is given in *Appendix A*. As indicated in the results section,

$$\varepsilon_{He} = \varepsilon_L.$$

A plot of X_{D_2}/F_{He} vs X_L and X_{HD}/F_{He} vs X_L is given in Figure III-11. It can be shown at $X_L = 0.0$ that

$$\frac{X_{D_2}}{F_{He}} = \frac{1}{\Sigma\phi} (\phi_5 + \phi_6) \quad [30]$$

$$\frac{X_{HD}}{F_{He}} = \frac{1}{\Sigma\phi} (\phi_4 + \phi_7) \quad [31]$$

$$\frac{X_{H_2}}{F_{He}} = \frac{1}{\Sigma\phi} (\phi_8) \quad [32]$$

It can also be shown that at $X_{He} = 0.0$:

$$\frac{X_{D_2}}{F_{He}} = \frac{1}{\Sigma\phi} (\phi_6) \quad [33]$$

$$\frac{X_{HD}}{F_{He}} = \frac{1}{\Sigma\phi} \left[\phi_7 + \phi_5 + \frac{k_{16}}{k_{15}} \frac{\varepsilon_L}{\varepsilon_{He}} (\phi_{10} + \phi_{11}) \right] \quad [34]$$

$$\frac{X_{H_2}}{F_{He}} = \infty \quad [35]$$

From these equations ϕ_5 , ϕ_6 , ϕ_8 , and $\phi_4 + \phi_7$ can be determined. The values obtained are $\phi_5 = \phi(D) = 0.295$, $\phi_6 = \phi(D_2) = 0.135$, $\phi_8 = \phi(H_2) = 0.107$ and $\phi_4 + \phi_7 = \phi(H) + \phi(HD) = 0.363$.

Rearranging equation [27] gives

$$\frac{\phi_5}{\frac{X_{D_2}}{\Sigma\phi} - \phi_6} = 1 + \frac{k_{17}}{k_{18}} \frac{X_L}{X_{He}} \quad [36]$$

A plot of equation [36] is shown in Figure III-12 from which a kinetic isotope effect, $k_{17}/k_{18} = 3.6$, was determined. We set $k_{15}/k_{16} =$

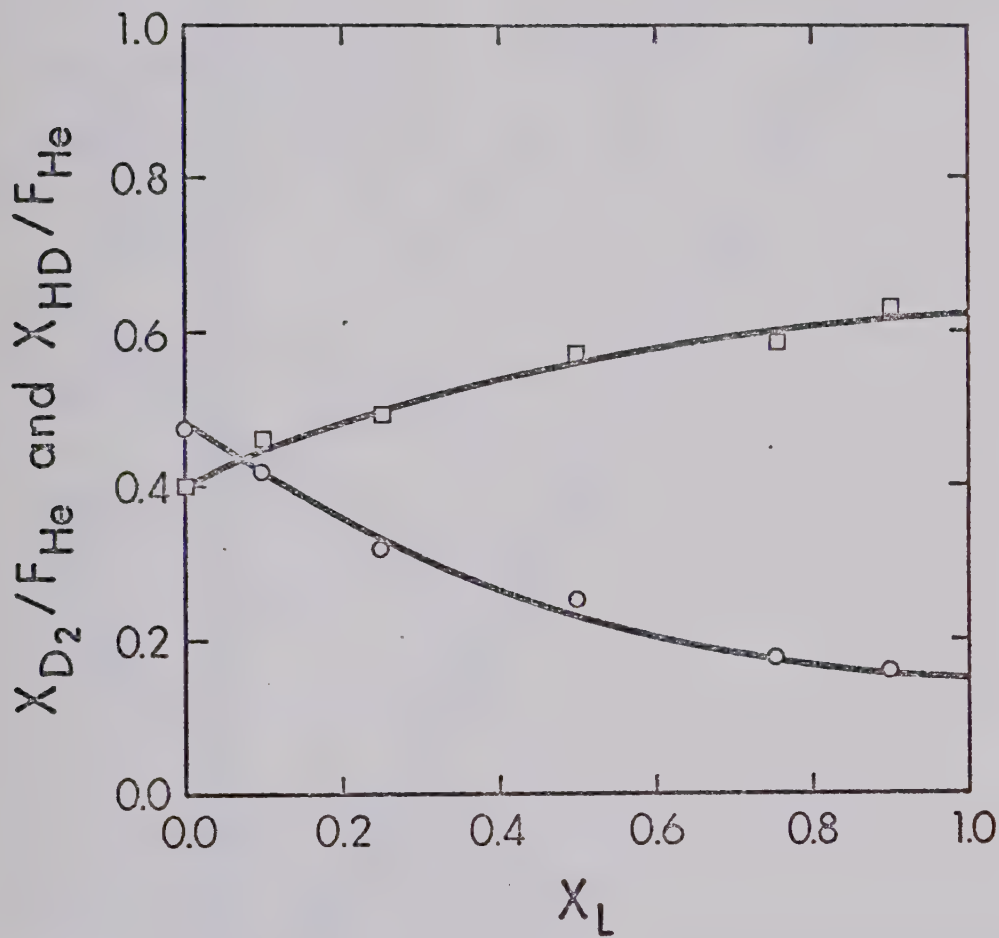


FIGURE III-11. X_{D_2}/F_{He} and X_{HD}/F_{He} as a Function of X_L from the Xenon Lamp Photolysis of Mixtures of Dimethylsilane and Dimethylsilane-d₂.

○ X_{D_2}/F_{He} , □ X_{HD}/F_{He}

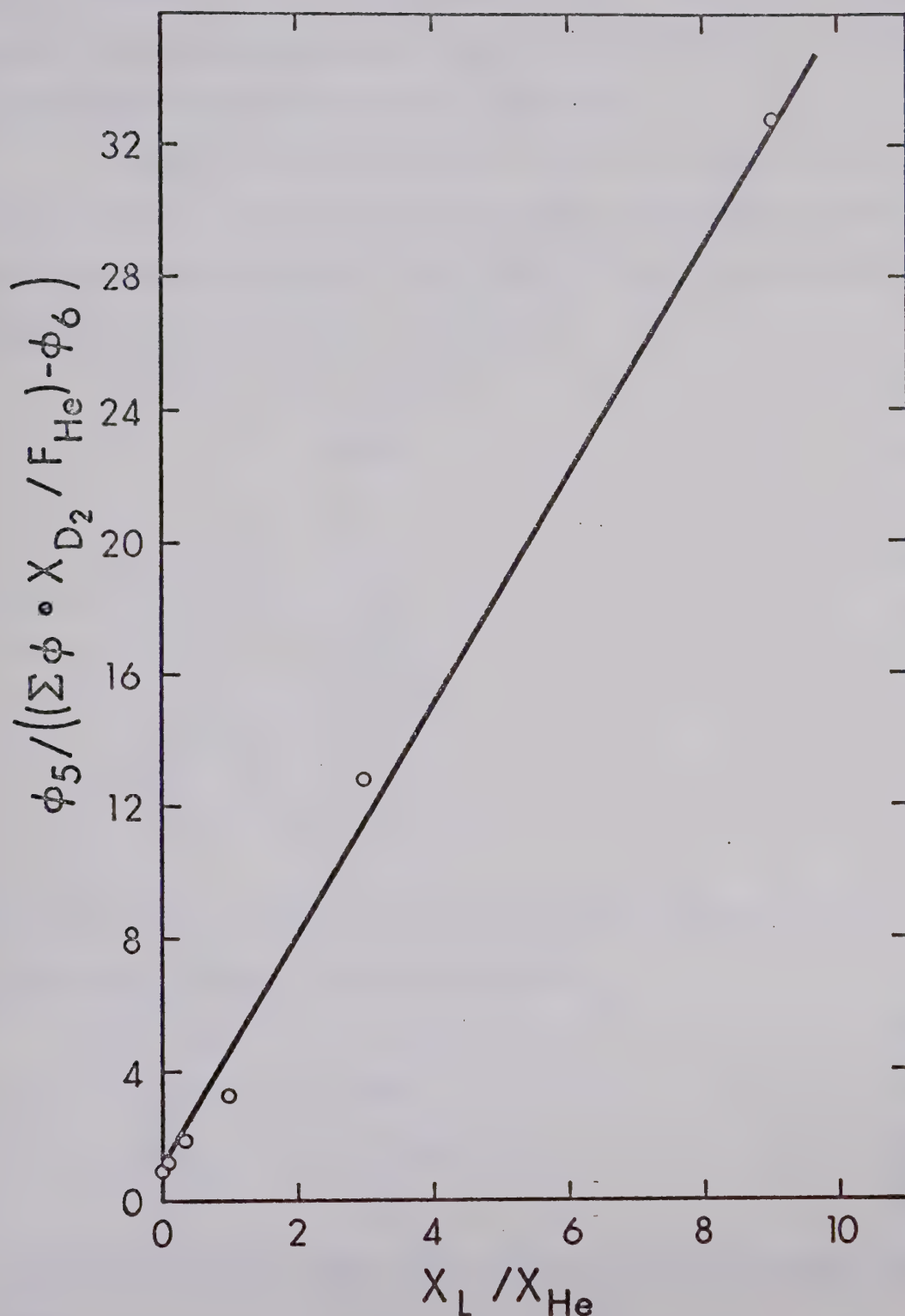
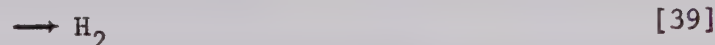
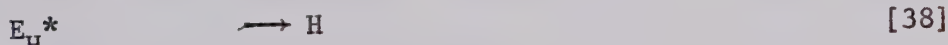


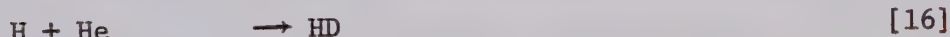
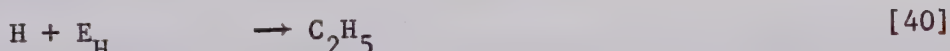
FIGURE III-12. A Plot in Accordance with Equation [36] to Obtain the Isotope Effect for Abstraction in the Xenon Lamp Photolysis of Mixtures for Dimethylsilane and Dimethylsilane-d₂.

k_{17}/k_{18} . That is, the isotope effect ratio for abstraction is independent of the attacking species. This is not unreasonable to a first approximation in gas phase reaction rate theory.

Owing to the primary isotope effect for hydrogen loss between He and L, ϕ_4 and ϕ_7 must be determined independently from the ethylene scavenger studies. The following kinetic scheme applies to this system, where E_H refers to ethylene.



The H and D atoms formed in the system would be expected to add to ethylene and abstract from dimethylsilane-d₂.



It has been shown (165-168) that the abstraction and exchange reactions





are of no importance under these conditions and can be ignored.

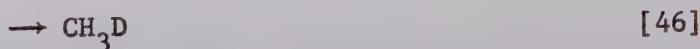
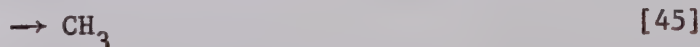
Steady state treatment of this set of equations gives the expression

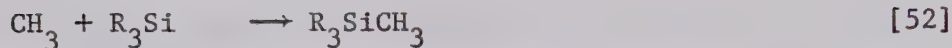
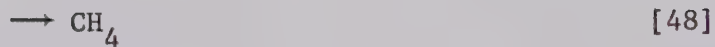
$$\frac{x_{HD}}{x_{D_2}} = \frac{\phi_7 + \frac{\phi_4 + \frac{\epsilon_{E_H}}{\epsilon_{He}} \frac{x_{E_H}}{x_{He}} \phi_{38}}{\frac{k_{40}}{k_{16}} \frac{x_{E_H}}{x_{He}} + 1}}{\phi_6 + \frac{\phi_5}{\frac{k_{41}}{k_{18}} \frac{x_{E_H}}{x_{He}} + 1}} \quad [44]$$

A complete kinetic derivation is given in *Appendix B*.

Since $k_{17} = 3.83 \times 10^{11}$ cc/mole-sec (56) based on a value of $k_{40} = 6.7 \times 10^{11}$ cc/mole-sec (56) and $k_{17}/k_{18} = 3.6$ (this work), then $k_{18} = 1.06 \times 10^{11}$ cc/mole-sec. Hence $k_{40}/k_{16} = k_{41}/k_{18} = 6.32$. Also, $\epsilon_{E_H} = 7850$ 1/mole-cm (98,169), $\epsilon_{He} = 13,155$ 1/mole-cm (this work) and $\phi_{38} = 0.58$ (170). Using the already derived values for ϕ_5 , ϕ_6 , $\phi_4 + \phi_7$ and the ethylene scavenging results we find that $\phi_4 = 0.101$ and $\phi_7 = 0.262$.

The question of molecular methane and methyl radical loss should also be considered. The relevant reactions are:





Kinetic treatment of this scheme does not lead to an explicit solution for the steady concentration of methyl radicals, but the problem can be solved by a different approach. It has been shown that all the ethane is formed by radical recombination. Hence:

$$(\text{CH}_3) = \left(\frac{\text{R}_{\text{C}_2\text{H}_6}}{k_{51}} \right)^{\frac{1}{2}} \quad [53]$$

where $\text{R}_{\text{C}_2\text{H}_6}$ is the rate of formation of ethane. Also, we know that at any given time:

$$\text{R}_{\text{C}_2\text{H}_6} = \phi_{\text{C}_2\text{H}_6} I \quad [54]$$

where $\phi_{\text{C}_2\text{H}_6}$ is the quantum yield of formation of ethane and I is the total photon input. A time study enabled us to determine the quantum yield of ethane formation at zero time (Table III-IV). Hence:

$$(\text{CH}_3) = \left(\frac{\phi_{\text{C}_2\text{H}_6}^0 I_a}{k_{51}} \right)^{\frac{1}{2}} \quad [55]$$

where $\phi_{\text{C}_2\text{H}_6}^0$ is the zero time quantum yield and I_a is the incident light intensity.

Since the rate of formation of CH_3D by abstraction is given by

$$\text{R}_{\text{CH}_3\text{D}}^A = k_{50} (\text{CH}_3) (\text{He}) \quad [56]$$

$$= \phi_{\text{CH}_3\text{D}}^{\text{A}} I_a \quad [57]$$

Then

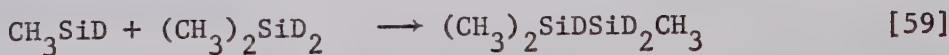
$$\phi_{\text{CH}_3\text{D}}^{\text{A}} = k_{50} \left(\frac{\phi_{\text{C}_2\text{H}_6}^{\circ}}{k_{51} I_a} \right)^{\frac{1}{2}} \quad (\text{He}) \quad [58]$$

Substitution of the appropriate numbers ($k_{50} = 3.38 \times 10^5 \text{ cc/mole-sec}$ (48), $k_{51} = 2.5 \times 10^{13} \text{ cc/mole-sec}$ (171,172)) show that $\phi_{\text{CH}_3\text{D}}^{\text{A}} = 0$. As explained previously, methyl radical abstraction from the methyl groups is several orders of magnitude slower than from the silicon end of the molecule, hence all the methane in the system is molecular methane and 26.5% is CH_4 and 73.5% is CH_3D .

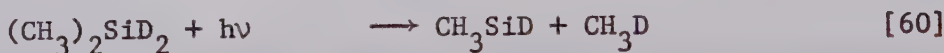
Having derived the quantum yields for the various isotopic hydrogen and methane species, we can now establish a mechanism for the overall photolysis on the basis of the deuterated molecule for clarity.

Although the final values for the primary mechanism (Table III-IX) can only be considered accurate to the second decimal place, additional significant figures will be carried during the derivation to avoid round-off errors.

The quantum yield of formation of Tri-MDS is 0.35 and nitric oxide showed it to be non-scavengable. Hence it must be formed by insertion of methylsilylene into substrate.



Methylsilylene could form in two possible primary steps.

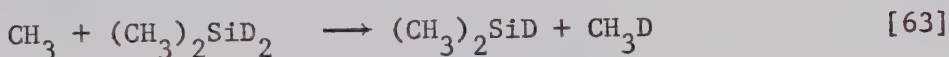


The total quantum yield of formation of methane is 0.20. From the

photolysis of $(\text{CH}_3)_2\text{SiD}_2$, Table III-VII, 26.5% of the methane is CH_4 and the remaining 73.5% is CH_3D . Since methyl radicals cannot abstract (47) from the methyl groups of DMS, then CH_4 must form in a molecular process with a quantum value of 0.053.

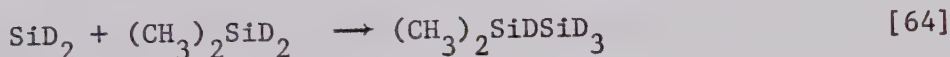


It has been shown previously that all the CH_3D is molecular and none forms by methyl radical abstraction.

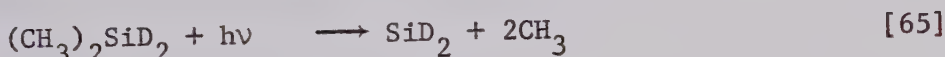


Hence $\phi_{60} = 0.147$ and $\phi_{61} = 0.203$.

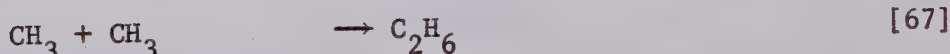
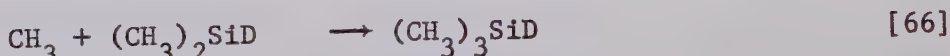
The quantum yield of formation of DMDS is 0.075 and nitric oxide showed it to be non-scavengable. It must form by an insertion reaction of silylene,



Since all the ethane was scavengable then silylene could only be formed by step [65] with a quantum yield of 0.075.



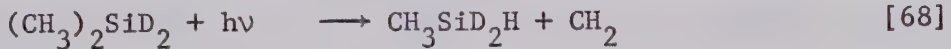
Nitric oxide studies showed that 83% of the Tri-MS and 100% of the ethane is scavengable so they would form by radical recombination reactions.



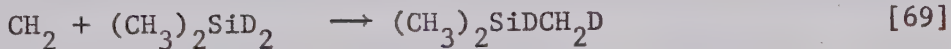
$\phi_{66} = 0.0913$ and $\phi_{67} = 0.15$. The total methyl radicals required to produce the observed produced is 83% $\phi(\text{Tri-MS}) + 2\phi(\text{C}_2\text{H}_6) = 0.3913$ whereas the total derived from the mechanism is 0.353. The difference

of 0.0383 must still be account for.

The quantum yield of formation of MMS is 0.035 and none of it is scavengeable. A likely mode of formation would be

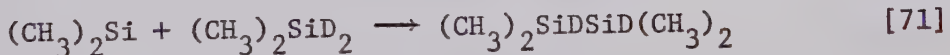


The CH_2 formed in step [68] would then insert into the carbon-hydrogen and silicon-hydrogen bonds of the substrate.

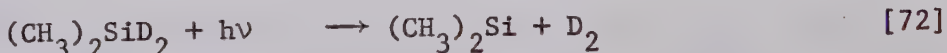


Seventeen percent of the Tri-MS was non-scavengeable and none of the MES was scavengeable, therefore $\phi_{69} + \phi_{70} = 0.0367$. This agrees very well with ϕ_{68} which is the sole source of methylene. Therefore methylene will insert into the silicon-hydrogen bond 3.12 times faster than into the carbon-hydrogen bond in this system.

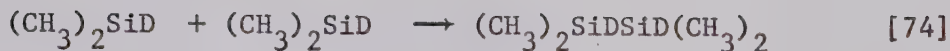
The quantum yield of formation of Tet-MDS is 0.135 and nitric oxide showed it to be 51% scavengeable. The non-scavengeable Tet-MDS would form by insertion of dimethylsilylene with a quantum yield of 0.06615.



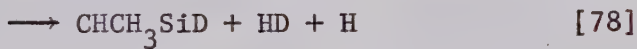
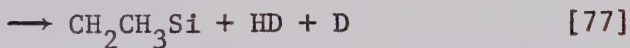
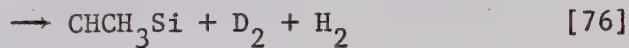
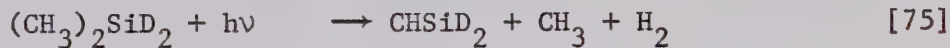
The dimethylsilylene could arise in two possible steps.



Since the relative importance of steps [72] and [73] cannot be determined, step [73] will be designated β and ϕ_{72} is then $0.06615 - \beta$. The scavengeable Tet-MDS would form by radical recombination.



So far we have accounted for all the products except hydrogen, methane and ethylene and the primary quantum yield up to this point is 0.57915. We still have to rationalize $\phi(\text{CH}_3) = 0.0383$, $\phi(\text{D}_2) = 0.06885 + \beta$, $\phi(\text{D}) = 0.092 - \beta$, $\phi(\text{HD}) = 0.262$, $\phi(\text{H}) = 0.101$, $\phi(\text{H}_2) = 0.107$ and $\phi(\text{C}_2\text{H}_4) = 0.015$. These must be accounted for in such a way that the silane fragments left behind after cleavage do not give measureable products, i.e. they must be 1,2 diradicals or multi-radicals that would contribute to polymer formation. Also, the total primary quantum yield must equal unity to within experimental error and the proposed steps must be in accordance with energetic considerations. There are many combinations of primary steps that would satisfy the above requirements and the scheme proposed here must be considered speculative.



$\phi_{75} = 0.0383$, $\phi_{76} = 0.06885 + \beta$, $\phi_{77} = 0.092 - 2\beta$, $\phi_{78} = 0.051$, $\phi_{79} = 0.05$, and $\phi_{80} = 0.119 + 2\beta$. The total primary quantum yield is $0.9983 + \beta$ and the limits on β are $0.0 \leq \beta \leq 0.06615$. The presence of ethylene among the products will be discussed later. The thirteen step mechanism is summarized in Table III-IX.

TABLE III-IX

 Primary Mechanism for the Xenon Lamp Photolysis of
 Dimethylsilane-d₂

$(\text{CH}_3)_2\text{SiD}_2 + h\nu$	$\xrightarrow{60}$	$\text{CH}_3\text{SiD} + \text{CH}_3\text{D}$	0.15
	$\xrightarrow{61}$	$\text{CH}_3\text{SiD} + \text{CH}_3 + \text{D}$	0.20
	$\xrightarrow{65}$	$\text{SiD}_2 + 2\text{CH}_3$	0.08
	$\xrightarrow{62}$	$\text{CH}_2\text{SiD}_2 + \text{CH}_4$	0.05
	$\xrightarrow{68}$	$\text{CH}_3\text{SiD}_2\text{H} + \text{CH}_2$	0.04
	$\xrightarrow{72}$	$(\text{CH}_3)_2\text{Si} + \text{D}_2$	0.07 - β
	$\xrightarrow{73}$	$(\text{CH}_3)_2\text{Si} + 2\text{D}$	β
	$\xrightarrow{75}$	$\text{CHSiD}_2 + \text{CH}_3 + \text{H}_2$	0.04
	$\xrightarrow{76}$	$\text{CHCH}_3\text{Si} + \text{D}_2 + \text{H}_2$	0.07 + β
	$\xrightarrow{77}$	$\text{CH}_2\text{CH}_3\text{Si} + \text{HD} + \text{D}$	0.09 - 2 β
	$\xrightarrow{78}$	$\text{CHCH}_3\text{SiD} + \text{HD} + \text{H}$	0.05
	$\xrightarrow{79}$	$\text{CH}_2\text{CH}_3\text{SiD}_2 + \text{H}$	0.05
	$\xrightarrow{80}$	$\text{CH}_2\text{CH}_3\text{SiD} + \text{HD}$	0.12 + 2 β
			1.01 + β

$$0 \leq \beta \leq 0.07$$

D. Discussion

From the data presented, it is evident that there are two main primary processes involved: the first is loss of molecular fragments such as H_2 , D_2 , HD , CH_3D and CH_4 ; the second is radical loss of H , D and CH_3 . There is also a minor process involving formation of methylene. The silane fragments left behind may be monoradicals and diradicals that give silane products or monoradicals, diradicals and multiradicals that end up in polymer. Product formation involves silicon-hydrogen bond cleavage, carbon-hydrogen bond cleavage and silicon-carbon bond cleavage. The occurrence of so many primary processes and products is probably of spectral origin since numerous repulsive surfaces and excited states are possible. Hence, fluctuation of the internal energy in the excited molecule would lead to decomposition along a great variety of surfaces and therefore to a large number of primary processes. That is, there can be a random accumulation of energy in one particular bond regardless of what moiety of the molecule does the absorbing.

Comparing this work with the 1470\AA photolysis of the carbon analog, propane (132,136-140), shows both similarities and differences. The differences arise from, and reflect on, the characteristic differences between the chemical nature of the carbon and silicon atoms. It would be useful to discuss at length the absorption spectrum of DMS and propane.

The absorption spectrum of propane has been extensively studied (119-123). It shows an absorption onset at approximately 1630\AA , and eight bands between 1590\AA and 1100\AA . These bands may be

broadly characterized as (σ, σ^*) -type transitions. The first three (1590 \AA , 1577 \AA and 1512 \AA) are weak and probably correspond to the promotion of one of the $(\text{C-C})\sigma$ electrons to a 3s molecular orbital.

It is reasonable to assume that it is the forbidden $^1\text{A}_1 \rightarrow ^1\text{A}_1$ transition. The other bands (1395 \AA , 1285 \AA , 1200 \AA , 1172 \AA and 1162 \AA) are stronger and probably correspond to the promotion of a $(\text{C-H})\sigma$ electron to the same excited orbital. There are methyl and methylene C-H bonds and it is not possible to make a full assignment at present. The extinction coefficient at 1470 \AA is approximately 3500 1/mole-cm and the radiative lifetime of the order of 10^{-8} sec.

Until this work was begun there had only been one report (92) on the vacuum ultraviolet spectra of the simple methylated silanes. Due to the preliminary nature of this account and in order to determine the effect of deuteration, the absorption spectra of all the simple silanes were recorded. The principal features of these spectra, shown in Figures III-7 to III-10 agree with the earlier data of Harada et al. (92), with the notable distinction that some structural features were resolved at the 1400 \AA maxima. This, taken in conjunction with the observation that decomposition of photoexcited silicon hydride molecules is unaffected by pressure up to at least 1000 torr but is strongly suppressed in the condensed phase (96), places the decomposition lifetime in the order of 10^{-11} sec. With a resolution of 0.15 \AA no structure is apparent near the onset of absorption.

The appearance of the windows with minima at 1540 \AA (tetra-methylsilane) and at 1500 \AA (trimethylfluorosilane) would seem to suggest that the main absorber in the 1500 \AA to 1600 \AA region in the

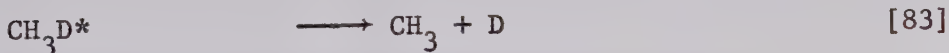
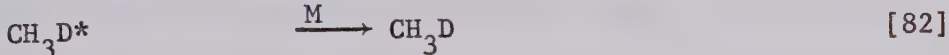
partially methylated silanes is the Si-H bond. The longer wavelength transitions are probably associated with the Si-C bond absorption and the structured maxima centered at 1400 \AA with the C-H bond absorption. Deuteration, as expected, has little effect on the spectra (98).

Substitution of fluorine for the tertiary hydrogen in trimethylsilane has the effects of: shifting the 1400 \AA maxima slightly to the blue; eliminating the structural features; and suppressing the intensity. These phenomena may be related to $d_{\pi} - p_{\pi}$ bonding between silicon and fluorine or to inductive effects.

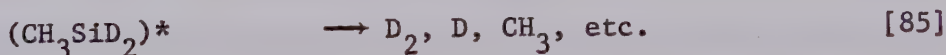
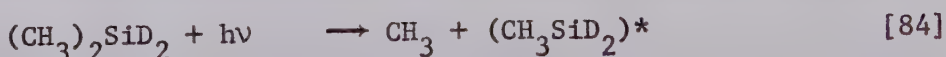
The spectrum of dimethylsilane in particular, shows an absorption onset at approximately 1750 \AA ; two strong bands at 1450 \AA and 1350 \AA ; very strong absorption from 1300 - 1100 \AA , with a maximum at 1120 \AA . The 1470 \AA resonance line of the xenon lamp coincides with the onset of the first strong transition. Although there is some fine structure in the spectrum, the excited states in this region (1100 - 1800 \AA) must be essentially repulsive. Since the absorption is strong at 1470 \AA then the transitions are allowed and the excited states are probably singlets. The extinction coefficient at 1470 \AA is 13,155 1/mole-cm and the radiative lifetime is of the same order as propane (10^{-8} sec). A comparison of the two spectra show that DMS is shifted by less than 100 \AA to the red, with respect to propane. Therefore it is not unreasonable to assume that the interpretation of the propane spectrum (meager as it is) can be applied to dimethylsilane. Hence we would expect the Si-C transition to lie at longer wavelengths, between 1650 and 1700 \AA , and have a small extinction coefficient. The bands at 1350 \AA and 1450 \AA would be associated with the Si-H bond.

Therefore the 1470A resonance line falls in the Si-H transition region and one would be tempted to assume that the main mode of decomposition would be Si-H cleavage. This, however, is not the case; C-Si cleavage and fragmentation are the major modes of decomposition. This is a clear indication that the energy in the excited molecule can randomize and cause decomposition along a variety of repulsive surfaces.

It is impossible at this point to decide whether the primary processes (Table III-IX) are parallel, competing reactions, or whether they encompass secondary reactions ensuing from only two or three primary steps. For example, steps [60] and [61] could occur independently or follow the sequence



The second alternative is not likely since the methane yield decreases to a plateau with increasing pressure (Figure III-2); furthermore, the excess energy carried away by the methane fragment would have to exceed 104 kcal/mole to cause fragmentation and it has been shown (98-106) that, in the photolysis of simple hydrocarbons, the excess photon energy is left behind in the parent fragment. It is possible however, that steps [61], [65] and [75] can be written as



Similarly, the combinations [75] + [76], [77] + [78] + [80], and [61] + [73] + [77] can be considered as originating from single primary steps. Energy delocalization in the excited state is undoubtedly responsible for the observed multiplicity of apparent primary steps.

It was necessary to postulate that approximately 47% of the primary mechanism gives rise to silane fragments that do not form measurable products but contribute to polymer formation. The six steps chosen are speculative and whereas there are many more possible choices, the ones chosen were done so to keep fragmentation at a minimum. Also, as noted in Chapter I, section B-2, the loss of more than two fragments in a primary process is not very likely. The use of β was made necessary because it was not possible to establish the relative importance of steps [72] and [73]. Thus the total primary quantum yield is $0.9983 + \beta$. If β were zero, then the primary quantum yield would be unity to within experimental error. Other values of β would mean that an adjustment would have to be made in steps [78], [79], and [80] to make the primary quantum yield unity.

A better understanding of the primary processes could possibly be achieved by considering the quantum yields for hydrogen, methane, methyl, and methylene formation. The values obtained were: $\phi(H) = 0.101$, $\phi(D) = 0.295$, $\phi(D_2) = 0.135$, $\phi(HD) = 0.262$, $\phi(H_2) = 0.107$, $\phi(CH_3D) = 0.147$, $\phi(CH_4) = 0.053$, $\phi(CH_3) = 0.391$, and $\phi(CH_2) = 0.035$. The need to correlate these easily measurable species (with the possible exception of methyl radicals) with the final silane products led to a somewhat unyielding mechanism which was not very informative. The main conclusion that could be drawn from the

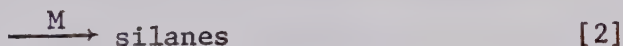
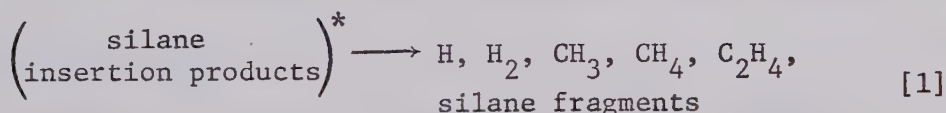
mechanism was that numerous (thirteen) parallel primary steps had to be postulated. This is in contrast to the photochemical decomposition of propane and the other simple hydrocarbons where few (four or five) primary steps (98-106) are adequate to explain the results. From the results presented above, we see that the quantum yield for elimination of molecular fragments is 0.739 and for elimination of radical species, 0.787.

It has been stated that all the unaccounted silane fragments contribute to polymer formation; although it is not possible to study the polymer deposition quantitatively, it is possible to get some idea of its composition from the proposed mechanism. All the H and D atoms would abstract from substrate to give dimethylsilyl radicals while the methyl radicals only undergo recombination. Thus, $\phi((\text{CH}_3)_2\text{SiD}) = 0.396$ and of this, 0.1377 recombine to yield scavengeable Tet-MDS and 0.0913 combine with methyl radicals to give Tri-MS. This leaves $\phi = 0.167$, or 42.2%, unaccounted for. Taking an average value for β of 0.0331, it can be shown that an average polymer unit has the approximate empirical formula: $\text{C}_2\text{H}_5\text{SiD}$.

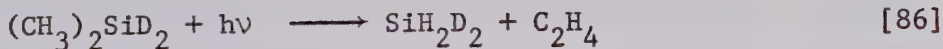
Methylene loss in the photolysis of monomethylsilane was considered but could not be verified; the occurrence of primary step [68] was definitely proven. As stated in section C, the quantum yield of MMS is equal to that of the insertion products of methylene. Methylene loss was also definitely proven in the 1470 \AA photolysis of propane (132,136-140), but was not considered important in the 1470 \AA photolysis of ethane (125-133). This is not unreasonable because CH_3SiHD_2 and $\text{CD}_3\text{CH}_2\text{D}$ can more easily carry away the excess energy

than can SiHD_3 and CHD_3 . It was shown (173) that methylene inserted into the Si-H bond of monomethylsilane 8.9 times faster than into the C-H bond. There would be a change in the insertion ratio for DMS because of a different bond ratio (3:1 for DMS, 1:1 for MMS) and steric factors. Indeed, it has been shown (174) that the ratio for dimethylsilane is 6.9 and for trimethylsilane, 0.80. The present work points to a value of 3.1 for dimethylsilane; this difference could be due to the large errors associated with the analysis of such small product yields in this study or to the different experimental variables between the two studies.

Ethylene was an important reaction product at low pressures and its mode of formation deserves comment. As stated earlier, it probably forms by fragmentation of the hot disilane insertion products:



It could not form in a primary step



because no monosilane was formed in the reaction. It would not form from a hot C_2H_6



because no non-scavengable C_2H_6 was detected among the reaction products. Molecular ethane would not be feasible because of the impossibility of intramolecular abstraction as in the case of CH_4 ,

CH_3D , etc. Therefore primary step [65] appears to be a true primary process and the following sequence does not occur.

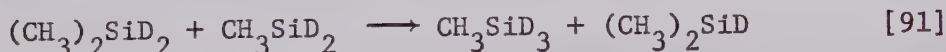
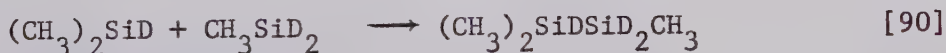


The pressure dependence of ethylene shows that its yield approached zero at about 400 torr; this reinforces the postulate that it comes from a vibrationally hot intermediate. Although this would mean that the quantum yield of the disilane insertion product would be different than indicated, the error is negligible as ethylene is the smallest measureable product. Thus ethylene was not considered in the mechanism derivation.

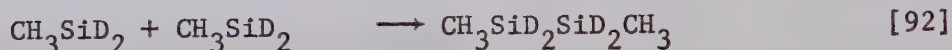
The initially formed silylenes, $(\text{CH}_3)_2\text{Si}$, CH_3SiD and SiD_2 can carry up to 145 kcal/mole excess energy and like methylene, inserted quantitatively. When they insert, there would be an additional gain in energy in the new molecule, due to bond formation. Since the silylenes (in contrast to methylene) inserted solely into the Si-H bond, then the disilane formed can carry up to 230 kcal of excess energy. Therefore reaction [1] would be facile at lower pressures: at higher pressures, these disilanes are stabilized. The diradical SiD_2 would carry the least excess energy (23 kcal) of the silylenes and thus it would be the least difficult to stabilize as shown by the pressure graphs (Figures III-1 and III-2). This is in spite of the fact that DMDS has less vibrational modes to disperse the excess energy than do Tri-MDS or Tet-MDS. These silanes would probably be formed in a singlet electronic excited state (Chapter I, section A-4).

The silylenes do not rearrange to give a 1,3 diradical or an olefin as in the case of ethylidene. The silylenes are in fact, quite stable.

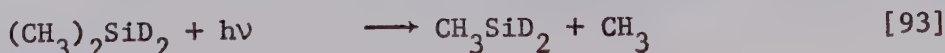
The addition of nitric oxide as a scavenger was necessary to sort out the mechanism (Table III-VI and Figure III-6). The appearance of Tri-MDSO and Tet-MDSO among the products was indicative of the presence of $(\text{CH}_3)_2\text{SiH}$ and CH_3SiH_2 radicals. There are two things to consider in interpreting the nitric oxide results. Firstly, any product yield that increases cannot be rationalized in quantitative terms due to the chain nature of the nitric oxide mechanism. On the other hand, the decrease of a product can be interpreted in quantitative terms because insertion reactions and molecular products are not affected by nitric oxide. The presence of the methylsilyl radical among the products should be examined further. It can be seen that the only products (Tri-MDS and MMS) that could conceivably arise from the monoradical, CH_3SiD_2 , are not affected by nitric oxide. That is, the following reactions do not take place.



Also there is no 1,2-DMDS formed in the DMS system. Therefore the reaction

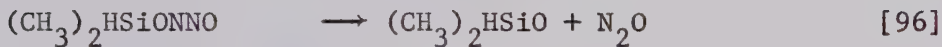
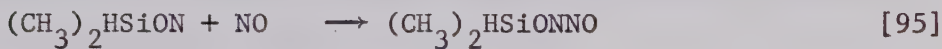
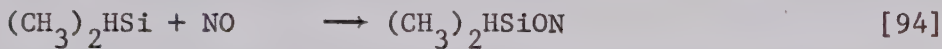


does not occur. Hence, the methylsilyl radical, which could arise only from the reaction

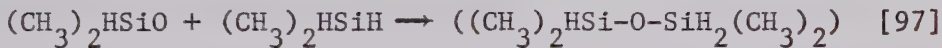


is not formed in the reaction; yet nitric oxide shows that it is present. To explain this ambiguity, it is necessary to examine the mechanism of the nitric oxide scavenging reaction.

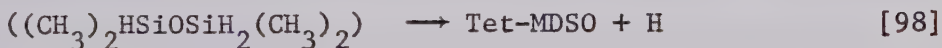
Combining the two mechanisms discussed previously (Chapter I, section A-8) and using the dimethylsilyl radical as an example, we can write the following sequence.



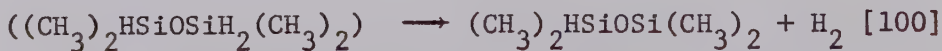
The dimethylsiloxy radical can now undergo a displacement with substrate. The first step would be the formation of the Si-O-Si bond



This reaction can be explained by the high affinity of silicon towards oxygen and the expansion of the valence shells of silicon by utilization of the vacant d-orbitals. The product could then undergo H or CH_3 loss to stabilize itself,

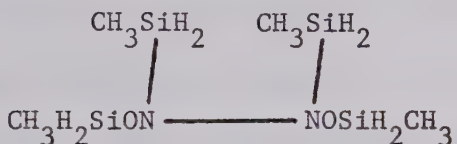


and thus give rise to the two main siloxanes. However, the intermediate can also lose molecular species such as H_2 and CH_4 that would leave behind different silyl radicals.



These new silyl radicals can react with nitric oxide and undergo the above sequence of reactions several times, giving rise to multioxygenated silanes and polymer.

The chain termination step in this reaction is not clear but it is not unreasonable to assume that a certain percentage of the siloxyl monoradicals or the N-O-silyl diradicals would end up in polymer. Also, the diradical could insert to give $(CH_3)_2^{\cdot}HSiONHSiH(CH_3)_2$ which could somehow decompose and/or end up in polymer. This is supported by evidence for such compounds as



in the mercury photosensitization of CH_3SiH_3 in the presence of nitric oxide (84). Several small peaks also appeared in the chromatogram at long retention times, and were impossible to identify positively; they were probably multioxygenated silanes (89).

All the C_2H_6 was scavengeable so the methyl radicals were obviously scavenged by nitric oxide. The mechanism for the scavenging of methyl radicals is in a state of extreme controversy (87). There were no peaks identified that could correspond to the scavenging of methyl radicals. The multioxygenated peaks mentioned earlier could help explain the methyl radical scavenging or the products formed might contribute to the formation of polymer.

The preceding results have given us a fairly lucid picture of the photochemistry of dimethylsilane. However several approximations and choices were made which require further explanation.

Firstly, let us discuss the kinetic derivation that led to the determination of the quantum yields and primary isotope effect for abstraction. It was stated that the quantum yields of steps [10] to [14] would equal those of steps [4] to [8] provided the corresponding rate constants were also identical. However, the rate constants are not equal owing to primary and secondary isotope effects for loss of the various hydrogen species from excited dimethylsilane and dimethylsilane-d₂. This point has been discussed in some detail by Rabinovitch (175) who showed that these effects can be quite important. It can be shown that as the excess energy in the excited molecule becomes large, say greater than 60 kcal/mole, then the primary isotope effect is given by,

$$\frac{k_H}{k_D} = \left(\frac{\mu_D}{\mu_H} \right)^{\frac{1}{2}} \quad [102]$$

where μ_H and μ_D are the reduced masses for motion along the reaction coordinate. The expression for the value of the secondary isotope effect is a lot more complex but it can be shown that its limiting value, when the excess energy of the excited species is large, is approximately 1.05. These values should enable us to obtain a ratio between the various rate constants mentioned above.

A comparison between equations [4] and [10] shows that k_4 is influenced by two secondary isotope effects. Therefore $k_{10} = (1.05)(1.05) k_4 = 1.10 k_4$. It can be seen that k_5 has one primary

and one secondary isotope effect; hence $k_{11} = (1.39)(1.05) k_5 = 1.46 k_5$. When we consider molecular loss, we will take the total mass of the leaving species (D_2 , HD , or H_2) to calculate the primary isotope effect. Hence $k_{12} = 1.37 k_6$; $k_{13} = (1.20)(1.05) k_7 = 1.26 k_7$ and $k_{14} = (1.05)(1.05) k_8 = 1.10 k_8$. It was shown earlier that:

$$(He)^* = \frac{I_a F_{He}}{k_4 + k_5 + k_6 + k_7 + k_8} \quad [25]$$

$$(L)^* = \frac{I_a F_L}{k_{10} + k_{11} + k_{12} + k_{13} + k_{14}} \quad [26]$$

which means that ϕ_4 to ϕ_8 are proportional to $(He)^*$ and ϕ_{10} to ϕ_{14} , to $(L)^*$. For the processes shown in equations [4] - [8] and [10] - [14] we have

$$\phi_4 \propto \frac{k_4}{k_4 + k_5 + k_6 + k_7 + k_8} \quad [103]$$

$$\phi_5 \propto \frac{k_5}{k_4 + k_5 + k_6 + k_7 + k_8} \quad [104]$$

etc.

$$\phi_{10} \propto \frac{k_{10}}{k_{10} + k_{11} + k_{12} + k_{13} + k_{14}} \quad [105]$$

$$\phi_{11} \propto \frac{k_{11}}{k_{10} + k_{11} + k_{12} + k_{13} + k_{14}} \quad [106]$$

etc.

Writing the ratios of the rate constants as $k_{10} = a k_4$, $k_{11} = b k_5$, $k_{12} = c k_6$, $k_{13} = d k_7$, and $k_{14} = e k_8$, where the values of a , b , c ,

d, and e are defined above, we see that ϕ_{10} to ϕ_{14} can be expressed in terms of k_4 to k_8 . However, there is no simple way to express ϕ_{10} in terms of ϕ_4 , ϕ_{11} in terms of ϕ_5 , etc. Therefore we cannot solve for all the quantum yields for the reasons explained in section C. The total primary quantum yields for both dimethylsilane and dimethylsilane-d₂ would be the same if there were no fluorescence, deactivation or chain processes and should equal 1.0. Although the total quantum yield should be equal in both cases, the individual quantum yields, ϕ_4 and ϕ_{10} , ϕ_5 , and ϕ_{11} , etc. need not be equal. This is because we are dealing with a "success" process. That is, (He)* and (L)* need not decompose in the same manner because of the difference in the rate constants for the various types of hydrogen loss. Even though we can obtain a reasonable ratio for the rate constants involved, we cannot obtain a simple ratio for the quantum yields because they represent complex interdependent rate constants. As explained earlier, the results of the ethylene scavenging studies were used to determine ϕ_4 and ϕ_7 .

The system used to differentiate between H and HD loss (ϕ_4 and ϕ_7) from the photolysis of dimethylsilane-d₂ should be further discussed. Mixtures of dimethylsilane-d₂ and ethylene were photolyzed and the X_{HD}/X_{D_2} ratio recorded. The kinetic scheme used involved k_4 to k_8 , and as discussed above, there are primary and secondary isotope effects for the various modes of hydrogen loss between He and L. It follows therefore that there is an isotope effect between k_4 , k_5 , k_6 , k_7 , and k_8 . This is automatically taken into account when discussing a mixture of He and L. However, in the He + E_H system

ratios for k_4 to k_8 must be determined. Using the isotope effects a, b, c, d, and e as mentioned above, we obtain the following rate constants: k_4/a , k_5/b , k_6/c , k_7/d , and k_8/e . The $X_{\text{HD}}/X_{\text{D}_2}$ ratio that was used to find the extent of H and HD loss is given by equation [44]. Since this equation has ϕ_4 , ϕ_5 , ϕ_6 , and ϕ_7 incorporated into it, which in turn are a function of the rate constants, then the results derived from the He system cannot be transposed to the L system. It is obvious that ϕ_4 , ϕ_5 , ϕ_6 , ϕ_7 , and ϕ_8 as derived above are legitimate within the He system.

The product quantum yields were determined only for the L system and were transferred to the He system in order to derive the mechanism. Any difference could be particularly noticeable in the determination of the relative amounts of molecular and radical methane which was dependent on the evaluation of $\phi_{\text{C}_2\text{H}_6}^\circ$, formed by recombination of two methyl radicals. The amounts of methyl radical and methane losses would be influenced by isotope effects in the same way that hydrogen loss would be. Hence $(\phi_{\text{C}_2\text{H}_6}^\circ)_L \neq (\phi_{\text{C}_2\text{H}_6}^\circ)_{\text{He}}$ and $(\phi_{\text{CH}_4}^\circ)_L \neq (\phi_{\text{CH}_3\text{D}}^\circ)_{\text{He}}$. Also, since the heavier products are formed after the loss of the various species in the primary steps then their absolute amounts would be influenced by isotope effects. Although the total primary quantum yield should be 1.0 in both the L and He systems, the relative amounts of the different products could be different: that is, one type of primary loss may be more important in one system than in the other. Results comparing the photolysis of $(\text{CH}_3)_2\text{SiH}_2$ and $(\text{CH}_3)_2\text{SiD}_2$ show that the total quantum yield of all the various products are approximately the same (to within 10%).

The existence of a primary photolysis isotope effect is dramatically illustrated by the following calculations. If we assume that the quantum yields of steps [4] - [8] are identical to those of steps [10] - [14] respectively then the values obtained for ϕ_4 and ϕ_7 ($\phi_4 = \phi(H) = 0.252$ and $\phi_7 = \phi(HD) = 0.111$) from equations [30] - [35] pertaining to the He/L system differ from those obtained by using ethylene as a scavenger ($\phi_4 = \phi(H) = 0.101$ and $\phi_7 = \phi(HD) = 0.262$). Hence the mechanism derived for the $(CH_3)_2SiD_2$ system cannot be conveniently applied to the $(CH_3)_2SiH_2$ system because of the presence of primary and secondary isotope effects for hydrogen loss.

CHAPTER IV

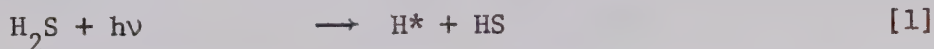
THE PHOTOLYSIS OF HYDROGEN SULPHIDE
IN THE PRESENCE OF DIMETHYLSILANE

The reactions of hydrogen atoms with silanes is an important part of the work described in the previous chapter, and since kinetic data for these systems are sparse, it was decided to examine this problem separately. In this study, the photolyses of H_2S , D_2S , and CH_2O have been employed as hydrogen atom sources. In particular, it was hoped that we could determine the rate constant for hydrogen abstraction from the simple silanes and compare the results with previous work (56). The present study should also enable us to establish some pertinent facts about (a) hot atom reactions with silanes - such as the relative role of abstraction and displacement; (b) the role of possible long lived intermediates and (c) the presence of short chains.

Hydrogen sulphide seemed an ideal source of hydrogen atoms. It exhibits a continuous absorption spectrum (176) over the region $1850 - 2700\text{\AA}$ with a maximum at about 2000\AA . The $HS-H$ bond strength is believed to be 90 ± 2 kcal/mole (177). Since the Cd 2288\AA resonance line was used as the light source, the excess energy carried mostly by the H -atom (178) would be of the order of 35 kcal/mole. The extinction coefficient of H_2S at 2288\AA is quite small, $170 L$ $\text{mole}^{-1} \text{cm}^{-1}$ (176). Therefore the amount of decomposition is small but yet large enough for accurate product analysis. Dimethylsilane

and the other simple methylated and nonmethylated silanes do not absorb at 2288 \AA (92,93).

The primary process in the photolysis of hydrogen sulphide in the 1850 - 2700 \AA spectral region is rupture of the HS-H bond to form (179) an HS ($^2\pi$) radical and a "hot" H (^2S) atom:



The majority of the "hot" H-atoms undergo thermalizing collisions before reaction and thus the symbol H^* refers to a distribution of translational energies. Additional steps in the photolysis of pure H_2S are:



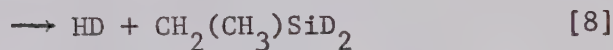
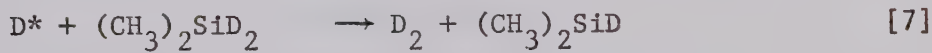
followed by the polymerization of S and S_2 to elemental sulphur which forms a solid coating on the cell walls. The predominant reaction removing SH is step [4] (180).

A. Results

1. The Photolysis of D_2S in the Presence of Dimethylsilane-d₂.

Previous work has shown that abstraction of a hydrogen from the silicon end of the simple methylated silanes is several orders of magnitude faster than from the methyl end (47). We first wanted to establish if the hot hydrogen atom produced in reaction [1] would react in the same way. Hence we photolyzed D_2S in the presence of

dimethylsilane-d₂ (hereafter referred to as DMS-d₂). The results are shown in Table IV-I, where the following reaction sequence is expected to hold:

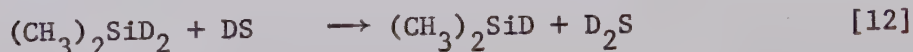
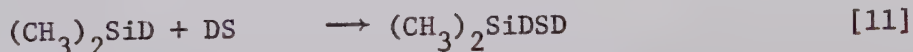


It is seen in the Table that there was a substantial impurity level in D₂S but can be accounted for in the calculations. X_{HD} increases slightly in the presence of DMS-d₂ due to reaction [8], or to some side reaction with a trace impurity. Even if the increase is real, it is obvious that reaction [8] is not very important.

In the photolysis of pure D₂S there was a great deal of sulphur deposited on the walls of the reaction cell due to the reactions



In the presence of the silane there was NO sulphur deposit. Therefore the DS radical is being removed by silane and does not disproportionate. Possible reactions are



It should be noted that reaction [12] is at best thermoneutral and probably endothermic. Silyl mercaptans are not very stable and would probably undergo a condensation reaction, analogous to

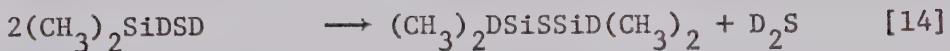
TABLE IV-I

Isotopic Composition of Hydrogen from the Cadmium Lamp
 Photolysis of Deuterium Sulphide in the Presence of
 Dimethylsilane-d₂^a

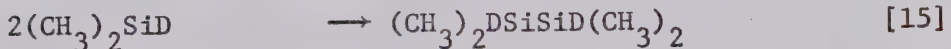
P(D ₂ S) mm	P(DMS-d ₂) mm	t min	X _{H₂}	X _{HD}	X _{D₂}	μmoles hydrogen
0.0	97.5	15	-	-	-	0.00
6.23	0	15	0.0203	0.118	0.862	5.49
5.83	100.8	15	0.0212	0.138	0.841	5.86
5.70	99.9	15	0.0221	0.138	0.844	4.69
5.40	99.9	15	0.0199	0.135	0.845	4.65

^a $\lambda = 2288\text{A}^{\circ}$

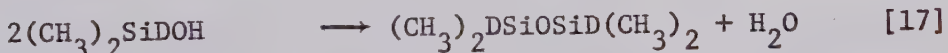
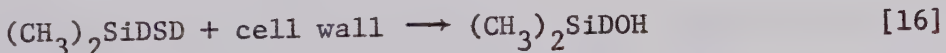
silylanols:



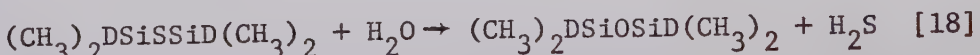
This sequence of reactions should give three condensable products, silylthioether (reaction [14]), silylthiol and tetramethyl-disilane, arising from radical recombination as shown in step [15]:



G.C. showed only two significant peaks, A and B, of approximately the same area. Mass spectrometric analysis showed that B was tetramethyl-disilane. Peak A gave the breakdown spectrum of tetramethyldisiloxane (Tet-MDSO) which is an impurity in DMS with the same retention time as peak A but is only a few per cent of peak A. Hence peak A either breaks down in the ion source and gives no mass spectrum, or Tet-MDSO is an exchange product of peak A originating in the mass spectrograph. The exchange of silylthiol on the cell wall to give silylanol which could then condense to Tet-MDSO, as indicated in reactions [16] and [17], is not very likely since D_2S does not exchange:



It is known however that silylthioethers can condense to siloxanes;

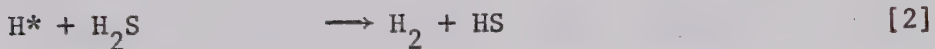
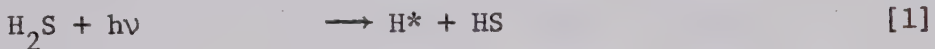


and reaction [18] could easily happen on the walls of the mass spectrograph. Alternatively, peak A could be silylthiol which gives a poor mass spectrum. This problem will be discussed later. It should be emphasized that there was no evidence of any significant amounts of methane, ethane, or monomethylsilane formation.

2. The Photolysis of H_2S in the Presence of Dimethylsilane-d₂.

Effect of Varying $\text{H}_2\text{S}/\text{DMS-d}_2$ Ratios at Constant Exposure Time.

In spite of the mysterious disappearance of the sulphur deposits mentioned previously, it was felt that it would still be possible to obtain a rate constant for hydrogen abstraction from dimethylsilane. The reaction scheme envisioned would be,



It was shown previously that reaction [8] is not important so therefore reaction [20] has been neglected in the scheme. The kinetic rate expression is

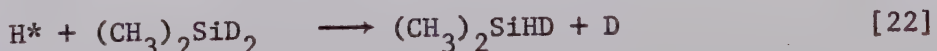
$$\frac{x_{\text{HD}}}{x_{\text{H}_2}} = \frac{k_{19}(\text{DMS-d}_2)}{k_2(\text{H}_2\text{S})} \quad [21]$$

The results are presented in Table IV-II.

The most startling observation is the large yields of D₂ and as can be seen, none of the major reactions [1] - [19] give rise to D₂. As noted previously, there were no sulphur deposits on the cell walls.

There are two possibilities that could give rise to the large amounts of D₂.

(a) A very efficient exchange reaction,



following by abstraction:

TABLE IV-II

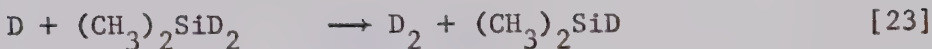
Isotopic Composition of Hydrogen from the Cadmium Lamp

Photolysis of Hydrogen Sulphide in the Presence

of Dimethylsilane-d₂. Constant Time^a

P(H ₂ S) mm	P(DMS-d ₂) mm	t min	X _{H₂}	X _{HD}	X _{D₂}	μmoles hydrogen
2.74	101.5	5	0.0401	0.223	0.736	1.33
4.40	102.5	5	0.0516	0.275	0.674	1.68
8.40	101.9	5	0.0734	0.326	0.601	2.52
12.60	101.9	5	0.106	0.373	0.521	3.39
17.40	101.8	5	0.162	0.433	0.405	3.18
23.40	104.3	5	0.241	0.455	0.305	3.39
20.30	99.4	5	0.217	0.454	0.328	3.70
14.20	104.2	5	0.125	0.393	0.483	3.06
20.0	20.9	5	0.626	0.340	0.0344	2.34
20.0	61.5	5	0.327	0.495	0.178	2.26
20.0	12.1	5	0.771	0.216	0.0128	1.76
20.0	15.3	5	0.749	0.234	0.0172	2.76

^a $\lambda = 2288\text{Å}$



(b) Secondary photolysis of silylthiol, silylthioether, or tetramethyldisilane.

3. Effect of Exposure Time at Constant $\text{H}_2\text{S}/\text{DMS-d}_2$ Ratios.

The results are presented in Table IV-III and shown graphically in Figure IV-1. The last two one-minute runs in the Table were allowed to remain for over one hour in the reaction cell after photolysis before the hydrogen was removed for mass spectral analysis. As can be seen, there is no post photolysis dark reaction taking place. The dramatic time dependence is quite evident, and suggests that D_2 is a secondary product. However, the possibility of the exchange reaction [22] cannot be ruled out as yet.

4. Test for Dark Reactions

The question of a dark reaction should also be considered:



This could account for the results in Table IV-II. A 1:1 mixture of H_2S and DMS-d_2 was allowed to stand overnight. The presence of $(\text{CH}_3)_2\text{SiHD}$ and $(\text{CH}_3)_2\text{SiH}_2$ was checked for, using a 100 Mc-NMR. Since these species were not found, there is obviously no dark reaction.

5. Effect of Added Carbon Dioxide

The question of the occurrence of the possible hot atom exchange reaction [22] can be further clarified by experiments with added CO_2 , Table IV-IV. As can be seen, there is no change in the isotope ratio with added CO_2 . From the work of Cvetanović (181)

TABLE IV-III

Isotopic Composition of Hydrogen from the Cadmium Lamp Photolysis
of Hydrogen Sulphide in the Presence of Dimethylsilane-d₂.

Constant H₂S/DMS-d₂ Ratio^a

P(H ₂ S) mm	P(DMS-d ₂) mm	t min	X _{H₂}	X _{HD}	X _{D₂}	μmoles hydrogen
6.03	99.4	15	0.0462	0.268	0.686	5.78
6.74	100.3	15	0.0481	0.280	0.672	6.04
6.40	102.0	5	0.0625	0.301	0.638	2.10
6.40	103.1	3	0.0725	0.326	0.602	1.43
6.30	105.0	1	0.200	0.477	0.324	0.278
6.60	101.5	1	0.164	0.443	0.393	0.439
6.70	103.2	1	0.167	0.468	0.366	0.354

^a $\lambda = 2288\text{\AA}$

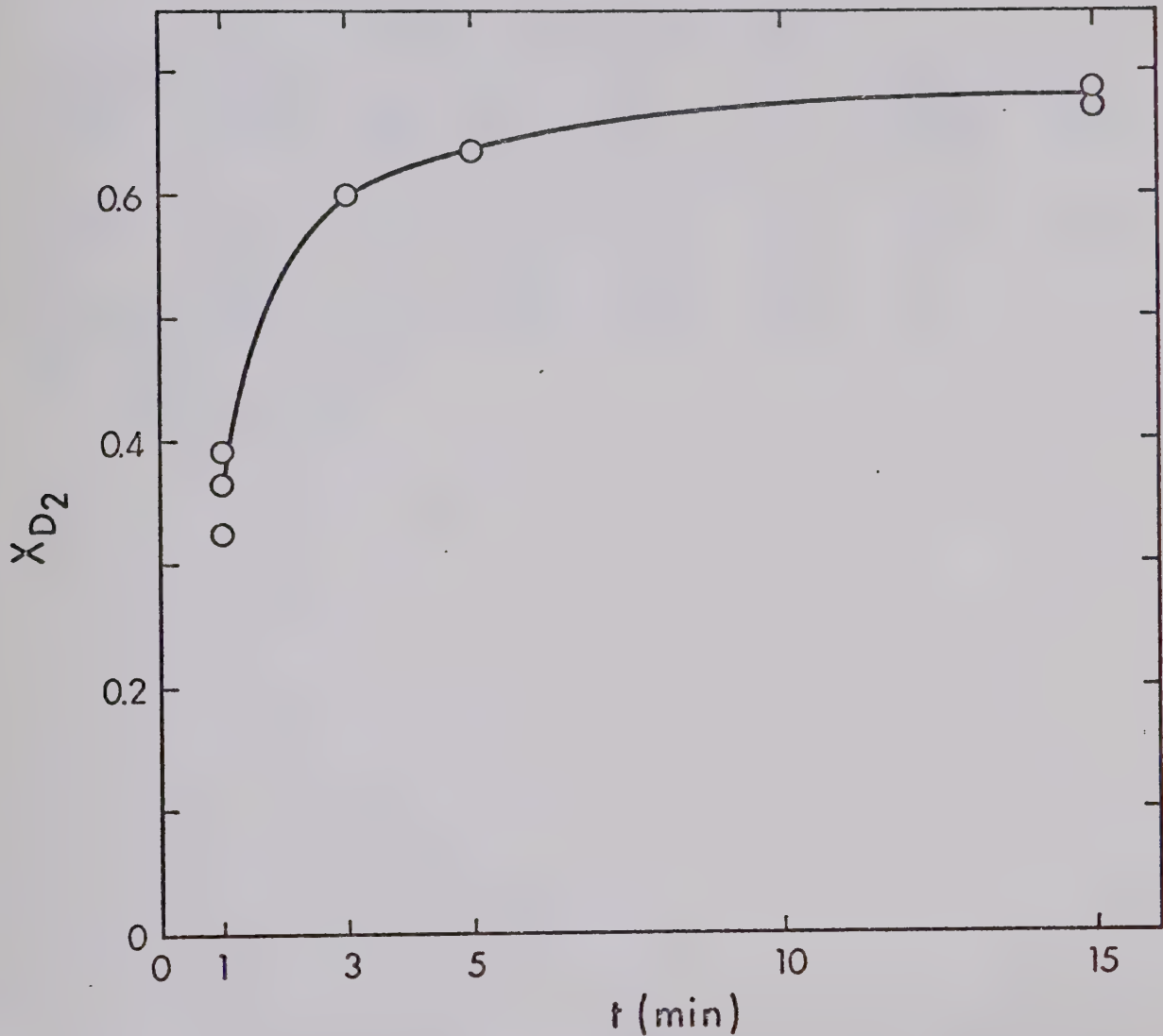


FIGURE IV-1. X_{D_2} as a Function of Time from Cadmium Lamp Photolysis of Hydrogen Sulphide in the Presence of Dimethylsilane-d₂. Constant H₂S/DMS-d₂ Ratio.

TABLE IV-IV

Isotopic Composition of Hydrogen from the Cadmium Lamp Photolysis
of Hydrogen Sulphide in the Presence of Dimethylsilane-d₂.

Effect of Added Carbon Dioxide^a

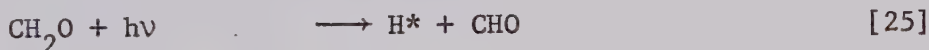
P(H ₂ S) mm	P(DMS-d ₂) mm	t min	X _{H₂}	X _{HD}	X _{D₂}	μmoles hydrogen	P(CO ₂) mm
7.13	99.9	15	0.0444	0.262	0.694	4.86	1015
0.41	11.2	15	0.0509	0.260	0.689	1.17	1033

^a $\lambda = 2288\text{A}^{\circ}$

on the H_2S /olefin system, one would expect CO_2 to thermalize the H^* atoms. This in turn should affect the exchange reaction [22] since Polanyi (182) has shown that exchange reactions are very energy-dependent. Hence it is obvious that reaction [22] is not the dominant mode of D atom formation.

6. The Photolysis of CH_2O in the Presence of Dimethylsilane-d₂.

The role of sulphur in the formation of D_2 was given by using a sulphur-free source of hydrogen atoms, namely the photolysis of formaldehyde. The CHO-H bond strength is approximately the same as the HS-H bond strength in hydrogen sulphide; 85-90 kcal/mole (183). Hence the H atom produced in the photolysis would carry 35 - 40 kcal excess energy at 2288 \AA and would be approximately thermoneutral at 3261 \AA . The primary step is



We will not consider molecular hydrogen formation or the complex photochemistry of formaldehyde (184) here. Table IV-V shows that there is no D_2 formed at 3261 \AA and only trace amounts when the full line system of the cadmium lamp is used. Hence we have to rule out reaction [22] as being important.

7. Photolysis of H_2S in the Presence of Trimethylsilane-d₁

The question of secondary photolysis in the $\text{H}_2\text{S}/\text{DMS-d}_2$ system should be considered in more detail. From previous work, Chapter III, we know that tetramethyldisilane and tetramethyldisiloxane do not photolyze at 2288 \AA . One possibility to consider is the photolysis of silylthioether:

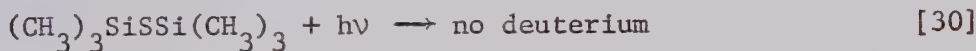
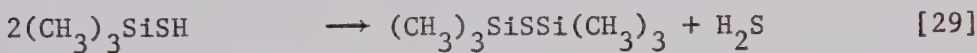
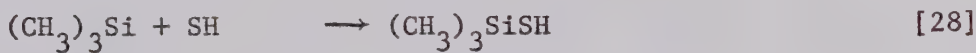
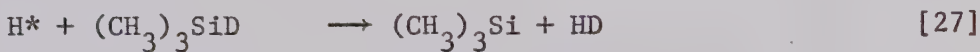
TABLE IV-V

Isotopic Composition of Hydrogen from the Cadmium Lamp Photolysis of
Formaldehyde in the Presence of Dimethylsilane-d₂

P(CH ₂ O) mm	P(DMS-d ₂) mm	t min	X _{H₂}	X _{HD}	X _{D₂}	μmoles hydrogen	Light Source
9.4	100.0	5	0.646	0.329	0.0252	1.17	2288A, 3261A ^o
15.6	104.0	10	0.315	0.685	0.0000	0.216	3261A ^o
26.5	107.8	30	0.495	0.505	0.0000	0.400	3261A ^o

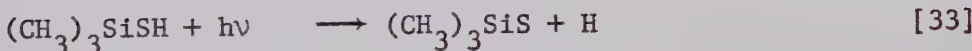
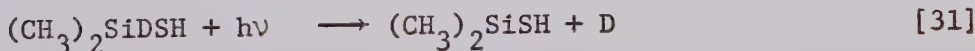


To check this possibility, H_2S was photolyzed in the presence of trimethylsilane-d₁ (hereafter called Tri-MS-d₁). The results are shown in Table IV-VI. Postulating a sequence of reactions for Tri-MS-d₁ similar to DMS-d₂,



As seen in Table IV-VI, large amounts of D_2 are formed and the D_2/HD ratio in this system was nearly identical to that obtained from the $\text{H}_2\text{S}/\text{DMS-d}_2$ system at equal D_2/H_2 levels. Hence we have to rule out the possibility of reaction [26] being the major mode of formation of D atoms.

The secondary photolysis of silylthiol should proceed via



However, reaction [33] would not explain the D_2 formed in the $\text{H}_2\text{S}/\text{Tri-MS-d}_1$ system. Also, reaction [32] may be more important than reaction [31] because the S-H bond would be the absorbing moiety at 2288 $^\circ\text{A}$ and not the Si-D bond. Hence we cannot yet explain the large amounts of D_2 formed in the $\text{H}_2\text{S}/\text{DMS-d}_2$ system.

TABLE IV-VI

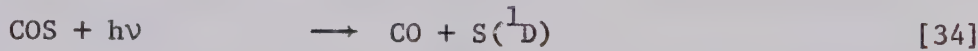
Isotopic Composition of Hydrogen from the Cadmium Lamp Photolysis
of Hydrogen Sulphide in the Presence of Trimethylsilane-d₁^a

P(H ₂ S) mm	P(Tri-MS-d ₁) mm	t min	X _{H₂}	X _{HD}	X _{D₂}	μmoles hydrogen
0.0	104.7	5	-	-	-	0.00
8.1	104.7	5	0.211	0.451	0.338	2.18

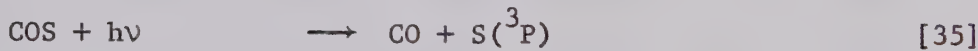
^a $\lambda = 2288\text{A}^{\circ}$

8. Photolysis of COS in the Presence of Dimethylsilane-d₂

That a sulphur containing product is somehow responsible for the high yields of D₂ was proven by auxiliary experiments using COS. The predominant primary process in the photolysis (163) of COS at 2288A is,



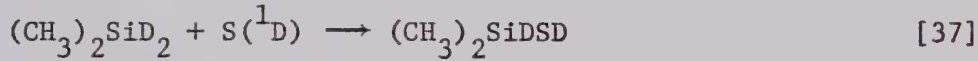
with a small contribution from the spin forbidden process



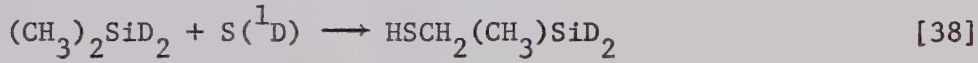
In the presence of paraffins, the S(¹D) atoms will insert to give mercaptans (185):



It has been shown (186) that in the case of methyl-silanes there is predominant insertion into the silicon-hydrogen bond,



although carbon-hydrogen insertion does take place.



The results are given in Table IV-VII. Large amounts of D₂ are formed, as well as the mercaptans formed via reactions [37] and [38]. Apparently these mercaptans photolyze readily to give H and D atoms which in turn abstract to give molecular hydrogen. The absorbing moiety would have to be the sulphur-deuterium or sulphur hydrogen bond (187,188).

IV-VII

Isotopic Composition of Hydrogen from the Cadmium Lamp
 Photolysis of Carbonyl Sulphide in the Presence
 of Dimethylsilane-d₂

P(COS) mm	P(DMS-d ₂)	X _{H₂}	X _{HD}	X _{D₂}	t (min)	μmoles hydrogen
10.3	102.0	0.0534	0.144	0.803	5	1.68
1.34	100.5	0.0802	0.160	0.760	30	1.59

9. Ultraviolet Absorption Study

If secondary photolysis is taking place, then the species responsible must compete favourably in absorption with hydrogen sulphide. To check this hypothesis, matched UV cells with 6.3 mm of H_2S and 102.6 mm of $(\text{CH}_3)_2\text{SiD}_2$ were prepared. The UV spectra were recorded against air in the $2000\text{\AA} - 2500\text{\AA}$ region. The H_2S spectrum had a value of $A \approx 2.6$ at 2288\AA . When the spectra of the cells were run against each other, a zero baseline was obtained. The sample cell was irradiated at 2288\AA line for fifteen minutes and the resulting spectrum recorded against the blank within three minutes. There was no increase in absorption. If there is an absorbing species formed in the system it has to have a lifetime shorter than three minutes.

The sample cell was further irradiated for fifteen minutes and the spectrum at 2288\AA measured within twelve seconds. A value of $A \approx 0.7$ was recorded, which did not change over a period of seven minutes. The sample was irradiated for another fifteen minutes, and the spectrum at 2288\AA measured within fifteen seconds. A value of $A \approx 0.09$ was recorded and did not change over a period of five minutes. This increase in absorption is obviously not due to the silylmercaptan intermediate or to any other intermediate as it is not strong enough. The absorption after such a long period of photolysis is probably due to the build-up of one of the final heavy products, A or/and B, mentioned earlier. However, since B is tetramethyldisilane and does not absorb 2288\AA radiation, then the small increase in absorption is due to compound A.

10. Flash Photolysis with Kinetic Absorption Spectroscopy

The possibility of the presence of a short-lived, strongly absorbing intermediate, was examined by the use of conventional flash photolysis coupled with kinetic absorption spectroscopy. The absorption was monitored between 2088 \AA and 2488 \AA . Flashing one torr $(\text{CH}_3)_2\text{SiD}_2$ in the 2000 \AA - 3000 \AA spectral range with delay times up to 1500 μsec verified that there was not a significant amount of absorption. A similar flash study using 0.05 torr H_2S established an absorption baseline. Next, a mixture of approximately 0.05 torr H_2S and 1 torr $(\text{CH}_3)_2\text{SiD}_2$ was flashed under the same conditions. The plate showed a small increase in absorption over the H_2S baseline, up to 300 μsec . After 300 μsec , the absorption became more intense than the H_2S background and continued to increase up to about 1500 μsec then began to decline.

These results prove the build-up and the start of decay within a short time period ($\approx 1500 \mu\text{sec}$) of an intensely absorbing intermediate. The most likely species is silylmercaptan, formed by the combination of a dimethylsilyl and a thiol radical.

11. Flash Photolysis with Mass Spectrometry

Finally, the transient presence of dimethylsilylthiol was detected in flash photolysis experiments using kinetic mass spectrometry. A ten per cent mixture of H_2S in $(\text{CH}_3)_2\text{SiH}_2$ was flashed in a Vycor cell and the resulting mixture bled into a mass spectrograph. The only significant m/e values recorded, after the 500 μsec delay time of the instrument, were 92, 91, 77, and 76. These masses correspond to $(\text{CH}_3)_2\text{SiHSH}^+$, $(\text{CH}_3)_2\text{SiHS}^+$, $\text{CH}_3\text{SiHSH}^+$, and CH_3SiHS^+ .

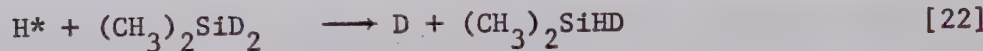
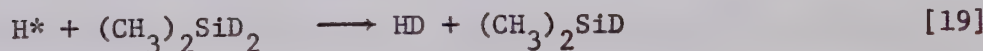
respectively. Further experiments showed that silylthiol had a half life in the order of a few milliseconds.

Although these m/e values were the only significant ones, there was some indication of m/e values of 150, 149, 135, and 134. These peaks would, if real, correspond to silylthioether formed as the condensation product of silylmercaptan. This point will be discussed later.

Similar studies on $\text{H}_2\text{S}/(\text{CH}_3)_3\text{SiH}$, $\text{H}_2\text{S}/\text{CH}_3\text{SiH}_3$, $\text{COS}/(\text{CH}_3)_3\text{SiH}$, $\text{COS}/(\text{CH}_3)_2\text{SiH}_2$, and $\text{COS}/\text{CH}_3\text{SiH}_3$ gave the parent and some fragment ions of the corresponding silylthiol with half lives in the order of a few milliseconds. The largest peaks were recorded with $(\text{CH}_3)_3\text{SiH}$, and decreased as methylation decreased. Experiments with $\text{H}_2\text{S}/\text{SiH}_4$ and COS/SiH_4 could not be meaningfully interpreted.

B. Discussion

The possibility of the occurrence of the exchange reaction [22] can be examined further kinetically. Let us consider the following kinetic scheme:



This is the simplest scheme that does not consider HS radicals as contributing to hydrogen production. It can be shown that:

$$\frac{X_{HD}}{X_{D_2}} = \frac{k_{19}}{k_{22}} + \left[\frac{k_{19}}{k_{22}} \cdot \frac{(k_{39} + k_{40})}{k_{23}} + \frac{k_{39}}{k_{23}} \right] \cdot \frac{(H_2S)}{((CH_3)_2SiD_2)} \quad [41]$$

The equation is derived in detail in *Appendix C*. A plot of equation [41] from the data in Table IV-II is shown in Figures IV-2 and IV-3. As can be seen, the results do not give a straight line as predicted. Other kinetic relationships were derived from the above reaction scheme but none fit the data. This kinetic treatment, in conjunction with the carbon dioxide cooling experiments and in particular, the use of formaldehyde as an alternative hydrogen atom source, definitely rules out the simple exchange reaction [22].

The marked time effect of X_{D_2} at constant $H_2S/DMS-d_2$ ratios was shown in Figure IV-1. In fact, X_{D_2} approaches zero at low exposure times and indicates the importance of secondary photolyses. It is difficult to see how an exchange reaction could be time dependent but the possibility can be checked quite easily because a long lived intermediate has to be involved. In the $H_2S/DMS-d_2$ system, such intermediates could be $((CH_3)_2SiD_2H)^*$ or $((CH_3)_2SiD_2SH)^*$ which might be expected to decompose to give D-atoms. However, when the reaction mixture was allowed to stand after a short period of photolysis (Table IV-III) there was essentially no change in the isotopic composition of hydrogen, and we can effectively rule out the presence of a long lived intermediate and the subsequent exchange reaction. Also, if an exchange reaction took place, it should release methyl radicals as well as deuterium atoms. The methyl

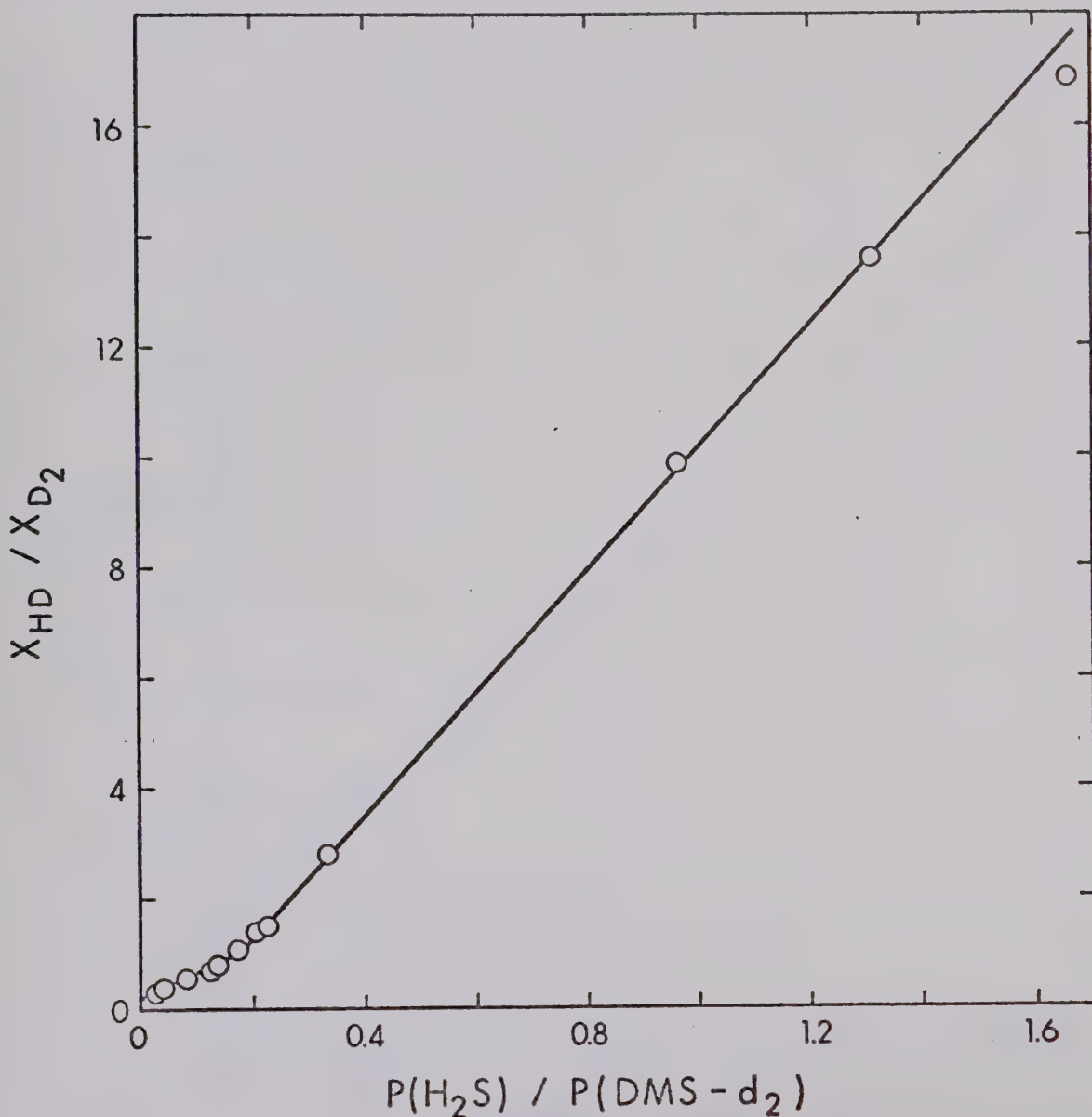


FIGURE IV-2. A Plot in Accordance with Equation [41] for the Cadmium Lamp Photolysis of Hydrogen Sulphide in the Presence of Dimethylsilane-d₂. Constant Time.

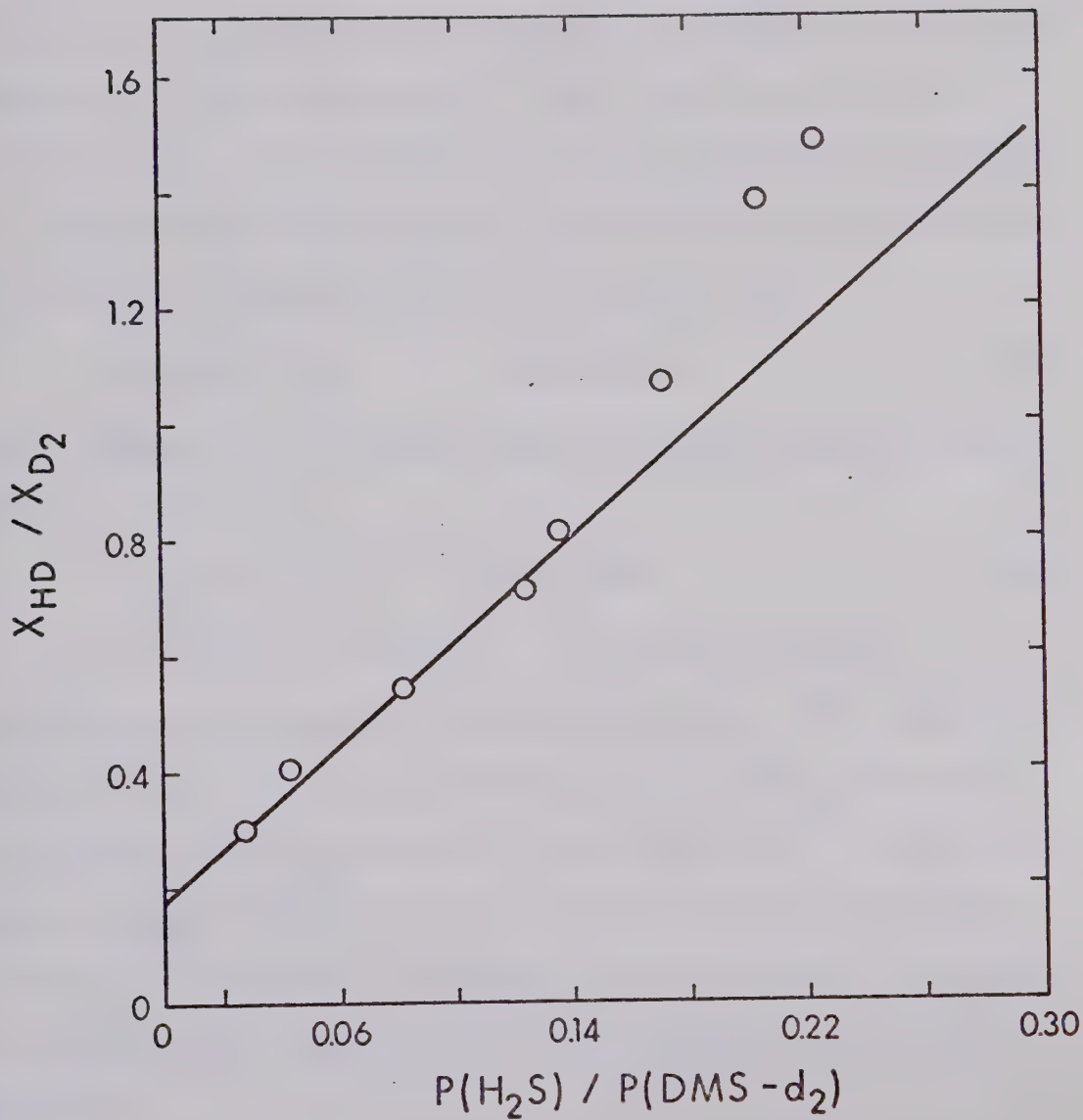
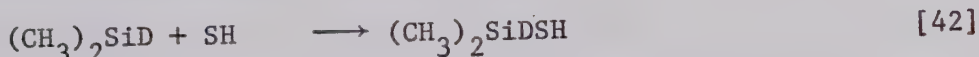


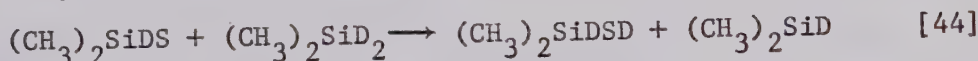
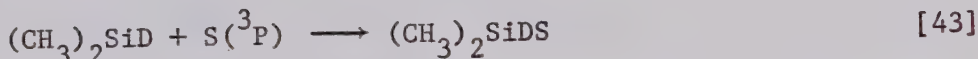
FIGURE IV-3. A Plot in Accordance with Equation [41] for the Cadmium Lamp Photolysis of Hydrogen Sulphide in the Presence of Dimethylsilane-d₂. Constant Time. Low H₂S/DMS-d₂ Ratios.

radicals would form methane by abstraction from substrate, and ethane, by radical recombination. The absence of methane, ethane and MMS among the products and the non-variance of the total hydrogen yield in Table IV-I rules out all types of exchange reactions.

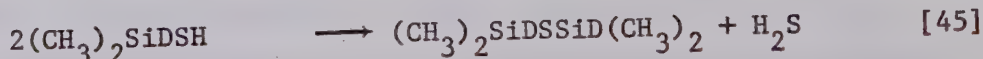
It has been mentioned that there were only two heavy products formed in the $D_2S/DMS-d_2$ system in about equal amounts, tetramethyl-disilane and A (silylthioether ?). Since there were no sulphur deposits, then all the DS or HS radicals were undoubtedly scavenged in a radical recombination reaction with the dimethylsilyl radicals, as indicated in reactions [11] and [42] respectively:



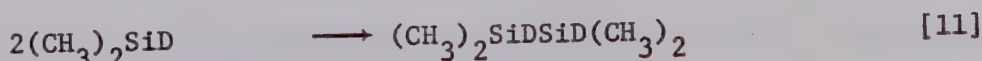
Another possible, but less likely means of silylmercaptan formation would be,



For clarity, let us consider the $H_2S/DMS-d_2$ system. The number of H atoms would equal the number of dimethylsilyl radicals which would now recombine with the SH radical to give $(CH_3)_2SiDSH$. Since there was no noticeable sulphur deposits, the HS radicals do not disportionate as indicated in reactions [3] and [4] to any great extent. If the sole fate of silylmercaptan were stabilization or disportionation,

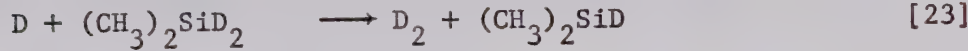
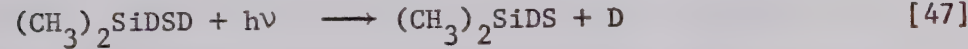
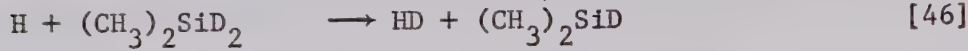
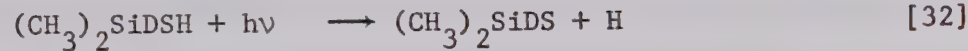
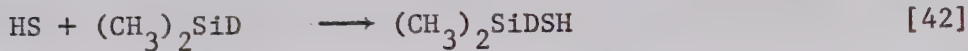
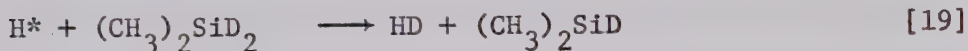


then tetramethyldisilane formation would be suppressed:



Therefore it seems that there is a surplus of dimethylsilyl radicals over HS radicals. This surplus would also explain why all the HS radicals are so effectively scavenged before they react with each other. Hence any mechanism proposed must create dimethylsilyl radicals as well as provide for D_2 formation.

The evidence indicates the following mechanism:



The $(CH_3)_2SiDS$ radical now acts as the chain carrier, producing, via reaction [44], $(CH_3)_2SiDSD$ which contributes to D atom formation in reaction [47] and molecular D_2 formation in reaction [23]. This reaction scheme gives a surplus of dimethylsilyl radicals which contribute to the formation of tetramethyldisilane.

This mechanism is an example of a photochemical chain.

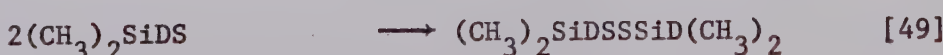
The length of this chain can be estimated by considering the yield of HD and D_2 when $P(DMS-d_2) \gg P(H_2S)$. It must be remembered that the chain length is time dependent. At small concentrations of H_2S , reaction [39] to form HD will not be very important so therefore all the HD will be formed in reactions [19] and [46]. Reaction [32] gives the first link in the photochemical chain formation of D_2 . If all the

$(\text{CH}_3)_2\text{SiDSH}$ undergoes reaction [32] then half the HD would be formed in reaction [19] and half in reaction [46]. Therefore the ratio $X_{\text{D}_2} / \frac{1}{2} X_{\text{HD}}$ will give the length of the photochemical chain at a given time. For example, (Table IV-III) the chain length decreases from ~ 5 for a 15 min. photolysis to ~ 1.5 , for a photolysis time of one minute.

Since this is a photochemical chain then the termination step would be the physical act of turning off the photolysis lamp. Silylmercaptan has been shown to be a stronger absorber than hydrogen sulphide, due to its large extinction coefficient rather than its concentration since the total conversion was less than five per cent in most cases. Silylmercaptan, although present in small but significant concentration, has a half life of the order of a few milliseconds and could not be detected at all using conventional ultraviolet spectroscopy. The suspected presence of tetramethyl-silylthioether among the products, and the short lifetime of silylmercaptan, support the hypothesis that silylmercaptan can somehow form silylthioether. That is, during the photolysis there is a competition between photochemical decomposition of silylmercaptan and its decay via reaction [45] and even more likely, reaction [48].



The occurrence of reaction [49] could not be proven because the disulphide formed would probably be unstable with respect to decomposition.



However, reaction [48] should predominate because of the large concentration of dimethylsilyl radicals present.

In any event, tetramethylsilylthioether is most likely the major reaction product labeled A. That it cannot be conveniently identified by conventional mass spectrometry is not surprising. As mentioned in section A-1, peak A gave the breakdown pattern of the oxygen analog - tetramethyldisiloxane. The condensation of silyl-thioethers to siloxanes is well known and could easily happen on the metal walls of the mass spectrograph. Sulphur-oxygen exchange has been noted in these experiments. For example, when D_2S was introduced into the mass spectrograph to ascertain its isotopic purity, only the spectrum of D_2O was obtained. The spectrum of H_2S can only be obtained when a large enough sample is introduced so that the mass spectrograph walls are purged. Hence it must be concluded that peak A is the silylthioether which gives a misleading mass spectrum.

CHAPTER V

SUMMARY AND CONCLUSIONS

The preceding chapters have given a fairly reasonable picture of the photochemistry of the simple silanes and in particular, of dimethylsilane. The direct photolysis of dimethylsilane was accomplished with a xenon resonance lamp and the reactions of H-atoms with dimethylsilane were examined separately. The resulting product distribution was accounted for in both studies, and mechanisms were proposed.

The photolytic decomposition of dimethylsilane yielded ten products and a polymer deposit on the cell window. By the use of pressure studies, time studies, scavengers, and deuterium labelling, it was possible to show that the decomposition was initiated by thirteen primary steps. Many of these steps can be further subdivided because they involve the loss of two fragments. The vacuum ultraviolet spectra of all the simple methylated silicon hydrides, their deuterated counterparts, and trimethylmonofluorosilane, were recorded and incorporated into the photolysis study. Although the 1470 \AA resonance line of the xenon lamp falls in the predominately silicon-hydrogen absorbing region, silicon-hydrogen cleavage is not the dominate mode of decomposition. That multifragmentation occurs to such a large extent, coupled with the need to postulate at least thirteen primary steps, is a clear indication of energy delocalization, that is, absorption of photon energy in one moiety can lead to

decomposition along a variety of pathways. The need to postulate such a complex mechanism is in contrast to the vacuum ultraviolet photochemical decomposition of the simple hydrocarbons.

The photolysis of hydrogen sulphide in the presence of dimethylsilane established that hot hydrogen atoms do not abstract from the carbon-hydrogen bond and do not undergo an exchange reaction. The presence of a strongly absorbing transient intermediate was needed to explain the isotopic hydrogen distribution. This silylmercaptan had a half-life in the order of a few milliseconds and reached a photostationary state during the photolysis. The silylthiol radical formed during the photolysis acted as a chain carrier. Such photochemical chains are not operative in the corresponding carbon systems and the high extinction coefficient of the silylmercaptan must indicate some type of interaction between the silicon and sulphur atoms. Indeed, the proposed condensation reaction for self-destruction of the silylmercaptan would indicate this.

The results on dimethylsilane have led to a revision (95, 189-191) of the proposed mechanism (92,93) for the photolysis of monomethylsilane, Table I-II. Several more HD-forming steps, analogous to [77] and [78] (Chapter III) were included in the primary sequence, all the methane was shown to form in a molecular process and the kinetic treatment became at least as complex as that described for dimethylsilane. The two systems thus exhibit many similarities in the primary fragmentation steps but, at present, quantum yield data at various wavelengths cannot be assessed on a structural basis.

The trends and findings of this study reflect on the physico-chemical differences between carbon and silicon and indicate the desirability of studying the photochemistry of elements other than the first row. The field of silicon photochemistry is a new one and it is obvious that more work is required before it is as well understood as hydrocarbon photochemistry. Future studies should include further photochemical photolyses of silanes and the recording of their spectra so that an attempt at correlation can be undertaken. The reaction of hydrogen and sulphur atoms with silanes is a virgin domain and thus such studies are most desirable. In particular, the flash photolysis of hydrogen and sulphur atom donors in the presence of silanes, using mass spectrometry and kinetic absorption spectroscopy to monitor the transients should yield much valuable information on silane reactions.

BIBLIOGRAPHY

1. J. G. Calvert and J. N. Pitts, Jr., *Photochemistry*, John Wiley and Sons, Inc., New York (1966).
2. V. Bažant, V. Chvalousky and J. Rathousky, *Organosilicon Compounds*, Academic Press, New York (1965).
3. C. J. Attridge, *Organometal Chem. Rev.*, A, 5, 323 (1970).
4. M. C. Flowers and L. E. Gusel'nikov, *J. Chem. Soc.*, B, 419 (1968).
5. R. S. Mulliken, *J. Am. Chem. Soc.*, 72, 4493 (1950).
6. B. E. Douglas and D. H. McDaniel, *Concepts and Models of Inorganic Chemistry*, Ginn, Boston, (1965), p. 58.
7. R. S. Mulliken, C. A. Rieke, D. Orloff and H. Orloff, *J. Chem. Phys.*, 17, 1248 (1948).
8. H. H. Jaffé, *J. Chem. Phys.*, 21, 258 (1953).
9. K. S. Pitzer, *J. Chem. Soc.*, 70, 2140 (1948).
10. C. E. Moore, *Atomic Energy Levels*, Natl. Bur. Std. U.S. Circ., 467, Vol. I (1948), Vol. II (1952), Vol. VIII (1958).
11. J. N. Murrell and M. Randic, *Valence Theory* (J. N. Murrell, S. F. A. Kettle and J. M. Tedder, eds.), John Wiley and Sons, New York (1965), p. 54.
12. E. A. V. Ebsworth, *Organometallic Compounds of the Group IV Elements*, Vol. I, ed. by A. G. MacDiarmid, Marcel Dekker, Inc., New York (1968).
13. B. G. Ramsy, *Electronic Transitions in Organometalloids*, Academic Press, Inc., New York (1969).
14. C. F. Shaw, III, and A. L. Allred, *Organometal Chem. Rev.*, A, 5, 95 (1970).

15. F. A. Cotton and G. Wilkinson, *Advanced Inorganic Chemistry*, second edition, Interscience, New York (1966), p. 103.
16. I. M. T. Davidson and I. L. Stephenson, *J. Chem. Soc.*, A, 282 (1968).
17. S. J. Band, I. M. T. Davidson and C. A. Lambert, *J. Chem. Soc.*, A, 2068 (1968).
18. P. Potzinger and F. W. Lampe, *J. Phys. Chem.*, 74, 719 (1970).
19. I. M. T. Davidson and C. A. Lambert, *Chem. Comm.*, 1276 (1969).
20. R. P. Clifford, B. G. Gowenlock, C. A. F. Johnson and J. Stevenson, *J. Organometal Chem.*, 34, 53 (1972).
21. G. G. Hess, F. W. Lampe and A. L. Yerger, *Annals N.Y. Acad. Sci.*, 136, 106 (1966).
22. A. E. Douglas, *Can. J. Phys.*, 35, 71 (1957).
23. O. P. Strausz, E. Jakubowski, H. S. Sandhu and H. E. Gunning, *J. Chem. Phys.*, 51, 552 (1969).
24. P. Potzinger and F. W. Lampe, *J. Phys. Chem.*, 74, 587 (1970).
25. R. L. Morehouse, J. J. Christiansen and W. Gordy, *J. Chem. Phys.*, 45, 1751 (1966).
26. G. S. Jackel and W. Gordy, *Phys. Rev.*, 176, 443 (1968).
27. J. H. Sharp and M. C. R. Symons, *J. Chem. Soc.*, A, 3068 (1970).
28. L. Pauling, *J. Chem. Phys.*, 51, 2767 (1969).
29. H. Sakurai, M. Murakami and M. Kumada, *J. Am. Chem. Soc.*, 91, 519 (1969).
30. U. Wannegat and C. Krüger, *Z. Anorg. Chem.*, 326, 304 (1964).
31. E. Eaborn, R. A. Jackson and R. Pearce, *Chem. Comm.*, 920 (1967).

32. R. A. Jackson, *Essays on Free Radical Chemistry*, Special Publication #24, The Chemical Society, Burlington House, London (1970), p. 295-321.

33. I. M. T. Davidson, *Quarterly Reviews*, 25, 111 (1971).

34. R. A. Jackson, *Advances in Free Radical Chemistry*, ed. G. H. Williams, Academic Press, New York (1969), p. 231.

35. W. Kirmse, *Carbene Chemistry*, second edition, Academic Press, New York (1971).

36. H. M. Frey, *Progress in Reactions Kinetics*, ed. G. Porter, V. 2, MacMillan Co., New York (1964).

37. W. H. Atwell and D. R. Weyenberg, *Angew Chem. Internat. Edit.*, 8, 469 (1969).

38. G. Herzberg and R. D. Verma, *Can. J. Phys.*, 42, 395 (1964).

39. I. Dubois, G. Herzberg and R. D. Verma, *J. Chem. Phys.*, 47, 2462 (1967).

40. P. C. Jordan, *J. Chem. Phys.*, 44, 3400 (1966).

41. D. E. Milligan and M. E. Jacox, *J. Chem. Phys.*, 52, 2594 (1970).

42. W. H. Atwell and D. R. Weyenberg, *J. Organometal Chem.*, 5, 594 (1966).

43. P. S. Skell and E. J. Goldstein, *J. Am. Chem. Soc.*, 86, 1442 (1964).

44. W. H. Atwell and D. R. Weyenberg, *J. Am. Chem. Soc.*, 90, 3438 (1968).

45. H. H. O'Neal, S. Pavlou, T. Lubin, M. A. Ring and L. Batt, *J. Phys. Chem.*, 75, 3945 (1971).

46. T. N. Bell and A. E. Platt, *J. Phys. Chem.*, 75, 603 (1971).

47. O. P. Strausz, E. Jakubowski, H. S. Sandhu and H. E. Gunning, *J. Chem. Phys.*, 51, 552 (1969); and references therein.

48. R. E. Berkley, Ph.D. Thesis, University of Alberta, 1970.
49. J. A. Kerr and D. M. Timbin, *Int. J. Chem. Kin.*, 3, 1 (1971); *ibid.*, 3, 69 (1971).
50. I. Safarik, R. Berkley and O. P. Strausz, *J. Chem. Phys.*, 54, 1919 (1971).
51. Y. Nagai, H. Matsumoto, M. Hayashi, E. Tajima, M. Ohtsuki and N. Sekikawa, *J. Organometal Chem.*, 29, 209 (1971).
52. E. R. Morris, J. C. J. Thynne, *Trans. Far. Soc.*, 66, 183 (1970).
53. T. N. Bell and A. E. Platt, *Int. J. Chem. Kin.*, 2, 299 (1970).
54. E. Jakubowski, H. S. Sandhu, H. E. Gunning and O. P. Strausz, *J. Chem. Phys.*, 52, 4242 (1970).
55. T. N. Bell and U. F. Zucker, *J. Phys. Chem.*, 74, 979 (1970).
56. K. Obi, H. S. Sandhu, H. E. Gunning and O. P. Strausz, to be published.
57. T. L. Pollock, H. S. Sandhu and O. P. Strausz, to be published.
58. Von M. A. Contineanu, D. Mihelcic and R. N. Schindler, *Ber. Bunsenges Physik Chem.*, 75, 426 (1971).
59. L. C. Glasgow, G. Albrich and P. Potzinger, *Chem. Phys. Lett.*, 14, 466 (1972).
60. W. L. Hase, W. G. Breiland, P. W. McGrath and J. W. Simons, *J. Phys. Chem.*, 76, 459 (1972).
61. W. L. Hase and J. W. Simons, *J. Organometal Chem.*, 32, 47 (1971).
62. W. L. Hase and J. W. Simons, *J. Chem. Phys.*, 54, 1277 (1971).
63. J. H. Purnell and R. Walsh, *Proc. Roy. Soc. (London)*, A, 293, 543 (1966).
64. M. A. Ring, M. J. Puentes and H. E. O'Neal, *J. Am. Chem. Soc.*, 92, 4845 (1970).

65. P. John and J. H. Purnell, *J. Organometal Chem.*, 29, 233 (1971).
66. I. M. T. Davidson, *J. Organometal Chem.*, 24, 97 (1970).
67. I. M. T. Davidson and C. A. Lambert, *J. Chem. Soc.*, A, 882 (1971).
68. M. Bowrey and J. H. Purnell, *Proc. Roy. Soc. (London)*, A, 321, 341 (1971); and references therein.
69. M. A. Ring, R. B. Baird and P. Estacio, *Inorg. Chem.*, 9, 1004 (1970).
70. P. Estacio, M. D. Sefcik, E. K. Chan and M. A. Ring, *Inorg. Chem.*, 9, 1068 (1970).
71. R. B. Baird, M. D. Sefcik and M. A. Ring, *Inorg. Chem.*, 10, 883 (1971).
72. H. Sakurai, A. Hosemi and M. Kumada, *Chem. Comm.*, 4 (1969).
73. C. Eaborn and J. M. Simmie, *Chem. Comm.*, 1426 (1968).
74. J. A. Connor, R. N. Haszeldine, G. J. Leigh and R. D. Sedgwick, *J. Chem. Soc.*, 768 (1967).
75. L. E. Gusel'nikov, N. S. Nametkin, T. Kh. Islamov, A. A. Sobtsov and V. M. Vdovin, *Bull. Acad. Sci. USSR, Div. Chem. Sci. (Eng. trans.)* 20, 71 (1971).
76. N. S. Nametkin, T. Kh. Islamov, L. E. Gusel'nikov, A. A. Sobtsov and V. M. Vdovin, *Bull. Acad. Sci. USSR, Div. Chem. Sci. (Eng. trans.)* 20, 76 (1971).
77. R. A. Shaw, *Pure Appl. Chem.*, 13, 297 (1966).
78. J. F. Schmidt and F. W. Lampe, *J. Phys. Chem.*, 73, 2706 (1969).
79. G. J. Mains and J. Dedinas, *J. Phys. Chem.*, 74, 3476 (1970).
80. G. H. Mains and J. Dedinas, *J. Phys. Chem.*, 74, 3483 (1970).
81. H. J. Emeleus and K. Stewart, *Trans. Far. Soc.*, 32, 1577 (1936).
82. A. J. Yarwood, O. P. Strausz and H. E. Gunning, *J. Chem. Phys.*, 41, 1705 (1964).

83. H. Niki and G. J. Mains, *J. Phys. Chem.*, 68, 304 (1964).
84. M. A. Nay, G. N. C. Woodall, O. P. Strausz and H. E. Gunning, *J. Am. Chem. Soc.*, 87, 179 (1965).
85. O. P. Strausz, T. L. Pollock, E. Jakubowski and H. E. Gunning, to be published.
86. A. H. Sehon and D. de B Darwent, *J. Chem. Phys.*, 23, 822 (1955).
87. J. Heicklen and N. Cohen, *Advances in Photochemistry*, Vol. 5, ed. W. A. Noyes, Jr., G. S. Hammond and J. N. Pitts, Jr., Interscience Publishers, New York (1968).
88. E. Kamaratos and F. W. Lampe, *J. Phys. Chem.*, 74, 2267 (1970).
89. T. L. Pollock, H. S. Sandhu and O. P. Strausz, to be published.
90. O. P. Strausz, K. Obi and W. K. Duholke, *J. Am. Chem. Soc.*, 90, 1359 (1968).
91. K. Obi, A. Clement, H. E. Gunning and O. P. Strausz, *J. Am. Chem. Soc.*, 91, 1622 (1969).
92. Y. Harada, J. N. Murrell and H. H. Sheena, *Chem. Phys. Lett.*, 1, 595 (1968).
93. A. G. Alexander, O. P. Strausz, R. Pottier and G. P. Semeluk, *Chem. Phys. Lett.*, 13, 608 (1972).
94. T. L. Pollock, H. Makada and O. P. Strausz, to be published.
95. A. G. Alexander, K. Obi and O. P. Strausz, to be published.
96. L. Gammie and O. P. Strausz, to be published.
97. M. A. Ring, G. D. Beverly, F. H. Koester and R. P. Hollandsworth, *Inorg. Chem.*, 8, 2033 (1969).
98. J. R. McNesby and H. Okabe, *Advances in Photochemistry*, 3, 157 (1964), ed. W. A. Noyes, Jr., G. S. Hammond and J. N. Pitts, Jr., Interscience Publishers (1964).

99. J. R. McNESBY, *Actions Chim. Biol. Radiat.*, 9, 39 (1966).
100. P. AUSLOOS and S. G. LIAS, *Radiat. Res. Rev.*, 1, 75 (1968).
101. L. W. SIECK, *Fundamental Processes in Radiation Chemistry*, edited by P. AUSLOOS, New York, Interscience (1968), p. 119.
102. A. D. BROADBENT, J. N. PITTS, JR. and E. WHITTLE, *Annual Survey of Photochemistry*, edited by N. J. TURRO, G. S. HAMMOND, J. N. PITTS, JR. and D. VALENTINE, JR., Wiley-Interscience, New York, 1, 422 (1967).
103. A. D. BROADBENT, J. N. PITTS, JR. and E. WHITTLE, *Annual Survey of Photochemistry*, edited by N. J. TURRO, G. S. HAMMOND, J. N. PITTS, JR. and D. VALENTINE, JR., Wiley-Interscience, New York, 2, 302 (1968).
104. D. PHILLIPS, *Specialist Periodical Reports - Photochemistry*, edited by D. BRYCE-SMITH, The Chemical Society, London, 1, 101 (July 1968 - June 1969).
105. D. PHILLIPS, *Specialist Periodical Reports - Photochemistry*, edited by D. BRYCE-SMITH, The Chemical Society, London, 2, 171 (July 1969 - June 1970).
106. P. J. AUSLOOS and S. G. LIAS, *Ann. Rev. Phys. Chem.*, 22, 85 (1971).
107. W. GROTH, *Z. Physik Chem. (Leipzig)*, B37, 307 (1937).
108. B. H. MAHAN, *J. Chem. Phys.*, 33, 959 (1960).
109. Reference 98, page 174.
110. Reference 98, page 173.
111. D. KATAKIS and H. TAUBE, *J. Chem. Phys.*, 36, 416 (1962).
112. P. WARNECK, *J. Chem. Phys.*, 41, 3435 (1964).
113. T. G. SLANGER, *J. Chem. Phys.*, 45, 4127 (1966).

114. A. -Y. Ung and H. I. Schiff, *Can. J. Chem.*, 44, 1981 (1966).
115. M. E. Jacox and D. E. Milligan, *J. Chem. Phys.*, 54, 919 (1971).
116. R. S. Sach, *Int. J. Radiat. Phys. Chem.*, 3, 45 (1971).
117. T. G. Slanger and G. Black, *J. Chem. Phys.*, 54, 1889 (1971).
118. L. F. Loucks and R. J. Cvetanović, *J. Chem. Phys.*, 56, 321 (1972).
119. H. Okabe and D. A. Becker, *J. Chem. Phys.*, 39, 2549 (1963).
120. B. A. Lombos, P. Sauvageau and C. Sandorfy, *Chem. Phys. Lett.*, 1, 382 (1967).
121. B. A. Lombos, P. Sauvageau and C. Sandorfy, *Chem. Phys. Lett.*, 1, 221 (1967).
122. B. A. Lombos, P. Sauvageau and C. Sandorfy, *J. Mol. Spec.*, 24, 253 (1967).
123. B. A. Lombos, P. Sauvageau and C. Sandorfy, *Chem. Phys. Lett.*, 1, 42 (1967).
124. R. A. Holroyd, *J. Am. Chem. Soc.*, 91, 2208 (1969).
125. H. Okabe and J. R. McNesby, *J. Chem. Phys.*, 34, 668 (1961).
126. K. Faltings, *Ber. Deut. Chem. Ges.*, 72B, 1207 (1939).
127. M. H. J. Wijnen, *J. Chem. Phys.*, 24, 85 (1956).
128. R. F. Hampson, Jr., J. R. McNesby, H. Akimoto and I. Tanaka, *J. Chem. Phys.*, 40, 1099 (1964).
129. R. F. Hampson, Jr., and J. R. McNesby, *J. Chem. Phys.*, 42, 2200 (1965).
130. H. Akimoto, K. Obi and I. Tanaka, *J. Chem. Phys.*, 42, 3864 (1965).
131. K. Obi and I. Tanaka, *J. Chem. Phys.*, 44, 424 (1966).

132. H. Akimoto and I. Tanaka, *Ber. Bunsenges Physik Chem.*, 72, 134 (1968).

133. S. G. Lias, G. J. Collin, R. E. Rebbert and P. Ausloos, *J. Chem. Phys.*, 52, 1841 (1970).

134. G. von Bünau, K. Nieswandt, D. Henneberg and G. Schomburg, *Ber. Bunsenges Physik Chem.*, 73, 891 (1969).

135. Y. Ogata, K. Obi, H. Akimoto and I. Tanaka, *Bull. Chem. Soc. Japan*, 44, 2671 (1971).

136. H. Okabe and J. R. McNesby, *J. Chem. Phys.*, 37, 1340 (1962).

137. P. Ausloos, S. G. Lias and I. B. Sandoval, *Disc. Faraday Soc.*, 36, 66 (1963).

138. P. Ausloos and S. G. Lias, *J. Chem. Phys.*, 44, 521 (1966).

139. P. Ausloos and S. G. Lias, *Ber. Bunsenges Physik Chem.*, 72, 187 (1968).

140. A. K. Dhingra and R. D. Koob, *J. Phys. Chem.*, 74, 4490 (1970).

141. K. Obi, H. Akimoto, Y. Ogata and I. Tanaka, *J. Chem. Phys.*, 55, 3822 (1971).

142. D. Peters, *J. Chem. Phys.*, 41, 1046 (1964).

143. S. Karplus and R. Bersohn, *J. Chem. Phys.*, 51, 2040 (1969).

144. E. Lindholm, *J. Chem. Phys.*, 52, 4921 (1970).

145. J. W. Raymonda and W. T. Simpson, *J. Chem. Phys.*, 47, 430 (1967).

146. R. Gorden, Jr., R. E. Rebbert and P. Ausloos, *Nat. Bur. Stand. Tech. Note*, 496, 31 (1969).

147. R. Gorden, Jr., R. E. Rebbert and P. Ausloos, *Nat. Bur. Stand. Tech. Note*, 496, 56 (1969).

148. Y. Tanaka, A. S. Jursa and F. J. LeBlanc, *J. Opt. Soc. Am.*, 48 304 (1958).

149. R. E. Huffman, Y. Tanaka and J. C. Larrabee, *Japan J. Appl. Phys.*, 4, Supp. 1, 494 (1965).

150. R. E. Huffman, J. C. Larrabee and Y. Tanaka, *Appl. Opt.*, 4, 1581 (1965).

151. P. Harteck, R. R. Reaves, Jr., and B. A. Thompson, *Z. Naturforsch.*, 19a, 2 (1964).

152. B. A. Thompson, R. R. Reaves, Jr., and P. Harteck, *J. Phys. Chem.*, 69, 3964 (1965).

153. W. D. Woolley and R. A. Back, *Can. J. Chem.*, 46, 295 (1968).

154. H. Akimoto and I. Tanaka, *Z. Electrochem.*, 72, 134 (1968).

155. P. Warneck, *Appl. Opt.*, 1, 721 (1962).

156. H. Okabe, *J. Opt. Soc. Am.*, 54, 478 (1964).

157. A. H. Laufer, J. A. Pirog and J. R. McNesby, *J. Opt. Soc. Am.*, 55, 64 (1965).

158. L. S. Nelson and G. P. Spindler, *Res. Sci. Instr.*, 29, 324 (1958).

159. R. A. Back and D. C. Walker, *J. Chem. Phys.*, 37, 2348 (1962).

160. R. E. Rebbert and P. Ausloos, *J. Am. Chem. Soc.*, 90, 7370 (1968).

161. J. A. R. Samson, *Techniques of Vacuum Ultraviolet Spectroscopy*, John Wiley and Sons, Inc., (1967).

162. R. W. Fair, A. Van Rooselaar and O. P. Strausz, *Can. J. Chem.*, 49, 1659 (1971).

163. O. P. Strausz, S. C. Barton, W. K. Duholke, H. E. Gunning and P. Kebarle, *Can. J. Chem.*, 49, 2048 (1971).

164. R. G. Schmitt and R. K. Brehm, *Appl. Opt.*, 5, 1111 (1966).

165. R. D. Penzhorn and B. de B. Darwent, *J. Chem. Phys.*, 55, 1508 (1971).

166. R. D. Penzhorn and B. de B. Darwent, *J. Chem. Phys.*, 55, 4148 (1971).

167. Y. Sano and S. Sato, *Bull Chem. Soc. Japan*, 44, 3213 (1972).

168. W. E. Falconer and W. A. Sunder, *Int. J. Chem. Kin.*, 4, 315 (1972).

169. M. Zelikoff and K. Watanabe, *J. Opt. Soc. Am.*, 43, 756 (1953).

170. L. C. Glasgow and P. Potzinger, *J. Phys. Chem.*, 76, 138 (1972).

171. H. E. van den Berg, A. B. Callear and R. J. Norstrom, *Chem. Phys. Lett.*, 4, 101 (1969).

172. N. Basco, D. G. L. James and R. D. Suart, *Int. J. Chem. Kin.*, 2, 215 (1970).

173. C. J. Mazak and J. W. Simons, *J. Am. Chem. Soc.*, 90, 2484 (1968).

174. W. L. Hase, W. G. Brieland and J. W. Simons, *J. Phys. Chem.*, 73, 4401 (1969).

175. B. S. Rabinovitch and D. W. Setser, *Advances in Photochemistry*, 3, 1 (1964).

176. C. F. Goodeve and N. O. Stein, *Trans. Faraday Soc.*, 27, 393 (1931).

177. J. A. Kerr, *Chem. Rev.*, 387 (1966).

178. R. G. Gann and J. Dubrin, *J. Chem. Phys.*, 47, 1867 (1967).

179. G. Herzberg, *Electronic Spectra of Polyatomic Molecules*, D. Van Nostrand Co., Inc., Princeton, N.J., 1966.

180. B. de B. Darwent, R. L. Wadlinger and Sr. M. J. Alland, *J. Phys. Chem.*, 71, 2346 (1967).

181. G. R. Woolley and R. J. Cvetanović, *J. Chem. Phys.*, 50, 4697 (1969).

182. P. J. Kuntz, E. M. Nemeth, J. C. Polanyi and W. H. Wong, *J. Chem. Phys.*, 52, 4654 (1970).

183. J. G. Calvert and J. N. Pitts, *Photochemistry*, p. 825, John Wiley and Sons, Inc., 1966.

184. B. A. De Graff and J. G. Calvert, *J. Am. Chem. Soc.*, 89 2247 (1967).

185. H. E. Gunning and O. P. Strausz, *Advan. Photochem.*, 4, 143 (1966).

186. M. A. Nay, O. P. Strausz and H. E. Gunning, unpublished results.

187. J. G. Calvert and J. N. Pitts, *Photochemistry*, p. 488, John Wiley and Sons, Inc., 1966.

188. E. Block, *Quart. Report Sulphur Chem.*, 4, 237 (1969).

189. A. G. Alexander, T. L. Pollock and O. P. Strausz, presented at the 25th Ann. N. W. Reg. Meeting of the Am. Chem. Soc., Seattle University, Seattle, June 19, 1970.

190. A. G. Alexander and O. P. Strausz, presented at the 54th Can. Chem. Conf., Halifax, Nova Scotia, May 31-June 2, 1971.

191. O. P. Strausz, A. G. Alexander, T. L. Pollock and K. Obi, presented at the 10th Informal Conf. Photochem., Stillwater, Oklahoma, May 14-18, 1972.

APPENDIX A

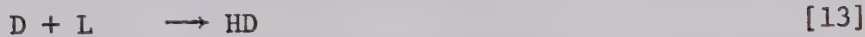
The photolysis of the simple methylated silanes can lead to various types of atomic and molecular loss of hydrogen. In order to sort out these possibilities, experiments were carried out with isotopically labelled substrate (on the silicon atom only). Various mixtures of undeuterated silane (hereafter referred to as L) and deuterated silane (hereafter referred to as He) were photolyzed and the isotopic hydrogen yields measured.

The following kinetic scheme was used to analyze the data; it is obvious that this scheme is applicable to any methylated silane. In this study, $\text{He} = (\text{CH}_3)_2\text{SiD}_2$ and $\text{L} = (\text{CH}_3)_2\text{SiH}_2$.

$\text{He} + \text{h}\nu$	\longrightarrow	He^*	$I_a F_{\text{He}}$
He^*	\longrightarrow	H	ϕ_1 [1]
	\longrightarrow	D	ϕ_2 [2]
	\longrightarrow	D_2	ϕ_3 [3]
	\longrightarrow	HD	ϕ_4 [4]
	\longrightarrow	H_2	ϕ_5 [5]
$\text{L} + \text{h}\nu$	\longrightarrow	L^*	$I_a F_{\text{L}}$
L^*	\longrightarrow	H	ϕ_6 [6]
	\longrightarrow	H	ϕ_7 [7]
	\longrightarrow	H_2	ϕ_8 [8]
	\longrightarrow	H_2	ϕ_9 [9]
	\longrightarrow	H_2	ϕ_{10} [10]

The H and D atoms formed in the system would only abstract from the

silicon end of the substrate (see Introduction).



We will not write the silane products formed from these equations because they do not contribute to hydrogen formation.

Equations [1] - [5] in the "heavy" (He) correspond to equations [6] - [10] in the "light" (L) silane. The following symbols will be used: $k_1 - k_{14}$ will refer to the rate constants for reactions [1] - [14]; $\phi_1 - \phi_{10}$ will refer to the primary quantum yields for reactions [1] - [10]; ϵ_L and ϵ_{He} refer to the extinction coefficients of L and He respectively; and I_a is the incident light intensity. Other expressions used are:

$$x_L = \frac{(L)}{(L) + (He)} \quad [15]$$

$$x_{He} = \frac{(He)}{(L) + (He)} \quad [16]$$

$$F_L = \frac{\epsilon_L(L)}{\epsilon_L(L) + \epsilon_{He}(He)} \quad [17]$$

$$F_{He} = \frac{\epsilon_{He}(He)}{\epsilon_L(L) + \epsilon_{He}(He)} \quad [18]$$

$$x_{H_2} = \frac{\text{Rate}(H_2)}{\text{Rate}(H_2 + HD + D_2)} \quad [19]$$

$$x_{HD} = \frac{\text{Rate}(HD)}{\text{Rate}(H_2 + HD + D_2)} \quad [20]$$

$$X_{D_2} = \frac{\text{Rate}(D_2)}{\text{Rate}(H_2 + HD + D_2)} \quad [21]$$

$$\Sigma\phi = \phi_1 + \phi_2 \dots \phi_{10} \quad [22]$$

= total experimental hydrogen quantum yield

Steady state treatment of the above reaction scheme gives:

$$(L^*) = \frac{I_a F_L}{k_6 + k_7 + k_8 + k_9 + k_{10}} \quad [23]$$

$$(He^*) = \frac{I_a F_{He}}{k_1 + k_2 + k_3 + k_4 + k_5} \quad [24]$$

$$(H) = \frac{k_1 (He^*) + (k_6 + k_7) (L^*)}{k_{11} (L) + k_{12} (He)} \quad [25]$$

$$(D) = \frac{k_2 (He^*)}{k_{13} (L) + k_{14} (He)} \quad [26]$$

The rate expressions for isotopic hydrogen formation are:

$$\text{Rate}(H_2) = k_5 (He^*) + (k_8 + k_9 + k_{10}) (L^*) + k_{11} (H) (L) \quad [27]$$

$$\text{Rate}(HD) = k_4 (He^*) + k_{12} (H) (He) + k_{13} (D) (L) \quad [28]$$

$$\text{Rate}(D_2) = k_3 (He^*) + k_{14} (D) (He) \quad [29]$$

$$\text{Rate}(H_2 + HD + D_2) = I_a \Sigma\phi \quad [30]$$

Thus we obtain:

$$X_{D_2} = \frac{1}{I_a \Sigma\phi} \left[k_3 (He^*) + \frac{k_{14} (He) k_2 (He^*)}{k_{13} (L) + k_{14} (He)} \right] \quad [31]$$

$$= \frac{1}{\Sigma\phi} \left[\left(\frac{k_3 (He^*)}{I_a F_{He}} \right) F_{He} + \frac{k_{14} X_{He}}{k_{13} X_L + k_{14} X_{He}} \left(\frac{k_2 (He^*)}{I_a F_{He}} \right) F_{He} \right] \quad [32]$$

$$\frac{x_{D_2}}{F_{He}} = \frac{1}{\Sigma\phi} \left[\phi_3 + \frac{k_{14}x_{He}}{k_{13}x_L + k_{14}x_{He}} \phi_2 \right] \quad [33]$$

A plot of $\frac{x_{D_2}}{F_{He}}$ vs x_L (see Figure III-11) enables the determination of ϕ_2 and ϕ_3 .

at $x_L = 0$

$$\frac{x_{D_2}}{F_{He}} = \frac{1}{\Sigma\phi} (\phi_3 + \phi_2) \quad [34]$$

at $x_L = 1.0$

$$\frac{x_{D_2}}{F_{He}} = \frac{1}{\Sigma\phi} (\phi_3) \quad [35]$$

A rearrangement of equation [33] gives:

$$\frac{\phi_2}{\frac{x_{D_2}}{F_{He}} - \phi_3} = 1 + \frac{k_{13}}{k_{14}} \frac{x_L}{x_{He}} \quad [36]$$

A plot of the L.H.S. of equation [36] vs $\frac{x_L}{x_{He}}$ will give the isotope effect k_{13}/k_{14} .

Similarly we obtain:

$$x_{HD} = \frac{1}{I_a \Sigma\phi} \left[k_4(\text{He}^*) + \frac{k_{12}(\text{He})k_1(\text{He}^*)}{k_{11}(\text{L}) + k_{12}(\text{He})} + \frac{k_{12}(\text{He})(k_6 + k_7)(\text{L}^*)}{k_{11}(\text{L}) + k_{12}(\text{He})} \right. \\ \left. + \frac{k_{13}(\text{L})k_2(\text{He}^*)}{k_{13}(\text{L}) + k_{14}(\text{He})} \right] \quad [37]$$

$$\begin{aligned}
&= \frac{1}{\Sigma\phi} \left[\left(\frac{k_4(\text{He}^*)}{I_a F_{\text{He}}} \right) F_{\text{He}} + \frac{k_{12} X_{\text{He}}}{k_{11} X_{\text{L}} + k_{12} X_{\text{He}}} \left(\frac{k_1(\text{He}^*)}{I_a F_{\text{He}}} \right) F_{\text{He}} \right. \\
&\quad \left. + \frac{k_{12} X_{\text{He}}}{k_{11} X_{\text{L}} + k_{12} X_{\text{He}}} \left(\frac{(k_6 + k_7)(\text{L}^*)}{I_a F_{\text{L}}} \right) F_{\text{L}} \right. \\
&\quad \left. + \frac{k_{13} X_{\text{L}}}{k_{13} X_{\text{L}} + k_{14} X_{\text{He}}} \left(\frac{k_2(\text{He}^*)}{I_a F_{\text{He}}} \right) F_{\text{He}} \right] \quad [38]
\end{aligned}$$

$$\begin{aligned}
\frac{X_{\text{HD}}}{F_{\text{He}}} &= \frac{1}{\Sigma\phi} \left[\phi_4 + \frac{k_{12} X_{\text{He}}}{k_{11} X_{\text{L}} + k_{12} X_{\text{He}}} \phi_1 \right. \\
&\quad \left. + \frac{k_{12} X_{\text{L}}}{k_{11} X_{\text{L}} + k_{12} X_{\text{He}}} (\phi_6 + \phi_7) \frac{\varepsilon_{\text{L}}}{\varepsilon_{\text{He}}} + \frac{k_{13} X_{\text{L}}}{k_{13} X_{\text{L}} + k_{14} X_{\text{He}}} \phi_2 \right] \\
&\quad [39]
\end{aligned}$$

A plot of $\frac{X_{\text{HD}}}{F_{\text{He}}}$ vs X_{L} (see Figure III-11) enables the determination of $\phi_1 + \phi_4$.

at $X_{\text{L}} = 0$

$$\frac{X_{\text{HD}}}{F_{\text{He}}} = \frac{1}{\Sigma\phi} \left(\phi_4 + \phi_1 \right) \quad [40]$$

at $X_{\text{L}} = 1.0$

$$\frac{X_{\text{HD}}}{F_{\text{He}}} = \frac{1}{\Sigma\phi} \left(\phi_4 + \phi_2 + \frac{k_{12}}{k_{11}} (\phi_6 + \phi_7) \frac{\varepsilon_{\text{L}}}{\varepsilon_{\text{He}}} \right) \quad [41]$$

Similarly we obtain:

$$\begin{aligned}
X_{\text{H}_2} &= \frac{1}{I_a \Sigma\phi} \left[k_5(\text{He}^*) + (k_8 + k_9 + k_{10})(\text{L}^*) + \frac{k_{11}(\text{L})k_1(\text{He}^*)}{k_{11}(\text{L}) + k_{12}(\text{He})} \right. \\
&\quad \left. + \frac{k_{11}(\text{L})(k_6 + k_7)(\text{L}^*)}{k_{11}(\text{L}) + k_{12}(\text{He})} \right] \quad [42]
\end{aligned}$$

$$\begin{aligned}
 &= \frac{1}{\Sigma\phi} \left[\left(\frac{k_5(\text{He}^*)}{I_a F_{\text{He}}} \right) F_{\text{He}} + \left(\frac{(k_8 + k_9 + k_{10})(\text{L}^*)}{I_a F_{\text{L}}} \right) F_{\text{L}} \right. \\
 &+ \frac{k_{11}(\text{L})}{k_{11}(\text{L}) + k_{12}(\text{He})} \left(\frac{k_1(\text{He}^*)}{I_a F_{\text{He}}} \right) F_{\text{He}} \\
 &\left. + \frac{k_{11}(\text{L})}{k_{11}(\text{L}) + k_{12}(\text{He})} \left(\frac{(k_6 + k_7)(\text{L}^*)}{I_a F_{\text{L}}} \right) F_{\text{L}} \right] \quad [43]
 \end{aligned}$$

$$\begin{aligned}
 \frac{X_{\text{H}_2}}{F_{\text{He}}} &= \frac{1}{\Sigma\phi} \left[\phi_5 + (\phi_8 + \phi_9 + \phi_{10}) \frac{X_{\text{L}}}{X_{\text{He}}} \frac{\epsilon_{\text{L}}}{\epsilon_{\text{He}}} \right. \\
 &\left. + \frac{k_{11}X_{\text{L}}}{k_{11}X_{\text{L}} + k_{12}X_{\text{He}}} \left(\phi_1 + \frac{\epsilon_{\text{L}}}{\epsilon_{\text{He}}} \frac{X_{\text{L}}}{X_{\text{He}}} (\phi_6 + \phi_7) \right) \right] \quad [44]
 \end{aligned}$$

A plot of this equation is not necessary because ϕ_5 is readily obtained from the photolysis of He alone.

at $X_{\text{L}} = 0$

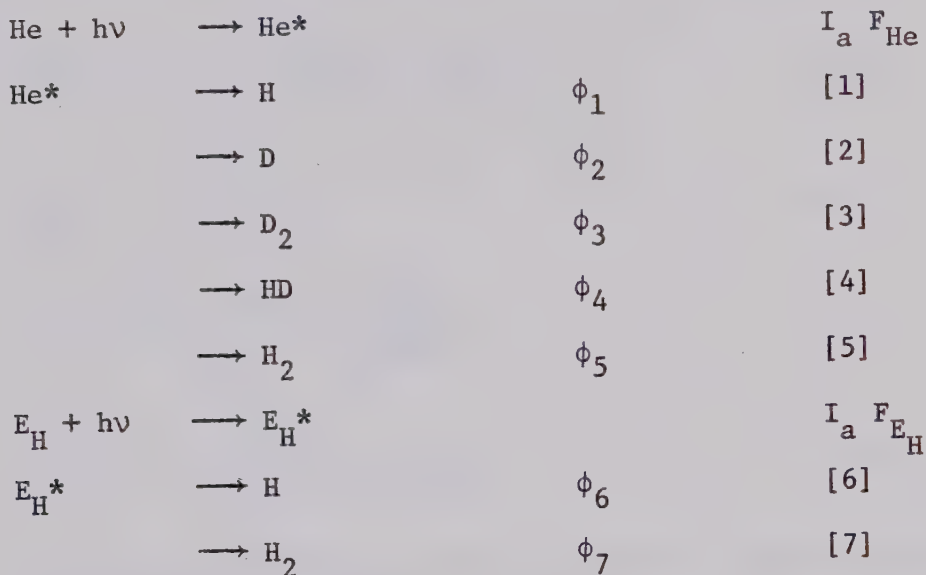
$$\frac{X_{\text{H}_2}}{F_{\text{He}}} = \frac{1}{\Sigma\phi} (\phi_5) \quad [45]$$

at $X_{\text{L}} = 1.0$

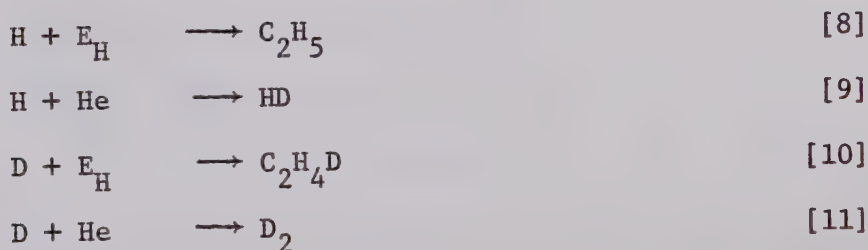
$$\frac{X_{\text{H}_2}}{F_{\text{He}}} = \infty \quad [46]$$

APPENDIX B

The photolysis of dimethylsilane-d₂ (He) in the presence of small amounts of ethylene (E_H) affords a convenient method of finding ϕ_1 and ϕ_4 separately (Appendix A). The kinetic scheme to be considered is given below.



The H and D atoms formed in the system would be expected to add to ethylene and abstract from dimethylsilane-d₂.



Symbols that differ from Appendix A are:

$$x_{He} = \frac{(He)}{(He) + (E_H)} \quad [12]$$

$$x_{E_H} = \frac{(E_H)}{(He) + (E_H)} \quad [13]$$

$$F_{He} = \frac{\varepsilon_{He}(He)}{\varepsilon_{He}(He) + \varepsilon_{E_H}(E_H)} \quad [14]$$

$$F_{E_H} = \frac{\varepsilon_{E_H}(E_H)}{\varepsilon_{He}(He) + \varepsilon_{E_H}(E_H)} \quad [15]$$

Steady state treatment of the above set of equations

gives:

$$(He^*) = \frac{I_a F_{He}}{k_1 + k_2 + k_3 + k_4 + k_5} \quad [16]$$

$$(E_H^*) = \frac{I_a F_{E_H}}{k_6 + k_7} \quad [17]$$

$$(H) = \frac{k_1(He^*) + k_6(E_H^*)}{k_8(E_H) + k_9(He)} \quad [18]$$

$$(D) = \frac{k_2(He^*)}{k_{10}(E_H) + k_{11}(He)} \quad [19]$$

The rate expressions for isotopic hydrogen formation are:

$$\text{Rate}(H_2) = k_5(He^*) + k_7(E_H^*) \quad [20]$$

$$\text{Rate}(HD) = k_4(He^*) + k_9(H)(He) \quad [21]$$

$$\text{Rate}(D_2) = k_3(He^*) + k_{11}(D)(He) \quad [22]$$

$$\begin{aligned} \text{Rate}(H_2 + HD + D_2) &= K \\ &= \text{constant} \end{aligned} \quad [23]$$

Hence we obtain:

$$\frac{x_{HD}}{x_{D_2}} = \frac{k_4(He^*) + k_9(He) \left(\frac{k_1(He^*) + k_6(E_H^*)}{k_8(E_H) + k_9(He)} \right)}{k_3(He^*) + k_{11}(He) \left(\frac{k_2(He^*)}{k_{10}(E_H) + k_{11}(He)} \right)} \quad [24]$$

$$= \frac{\frac{k_4(\text{He}^*)}{I_a F_{\text{He}}} + \frac{k_1(\text{He}^*)}{I_a F_{\text{He}}} + \frac{k_6(E_{\text{H}}^*)}{I_a F_{\text{E}_H}} + \frac{I_a F_{\text{E}_H}}{I_a F_{\text{He}}}}{\frac{k_8}{k_9} \frac{X_{\text{E}_H}}{X_{\text{He}}} + 1} \quad [25]$$

$$+ \frac{\frac{k_3(\text{He}^*)}{I_a F_{\text{He}}} + \frac{k_2(\text{He}^*)}{I_a F_{\text{He}}}}{\frac{k_{10}}{k_{11}} \frac{X_{\text{E}_H}}{X_{\text{He}}} + 1}$$

$$\frac{X_{\text{HD}}}{X_{\text{D}_2}} = \frac{\phi_4 + \frac{\phi_1 + \frac{\varepsilon_{\text{E}_H}}{\varepsilon_{\text{He}}} \frac{X_{\text{E}_H}}{X_{\text{He}}} \phi_6}{\frac{k_8}{k_9} \frac{X_{\text{E}_H}}{X_{\text{He}}} + 1}}}{\phi_3 + \frac{\phi_2}{\frac{k_{10}}{k_{11}} \frac{X_{\text{E}_H}}{X_{\text{He}}} + 1}} \quad [26]$$

APPENDIX C

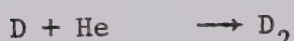
The photolysis of H_2S in the presence of DMS-d_2 (He) leads to the formation of large amounts of D_2 . The following kinetic scheme was used to examine the possibility of a simple exchange reaction.

 I_a 

[1]



[2]



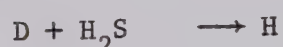
[3]



[4]



[5]



[6]

Steady state treatment of the above set of equations gives:

$$\frac{(\text{H})}{(\text{D})} = \frac{k_3(\text{He}) + (k_5 + k_6)(\text{H}_2\text{S})}{k_2(\text{He})} \quad [7]$$

The rate expressions for hydrogen formation are:

$$\text{Rate}(\text{H}_2) = k_4(\text{H})(\text{H}_2\text{S}) \quad [8]$$

$$\text{Rate}(\text{HD}) = k_1(\text{H})(\text{He}) + k_5(\text{D})(\text{H}_2\text{S}) \quad [9]$$

$$\text{Rate}(\text{D}_2) = k_3(\text{D})(\text{He}) \quad [10]$$

$$\begin{aligned} \text{Rate}(\text{H}_2 + \text{HD} + \text{D}_2) &= K \\ &= \text{constant} \end{aligned} \quad [11]$$

Hence we obtain

$$\frac{x_{\text{HD}}}{x_{\text{D}_2}} = \frac{k_1(\text{H})(\text{He}) + k_5(\text{D})(\text{H}_2\text{S})}{k_3(\text{He})(\text{D})} \quad [12]$$

$$= \frac{k_1}{k_3} \frac{(\text{H})}{(\text{D})} + \frac{k_5}{k_3} \frac{(\text{H}_2\text{S})}{(\text{He})} \quad [13]$$

$$= \frac{k_1}{k_2} + \left[\frac{k_1}{k_2} \frac{(k_5 + k_6)}{k_3} + \frac{k_5}{k_3} \right] \frac{(H_2S)}{(He)} \quad [14]$$

B30037